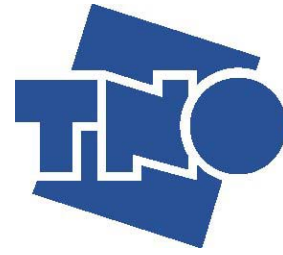




**Universiteit Utrecht**



Modeling of the erosion phases during the  
Mesozoic in The Broad Fourteens,  
offshore the Netherlands

*Master Thesis*

***F.M.J. van Lieshout***

*Supervisors:*

***Prof. Dr. P. L. de Boer***  
*University of Utrecht*

***Dr. J.H ten Veen***  
*TNO, Bouw en Ondergrond, Utrecht*

*August 2010*



---

## **Abstract**

In this report estimates of erosion in the Broad Fourteens during the Mesozoic are presented. This is done by using, among others, a new 3D seismic model of this area provide by the National Geological Survey, TNO.

Results show that most erosion occurred in the southeastern part of the Broad Fourteens Basin. The maximum erosion of 3100 meter is calculated for well P06-02. This is also the area where the most sediment is deposited during the Mesozoic. Erosion values are presented as erosion maps running from the Triassic till the Cretaceous. The erosion maps show that mainly the Triassic sediments are removed from the platforms and highs, while the Jurassic and essentially the Cretaceous are removed in the basin. The erosion maps of the Lower and Upper Cretaceous show a decreasing distribution of the amount of erosion from the southeastern part of the basin towards the northwestern part. By looking at the fault systems, cross sections and the amount of erosion, of this period, it is therefore stated that the erosion started first in the southern part of the basin (Late Turonian) and then moved up northwards (Late Coniacian- Early Santonian).

The most sediment was removed in the Broad Fourteens Basin during the Sub Hercynian tectonic event and had therefore the most influence on the general structure of the basin.

---

Keywords:

*North Sea, Broad Fourteens, Mesozoic, erosion, 3D, model*



# Table of Contents

<b>1. Introduction</b>	<b>7</b>
1.1 Aim	7
1.2 The North Sea	8
<i>Tectonic History of the North Sea</i>	
1.3 Broad Fourteens	9
1.3.1 <i>General Setting</i>	
1.3.2 <i>Time Periods &amp; Tectonic Phases in the Broad Fourteens area</i>	
<b>2. Data &amp; Methods</b>	<b>18</b>
2.1. Well selection	18
2.2 The structural elements map	18
2.3 Well-data; logs and cores	19
2.3.1 Vitrinite Reflectance (Vr or R <sub>o</sub> )	
2.4 Seismic data, the 3D layer model	20
2.5 Basic assumptions	
2.6 The Method	21
2.6.1 Backstripping	
2.6.2 Techniques	
2.6.3 Programs used	
2.7 Scenario's	27
2.7.1 Sedimentation and erosion	
<i>Erosion due to the Kimmerian tectonic phases</i>	
<i>Erosion due to the Sub Hercynian &amp; Laramide tectonic phase</i>	
2.7.2 Scenario's	
<i>Scenario 1</i>	
<i>Scenario 2</i>	
<i>Scenario 3</i>	
<b>3. Results</b>	<b>30</b>
3.1 The Basin	30
3.2 The Low Platforms	32
3.3 The High Platforms and Highs	33
3.4 The erosion maps	34
<b>4. Discussion</b>	<b>36</b>
4.1 Structural elements	36
4.2 The input data	36
4.3 Basic Assumptions	36
4.4 Evolution of the Broad Fourteens Basin	37
4.5 The erosion maps	38
4.5.1 Erosion maps of the Early and Late Triassic	
4.5.2 Erosion maps of the Early and Late Jurassic	
4.5.3 Erosion maps of the Early and Late Cretaceous	
4.5.4 Comparison with other reports	

<b>5. Conclusion</b>	<b>40</b>
<b>6. Recommendations</b>	<b>41</b>
<b>7. Acknowledgements</b>	<b>41</b>
<b>8. Appendix</b>	<b>42</b>
Appendix A:	
Workflow	43
Appendix B:	
Selected wells	46
Appendix C:	
Boundary conditions	
Well K14-01 and P06-04	49
Appendix D:	
The Burial maps and the Maturity diagrams	62
Appendix E:	
The Erosion maps	<b>68</b>
<b>9. References</b>	<b>71</b>
<b>10. Figures</b>	

# 1. Introduction:

## 1.1 Aim

The North Sea Basin is an important hydrocarbon producing area since the middle of the 20<sup>th</sup> century [4]. The geological evolution of the North Sea area therefore has been studied intensely. For more detail, the basins of the North Sea also have been studied to understand the local evolution. To reconstruct the evolution of a basin, features like sediment characteristics, compaction, erosion and chronology have to be known.

Unfortunately, not all features can be measured precisely, such as erosion. Knowing the original thickness of an eroded sequence and its distribution, however, is important as it provides important constraints on the style of inversion and on the fluid-flow system before and during tectonic events [5-7] i.e., the entire evolution of the basin.

The aim of this research is to create erosion maps with 3D information of the Mesozoic erosion phases in the Dutch part of the North Sea Basin. The Broad Fourteens, an offshore basin in The Netherlands North Sea, is used as a case study. Earlier erosion maps, which have been made, of this area, were based on 1D data and are therefore less accurate [6]. In this research, well data, seismic data and a 3D subsurface model of the area will be used in order to reconstruct the amount of erosion. The data sets are provided by TNO, including vitrinite reflectance data, temperature data and composite well logs.

With the wide range of data available several erosion maps are able to be created, which are more detailed and can be used for further 3D modeling of palaeo surface reconstruction. As this is needed in, for instance the hydrocarbon industry, the erosion determination thus has a direct economical relevance.

Other issues which are relevant:

1. *-Did erosion rates vary laterally?*
2. *-What controls the rate of uplift and subsidence?*
3. *-Can a better estimate of the palaeo thickness per unit be made?*
4. *-Are the results of such quality to make better hydrocarbon system predictions?*

This report briefly discusses the tectonic history of the North Sea in Chapter 1.2, which is followed by a description of the general setting and the history of the Broad Fourteens basin in Chapter 1.3.

Chapter 2 describes in detail the data and the methods, which were used to determine the erosion in the basin. The results of these methods are presented in Chapter 3. In this chapter the backstripped wells, which fit the best with the measured data, together with graphics are shown and discussed. In Chapter 4 all these results are discussed and interpreted. Also the assumptions are discussed and explained as these have much influence on the input and output of the model.

This all is summarized and concluded in Chapter 5. Some recommendations are made for future work in Chapter 6.

Chapter 8 includes the Appendix, and contains the selected wells, a list of assumptions made, the burial maps, the maturity diagrams and the erosion maps made.

## 1.2 The North Sea:

### 1.2.1 Tectonic history of the North Sea

The tectonic history of Western Europe and the North Sea is controlled by the convergence of three large continental plates: Gondwana, Laurentia and Baltica. It was the collision of these three plates that formed the supercontinent Pangea during Ordovician to Permian times. The creation of the Pre-Mesozoic supercontinent Pangea is characterized by the Caledonian and Variscan orogeny. These two events formed the initial highs and characterized the basement.

During the Late Devonian the North Sea area was located at equatorial regions and formed a depression between the Caledonian and Variscan orogeny.

It was during the Late Carboniferous that a major wrench fault through the North Sea caused a thermal destabilization of the lithosphere [8, 9]. Old fault systems were reactivated and intrusive and extrusive magmatism, such as in the Oslo Graben, played an important role in the formation of the North Sea basin [10]. At the end of the Early Permian the thermal activity declined and the lithosphere experienced a thermal relaxation, which caused two major basins to develop, the Northern and Southern Permian Basin.

It was at the beginning of the Mesozoic (251.0 Ma to 65.5 Ma) Pangea started to break up, the Atlantic between Greenland and Norway opened (251.0 to 199.6 Ma) and the North Sea area started to subside [11]. An eastern branch of this break-up started to extend towards the North Sea area during the Triassic, which resulted in the Hardegsen tectonic phase in North Sea [12, 13]. The tectonic event resulted in a major uplift in the centre of the Netherlands, the Netherlands Swell during the Early Trias. The uplift of this domal structure caused a stronger subsidence of area next to it, such as for the West Netherlands Basin, the Off Holland Low and the Roer Valley Graben. These three grabens are important elements in the development of the Netherlands and the Dutch part of the North Sea.

During the Jurassic (199.6 to 145.5 Ma), the breaking up of supercontinent Pangaea continued and sea level started to rise. With the deepening of the sea during the Early Jurassic anoxic bottom waters started to develop the deposition of organic-rich sediments, these would later form important source rocks for oil and gas. A gradual drop of sea level starting in Middle Jurassic was accompanied by clastic and sand deposition. Today these comprise major Late Jurassic reservoirs. Continental spreading continued during Middle Jurassic and resulted in the opening of the North Atlantic.

At the end of the Jurassic till the end of the Ryazanian another large rifting phase took place. This expansion was caused by the 'Late-Kimmerian' rifting tectonic phase and was the cause of the deposition of shallow marine to marine sediments in the Dutch North Sea basin. Many clay and fine sandstone sediments were deposited during this time which can be found as the Delfland and Rijnland Group (SLD and KN).

Rifting started to concentrate more between Norway and Greenland at the end of the Early Cretaceous, and sea level started to rise in the North Sea. The rifting phase in the southern part of the North Sea was mostly reduced at the beginning of the Late Cretaceous when the stress regime changed from extensional to compressional. This Sub Hercynian tectonic event caused normal faults to reactivate as reverse faults resulting in a phase of uplift.

The intensity and timing of the inversion for all basins in the North Sea is different, with the largest inversion for the Broad Fourteens basin and the West Netherlands basin [5].

At the start of the Danian the inversion stopped, which resulted in thermal relaxation of the lithosphere and the start of sedimentary loading. The development of the North Sea from



Eocene to present is characterised by an almost continuous regional subsidence and basin sedimentation. A final inversion can be found in regional unconformities with a maximum offset of 200 meters in the centre, probably caused by the Pyrenean orogenic phase [14, 15]

### 1.3 Broad Fourteens

#### 1.3.1 General Setting:

The Broad Fourteens Basin forms a NW-SE trending extensional basin in the southern part of the Dutch sector of the North Sea. It is believed that the basin started to establish during the Late Permian – Early Triassic. This can be stated, as from the Triassic, the thicknesses per stratigraphic unit increase towards the centre of the basin [16]. The now inverted basin is 120 km long and 45 wide and is bounded by several other basins. To the west the basin is bounded by the Sole Pit Basin, to the northeast by the Dutch Central Graben, the Terschelling Basin and the Vlieland Basin. The Central Netherlands Basin and the West Netherlands Basin bound the basin to its southeast (figure 1).

The Broad Fourteens Basin overlies partly the southern part of the Southern Permian Basin. This results in the fact, that only under the northern margin of the basin Zechstein salt can be found (>500 m). The southern part is underlain by Zechstein carbonate and clastic sediments [6, 7]. It is believed that this difference in subsurface causes the difference in present-day structural styles between the southern and northern part of the basin. This is because the salt acts as a gliding surface and the siliclastic sediments behave brittle to stresses acting upon the area (figure 2).

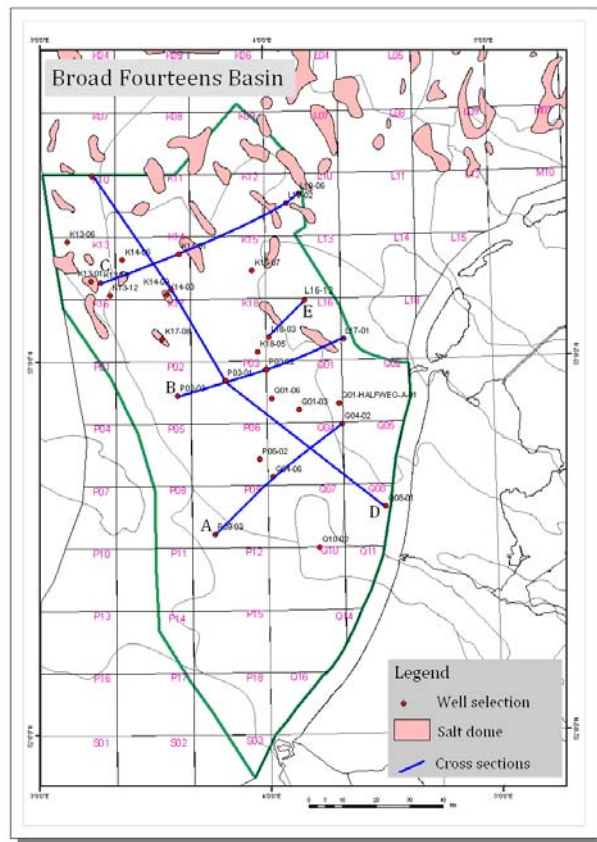
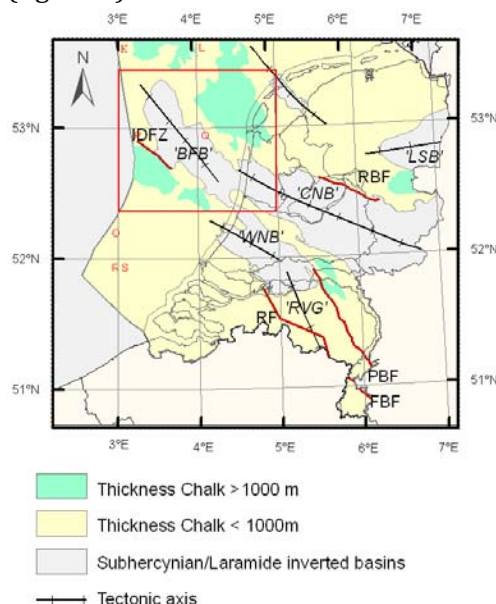


**Figure 1: The Broad Fourteens Basin**, is situated to the West of the Netherlands in the offshore area of the Dutch North Sea. Visible are the cross sections A, B, C, D and E used during the estimation of the erosion and the tectonic axis of the basin.

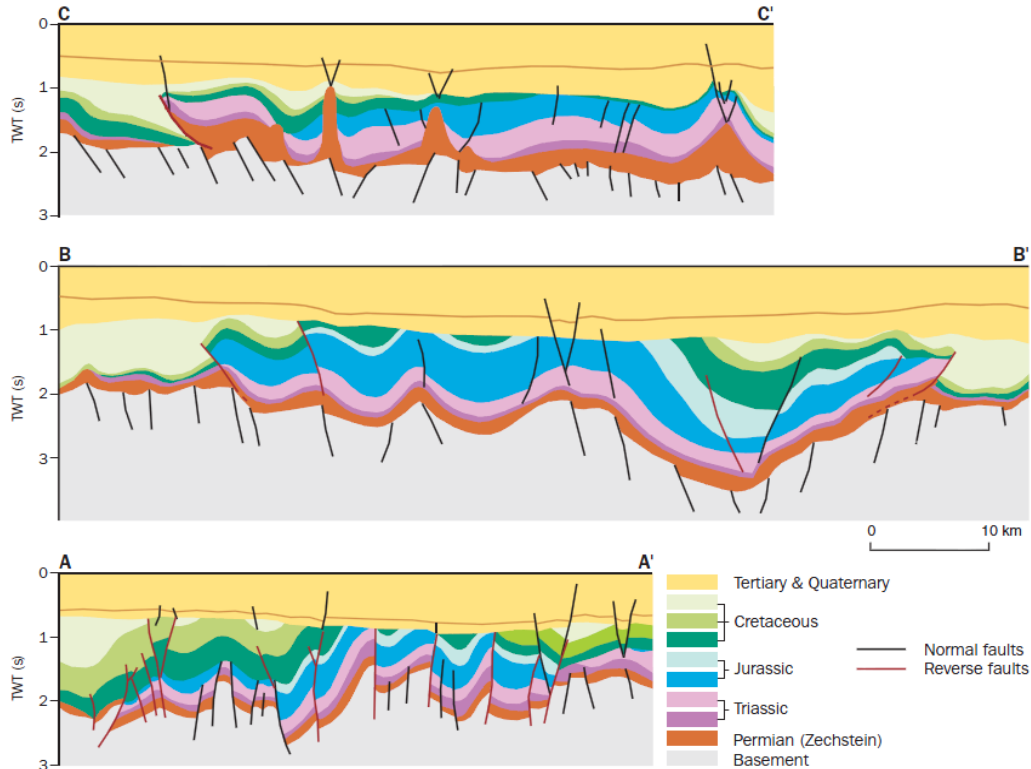


**Figure 2: Cross sections, showing the morphology of sediments due to salt tectonics.** The cross sections represent the same cross sections as in figure 1. In this figure the influence of the brittle to the more ductile manner of movement of the salt can be seen. (after Nalpas, 1995)

The study of the stratigraphic sequence per well and the geological structure of the basin indicate a complex evolution with periods of subsidence and inversion [4, 11, 15]. They show that over time major tectonic events such as the Kimmerian phases and the Sub Hercynian tectonic phase had a major influence on the development of the basin [6, 7, 11, 14, 15, 17-20]. Inversion, subsidence, erosion and sedimentation have given the basin a complex structural and sedimentological history. The most important tectonic events are summarized in Table 1.

In general it is believed that the structure of the present-day Broad Fourteens Basin is the effect of [6, 11, 13, 15]:

- The presence or absence of Zechstein salts.
- The angle between the normal faults and the shortening direction during inversion
- The thickness variation of the Mesozoic sedimentary cover throughout the basin
- Salt structures along the faults during inversion

**Table 1:** The important tectonic events in the Dutch part of the North Sea between Carboniferous and Present. The table is based on information gathered from many other reports [6, 8, 11, 13-16, 19, 21, 22].

<b>Tectonic event</b>	<b>Age</b>	<b>Structural influence</b>
<b>Variscan/Hercynian Orogeny</b>	Carboniferous- Permian	
The Saalian Phase	Early Permian	-Compression and wrench faulting
<b>Break up of Pangea</b>		
Hardegsen Tectonic Phase ( <i>End of the Scythian Hardegsen/Solling Unconformity</i> )	Early Trias - Lower Germanic Group	-Unconformity at base Upper Germanic Trias Group -Extension and subsidence
Early Kimmerian pulse I and II	Late Triassic - Early Jurassic	-Exclusively controlled by the Artic-North Atlantic rift system -Extension and subsidence
Late Kimmerian I pulse	Oxfordian-Valangian	-Stretching -Rapid subsidence basin -Uplift of its flanks
Late Kimmerian II tectonic pulse	Early Cretaceous Ryazanian	-Intensified uplift and erosion -Drop in sea level
<b>Alpine Orogeny</b>		
Austrian Phase	Early Cretaceous Aptian-Albian	-Local uplift -Erosion -Emplacement of magmatic intrusions in B14
Sub Hercynian Phase	Turonian to Maastrichtian	-Compression -Strong inversion -Uplift of centre of the basin -Erosion -Deposition outside the basin
Laramide Tectonic Phase	Mid-Palaeocene	-Inversion/crustal shorting, -Floor uplifted
Pyrenean Event	Eocene-Oligocene	-Uplift of basin -400-500 m of erosion of Lower Tertiary deposits in southern part -Stress orientation N-S -Compressive reactivation -200 m uplift of the centre

### 1.3.2 Time Periods & Tectonic Phases in the Broad Fourteens area

The stratigraphy in the Broad Fourteens is described in detail in many reports. The overview given here is based on [6, 16, 19-22]. A global overview of the sedimentary succession, including the depositional environment, is given in Table 2.

Over 500 wells have been drilled in the Broad Fourteens Basin. About 100 wells penetrate as deep as the Carboniferous Limburg Group (DC). Rock this old or older found in the basin is interpreted as Basement.

#### **The Carboniferous:**

During the Carboniferous the Dutch sector of the North Sea was a foredeep basin of the **Variscan orogeny**. During the Late Carboniferous and the Early Permian the basin became transected by a wrench fault system in the basement [19]. This resulted in several pull-apart basins in western Poland and Northeastern Germany. Sedimentation of clastics and volcanics was the result [13].

More to the end of the Carboniferous sedimentation changed into a succession of mostly lacustrine, deltaic and fluvial fine-grained sediments, which can be interbedded with local coal seams.

Sedimentation ended as a result of a thermal uplift in the southern North Sea during Stephanian-Early Permian times, **the Saalian phase**. This uplift of the sediment above sea-level resulted in a widespread differential erosion of hundreds to thousands of meters of sediment. [21-23].

#### **The Early Permian:**

After the Saalian uplift at the end of the Early Permian, the Northern and Southern Permian Basins began to subside in response to thermal relaxation of the lithosphere [11, 13]. From that period on the two basins were filled with continental to shallow marine Upper Rotliegend sediments (RO). In the deeper parts of the two Permian basins, in the centre, the Silverpit Formation (ROCL) claystones, siltstones and evaporates were deposited, followed by Late Permian Zechstein salt. This led to a maximum total thickness of 2000 m in the Northern and 3500 m in the Southern Permian Basin [11]. Sedimentation on platforms or on highs started later or did not occur.

As there was a periodically hot and arid climate, the area towards the south of the two basins were deposited with sediments of the Slochteren Formation (ROSL), such as dune sands, sabkha and desert-lake deposits [4]. This formation also covers most of the later Broad Fourteens basin.

#### **The Late Permian:**

##### ***The Thuringian***

The Late Permian started with the rifting between Greenland and Scandinavia causing a phase of transgression in the Northern and Southern Permian Basins [4]. Due to periodic closure of the connection between the basins and the open sea, a cyclical sequence of evaporites, carbonates and minor clastics were deposited, the Zechstein Formation (ZE).

Due to the subdivision of the Southern Permian Basin into several tectonic structural elements, there was a widespread accumulation difference of the Zechstein Formation during the Late Permian. This resulted in a general decrease of salt from the north (500 m) towards the south (0 m) and the deposition of fine-grained clastics, carbonates and anhydrite on the platforms in the south. Due to salt movement, however, maximum Zechstein salt thicknesses can reach up to 3500 m [24] (figure 3).

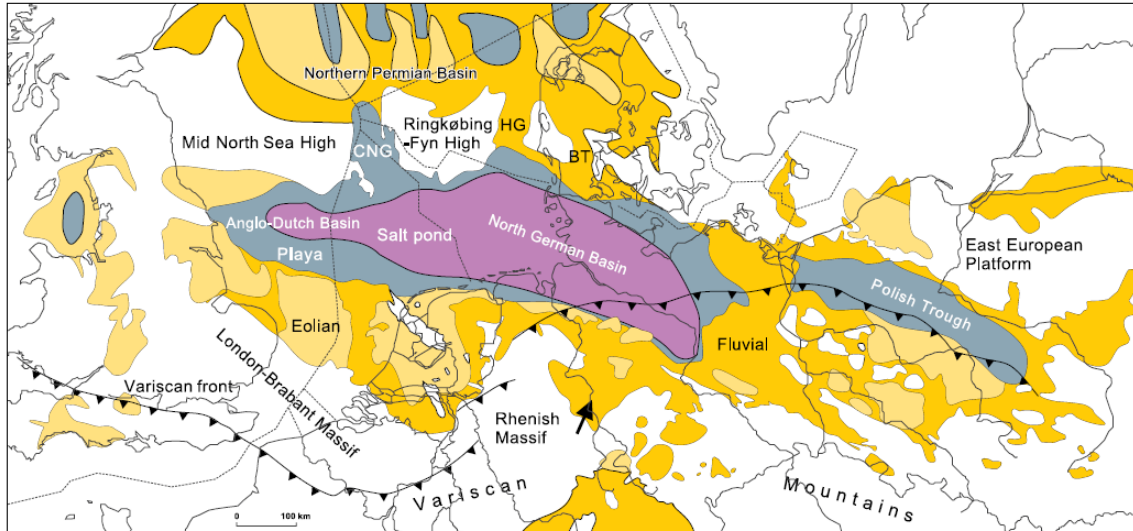


**Figure 3: Distribution map during the Late Permian, showing the shape and sedimentation of the Southern Permian Basin**

### Triassic:

During the Triassic the Northern and Southern Permian Basin kept subsiding due to lithospheric cooling and contraction. Due to differential subsidence and the withdrawal of the sea, a difference in thickness of Triassic sediment was created between the two basins [11]. The Lower Trias Group (RB) was deposited throughout the Dutch part of the North Sea.

The uplift of the swells is characterized by the erosion of the tops and the creation of the base of the Solling Unconformity. Sedimentation continued in the basins with the Muschelkalk and the Keuper Formation (RNMU, RNKP) while also the depositional environment changed to a marine climate.

Due to **the Hardegsen tectonic** phase during the Early Trias, basins such as the Dutch Central Graben, the Roer Valley Graben and the Off Holland Low subsided relatively faster than their surroundings [25]. The thickest Triassic sediment package can therefore be found in these grabens, with respectively 1500-2000 m in the Dutch Central Graben and 1000-1500 m in the Roer Valley and Off Holland Low.

### Jurassic:

As a result of the opening of the North Atlantic Ocean and the Tethys Ocean at the end of the Triassic, a new rifting event (**the Early Kimmerian tectonic phase**) took control in the basins and developed an open marine environment. It was during this time the Off Holland Low got the shapes of the Broad Fourteens Basins.

Sedimentation during that time covered the basin with clays of the Sleen and Aalburg Formation (ATRT, ATAL), which now can be found up to 5000 m depth in the basin [19].

With the open marine system being restricted during the *Toarcian*, conditions became anoxic and can be correlated with the deposition of the bituminous clays of the Posidonia Shale Formation (ATPO).

As the depositional environment changed from open marine to shallow marine, due to the thermal uplift of the Central North Sea Dome, the clays of the Werkendam Formation (ATWD) and the sandy carbonates of the Brabant Formation (ATBR) were deposited [13,

16]. The sedimentation ended in the Late Oxfordian when the Broad Fourteens became subaerial due to eustatic sea-level changes and domal uplift. This resulted in the erosion of the Jurassic sediments.

The Kimmeridgian started with the deposition of clastic material, indicating the start of the first pulse of **the Late Kimmerian tectonic phase** [11, 15, 21]. The Late Kimmerian I rifting phase caused a rapid subsidence of the Broad Fourteens Basin and a rise of the flanks. The basin was filled by the Delfland Subgroup (SLD) which thickens from the lower platforms towards the basin, up to 800 m [26]. Due to this rapid tectonic pulse Jurassic sediments can now be found which are over a 3000 meter thick. As sedimentation in the basin continued, it is thought that erosion still occurred at the platforms and highs of the Broad Fourteens Basin. This caused that no Delfland can now be found here. The elevated platforms and highs result now in a deep incision of the buildup stratigraphy through the Jurassic and Triassic and in some parts also the Permian sediments [15]. With the low sea level and an induced tectonic pulse (Late Kimmerian II) at the start of the Early Cretaceous, the erosion on the flanks was intensified.

#### **Cretaceous:**

With the start of the *Valanginian* the sea again transgressed into the Broad Fourteens Basin which led to the deposition of the Members of the Vlieland Claystone Formation (KNNC) and the Vlieland Sandstone Formation (KNNS). During the deposition the basin continued to subside differentially [5].

During *Aptian-Albian* times the Broad Fourteens was filled by a thick package of clays and sands of the Holland Formation (KNGL). With the continuation of subsidence of the basins and a major sea level rise, the remaining highs were covered by the sea. This resulted in favorable conditions for widespread deposition of limestone and marly chalk of the Texel and Ommeland Formations (CKTX and CKGR) [5].

The sedimentation in the basin was interrupted by an intense period of inversion, during *Turonian* times. This period, the **Sub Hercynian** tectonic event, is thought to be induced by the start of the compressional stresses from the Alpine collision. The inversion took place till *Campanian* times but was closely followed by the **Laramide** tectonic phase (Early Paleocene). It is therefore that the difference in effect of the two tectonic pulses are often hard to distinguish in seismic sections and composite well logs [27]. The effect of the inversion is thought to have started in the Albian, in the central part of the basin. Its margins started likely during the early Maastrichtian [26]

The clear variations in inversion style can be related to the variations in Zechstein salt thicknesses [6, 26]. The Zechstein salt in the northern and the middle part of the Broad Fourteens Basin served as the underlying surface for décollement faulting for the overlying sediments. As for in the southern part of the basin the Zechstein salt was absent. This difference can be seen in the general structure of the basin, as the northern part is controlled by, salt diapirism and folding as the southern part is more controlled by strong faulting, which even pass downward to the basement (figure 2).

As a result of the Sub Hercynian inversion the Rijnland Group (KN) in the Broad Fourteens is locally absent or strongly reduced by erosion [19, 21]. The deposition of the Chalk Gorup (CK) continued on the Jurassic Platforms and on the Highs at the margins of the basins, during the Sub Hercynian and the Laramide. More than 1800 m of Chalk is preserved here,

whereas in the centre of the Broad Fourteens Basin it has partly or completely been removed [6, 15, 19]. The end of the inversion period has been characterized by a relative thin layer (<50 m) of the Ekofisk Formation (CKEK), which mostly can be found at the margins of the basin.

**Tertiary:**

Sedimentation in the Tertiary resulted in a marine deposited of fine-grained clastics of mostly the Landen and Dongen Formation (respectively NLLF and NLFF).

**The Pyrenean tectonic phase** resulted in a regional uplift in the southern part of the basin and caused 400 to 500 m to be eroded of the Lower Tertiary [6, 18]. The sedimentation from Early Oligocene on occurred mainly in depocenters outside the area of the Broad Fourteens Basin. During Miocene and Early Pleistocene sediments from the Upper North Sea Group (N) were deposited as top of the total sediment package.

The compressional stresses that are still induced by the Alpine collision, still cause for the maximum horizontal stresses in the North Sea area. The strength is however reduced.

Table 2: Simplified succession of the Broad Fourteens Basin

Group and Formation	Age (ICS, 2003)	Depositional environment	Tectonic Pulses
<b>North Sea Supergroup (N)</b> <b>-Upper North Sea Group (NU)</b>  <b>-Middle North Sea Group (NM)</b>  <b>-Lower North Sea Group (NL)</b> - Dongen Formation - Landen Formation	<b>Tertiary</b> - Middle Miocene- Holocene	-Shallow marine, fluvial, paralic, lacustrine -Predominantly marine	
	- Late Eocene- Early Miocene		
	-Early Paleocene- Middle Eocene	-Marine	
<b>Chalk Group (CK)</b> -Ekofisk Formation (CKEK)  -Ommeland Formation (CKGR)  -Texel Formation (CKTX)	<b>Late Cretaceous</b> - Late Maastrichtian- Danian	-Shallow open marine	-Laramide
	-Turonian-Late Maastrichtian		-Sub Hercynian
	- Cenomanian		
<b>Rijnland Group (KN)</b> - Holland Formation (KNGL)  - Vlieland Claystone Formation (KNNC) -Vlieland Sandstone Formation (KNNS)	<b>Early Cretaceous</b> -Albian	-Moderately to fairly deep marine	
	- Valanginian- Aptian	-Coastal to shallow and fairly deep marine	
<b>Schieland Group (SL)</b> - Delfland Subgroup (SLD)	<b>Late Jurassic-Early Cretaceous</b> -Kimmeridgian- Early Valanginian	-Continental to paralic; shallow marine	



<b>Altena Group (AT)</b> - Brabant Formation (ATBR) - Werkendam Formation (ATWD) - Posidonia Shale Formation (ATPO) - Aalburg Formation (ATAL) - Sleen Formation (ATRT)	<b>Early to Middle Jurassic</b> - Hettangian-Oxfordian	- Shallow, open marine  - Marine, anoxic  - Shallow to fairly deep open marine	- Late Kimmerian I
<b>Upper Germanic Trias Group (RN)</b> - Keuper Formation (RNKP) - Muschelkalk Formation (RNMU) - Röt Formation (RNRO) - Soling Formation (RNSO)  <b>Lower Germanic Trias Group (RB)</b> - Main Buntersandstein Formation (RBM)	<b>Triassic</b> - Middle-Late Triassic	- Alternating shallow, restricted, marine - Playa lake, floodplains	- Early Kimmerian
	- Early Triassic	- Lacustrine, fluvial, Aeolian	- Hardegsen
<b>Zechstein Group (ZE)</b>	<b>Late Permian</b>	Playa lake Permimarine to shallow, highly restricted marine	
<b>Upper Rotliegend Group (RO)</b> - Slochteren Formation (ROSL) - Silverpit Formation (ROCL)	<b>Middle to early Late Permian</b>	- Aeolian, Fluvial, sheetflood  - Lake, Playa lake	- Saalian
<b>Limburg Group (DC)</b> - Maurits Formation (DCCU) - Baarlo Formation (DCCB) - Ruurlo Formation (DCCR)	<b>Carboniferous</b> - Westphalian	- Fluvial  - Deltaic	

## **2. Data & Methods:**

This research aims to reconstruct the amount of sediments that are removed during the Mesozoic in the Broad Fourteens. Till now erosion values of this basin are based on 1D well log information [6, 14]. To generate erosion values for the Broad Fourteens basin well log information, including core data, and a seismic based, 3D structural model of the basin are used. The erosion is determined, per sub-element of the basin, in which it is pursuit to gain a better determination of the evolution of the basin.

In the section below the approach is discussed together with further extension of the data used. The first step is the selection of the wells that are used during the research. This includes choosing the wells and which wells contain useable data. During the second step it is determined which technique can be used to estimate the erosion and which approach is used in this research. The last step is to determine the scenario's that are to be tested. The results of these scenarios are discussed later.

The workflow is visualized in Appendix A. Here all the steps taken during the research are shown in one figure.

### ***2.1 Well selection***

Over 500 wells have been drilled in the Broad Fourteens basin. From all these wells the composite well logs are known, and provide by TNO. Not all wells are cored and/or measured for their geophysical characteristics and are therefore not useful for this research.

The characteristic geophysical values include data on: porosity, permeability, pressure, reflective, present day temperature and stratigraphic data. During this research, wells are used that contain two or more important measured variables. Wells with vitrinite reflectance data are preferred as these are sensitive for initial burial depth.

With the selection of a well not only the data from the well are important, but also its position in the basin, its depth, its structural modifications due to faults or folds and external structures that could have influenced the stratigraphy, such as salt domes or extrusive rock.

Together with all these data, the wells are selected based on a structural elements map that divides the Broad Fourteens basin in several smaller areas. Because it is believed that a greater selection of suitable wells per structural element will give better erosion estimates, it is tried to select three or more wells per structural element.

Within the selection, the wells with vitrinite reflectance are looked at first. This is because this variable gives the most detailed information about the burial history of the wells. Also wells surrounding a well with vitrinite reflectance data are selected, because these wells will be used as comparison. In total 30 Wells out of the more than 500 wells in the Broad Fourteens basin were selected to perform the burial history simulation. Their results are also written done in Appendix B.

The final erosion maps are therefore based on these 30 wells.

### ***2.2 The structural elements map***

The structural elements map is based on the presence and absence of stratigraphic units in the Broad Fourteens basin (figure 4). These areas are defined as different structural elements and are used in the reconstruction of the evolution of the basin.

One has to note that the absence of stratigraphical layers, however, does not necessarily represent erosion. It could also represent a period of non-deposition.

Figure 4 (also Chapter 10) shows several large elements, which together represent a large part of the entire Broad Fourteens Basin: 5 basin elements (green), 4 low platforms (yellow), 2 high platforms and 1 high (both blue) are chosen to represent the entire basin. These elements are shown on the larger figure in Chapter 10. Noticeable is a NW-SE trend in most of the structural elements, corresponding to the rifting and the later inversion axis.

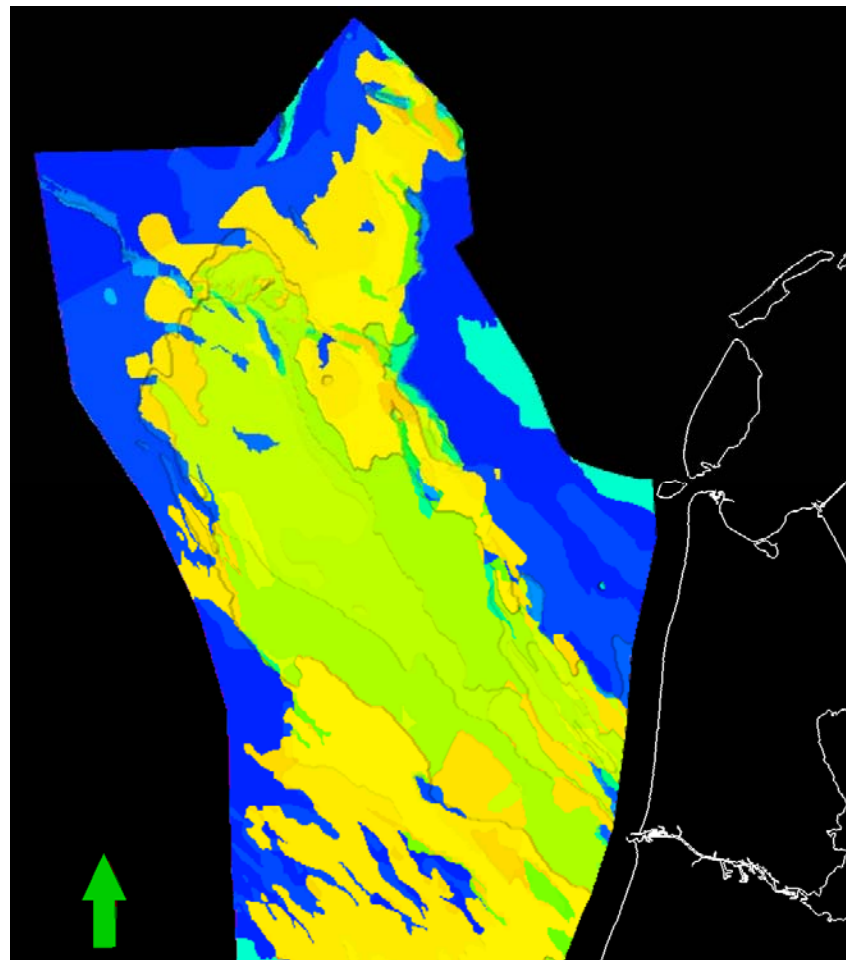
### **2.3 Well-data; logs and cores**

Well logs and measurements of the cores show the geophysical characteristics along the borehole. Well logs describe, for example, the amount of sand versus clay represented by the gamma ray or the resistivity of a unit, which is then used to determine the porosity, all correlated with depth. With this data also the sedimentary units are determined and divided from each other and is used for the interpretation of the subsurface [28].

By taking cores during the drilling, the physical characteristics of the well can be measured, such as the permeability and the vitrinite reflectance. Unfortunately, taking cores is an expensive process and therefore not all the wells are cored and not all the cores have been sampled.

From the more than 500 drilled wells in the Broad Fourteens only 103 wells contain porosity and permeability data. From these, only 40 wells in the basin contain vitrinite reflectance data and 71 wells contain measured pressure data.

**Figure 4: The structural element map, showing the three main elements used for the selection of the wells. Here green, yellow and blue represent respectively the basin, the low platforms and the high platform with the highs**



### **2.3.1 Vitrinite Reflectance ( $V_r$ or $R_o$ )**

Especially the vitrinite data is an important data set in this research. The reflectance of the vitrinite group of the macerals show a smoothly and predictable correlation with temperature and is therefore very useful as an indicator of maturity of organic materials.

To ensure reliable results, a reasonable amount of determinations need to be carried out (e.g. 20) on the same sample. Vitrinite reflectance is shown to be a very good maturity indicator above the 0.7 or 0.8%  $R_o$ . Below these values vitrinite reflectance tends to become unreliable. At temperatures equivalent to depths of >4 km the vitrinite maceral increases anisotropic, which makes taking correct measurements more difficult [29].

In the tables provided by TNO a column with the reliability of the measurements is presented. The vitrinite table is provided with a column representing the amount of measurements that have been taken from one sample. To give this data its reliability, the method stated in Allen & Allen (2005) [29] and mentioned above is taken into account. In the maturity diagrams the reliability given to the values is shown by using different symbols (see the legend accompanying Appendix D).

A great drawback in using vitrinite data for the determination of the maturity history is the possibility of reworking of the organic material. This leads to a strongly bimodal distribution of the vitrinite reflectance. Also the high variety of possible features that can be adept to determine the erosion values should be taken into account, when modeling the wells [30, 31].

The vitrinite data from TNO shows measurements over large parts of the well depths, while the other data sets, including e.g. temperature, porosity and pressure, are only section measurements and are not measured for the well depth. Therefore, taking the above into account, the erosion values determined during this research were mainly based on the vitrinite reflectance. The other data sets were used as supporting and correlating data.

### **2.4 Seismic-data; the 3D layer model, inc. faults**

For some important wells, erosion estimates could not be based on the measured and modeled vitrinite reflectance data, because there was no such data. For these wells the 3D seismic data of the area plays an important role, to make an estimate of the erosion. The interpretation of the seismic gives the first order of sediment that has been removed. The seismic data used in this report includes a 3D layer model of the studied area provided and interpreted by TNO. It is based on new 3D seismic and the seismic velocity model of Van Dalfsen *et al.* (2006) [32, 33]. The model shows the interpretation of horizons of the main stratigraphical units and the faults in the basin. By creating 2D lines through the model, crossing the wells, a good view is obtained of the tectonic movement, the timing of sedimentation and the amount of sediment removed.

### **2.5 Basic Assumptions**

Basic assumptions have to be made before modeling can start. These assumptions have great influence on the resulting burial history and maturity diagram and therefore should be taken with care. For two wells in the Broad Fourteens, well K14-01 and P06-04, the values for the palaeo sea level, the surface temperature and the heat flow, were calculated over a time period from 330 Ma till present and were provided for this research [34]. For all other wells, used during modeling, the basic assumptions were based on the values of these two wells and were manually adapted. In the Discussion below, these assumptions are further described.

## 2.6 The Method

### 2.6.1 Backstripping

The principal of backstripping is to use the present day stratigraphic record to determine the contribution of different geological processes and geometry of the basin at a time in the past.

The method of backstripping and the reconstruction of the burial history of a well was as concept originally put forward Watts & Ryan (1976)[35]. They expressed backstripping of a single layer as:

$$\therefore Y_i = W_{di} + S_i^* \left[ \frac{(\rho_m - \bar{\rho}_{si})}{(\rho_m - \rho_w)} \right] - \Delta_{sli} \frac{\rho_m}{(\rho_m - \rho_w)}$$

in which the first term expresses the water depth variation term, the second part the sediment loading term and the third part expresses the sea-level loading term.

This formula can also be used for multiple layer backstripping. This is however, much more complicated. To backstrip multiple layers, all the stratigraphic layers need to be restored individually in sequence and need to be determined for each time step. In this research, therefore, a modeling program is used, which will use this method and will make the calculations.

The method uses the information on the lithology, the ages and the depths of the main stratigraphic units, to quantitatively estimate the depth of the base through time as sediment and water is added or removed.

By comparing the backstripped curve with the theoretical curve it is possible to determine the mechanism that controlled the formation of the basin.

Throughout the years many reports have been written and used the backstrip concept to specify and determine erosion values in offshore sedimentary basins [2, 30, 36-38]. This has created a variety of methodologies that can be subdivided in four different techniques that can be used for defining erosion; tectonic based, thermal based, compaction based and stratigraphic correlation based. They are discussed in short.

## 2.6.2 Techniques:

### 2.6.2.1 Tectonic based:

This method is based on the stretching model of McKenzie [1], which calculates the subsidence of a basin by assuming an initial faulted synrift stage followed by an exponentially decreasing thermally driven subsidence. The model provides insight into the thermal and mechanical processes influencing the lithospheric stretching, and thus the evolution of the basin. Then, by comparing the model with the observed tectonic subsidence obtained by using well data, an estimate of the timing and amount of erosion can be made (figure 5) [39].

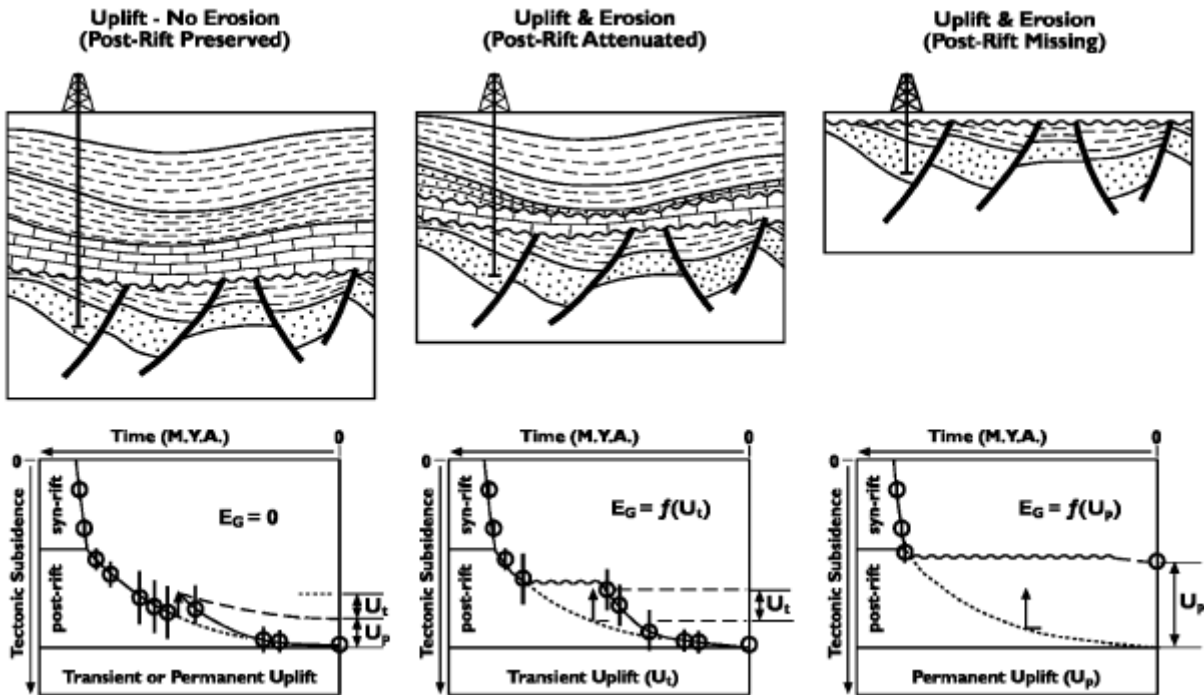


**Figure 5: Tectonic based erosion determination.** Three examples where erosion is estimated by correlating water-loaded basement subsidence curves with theoretical subsidence curves (dashed) gathered from the lithospheric stretching model of McKenzie [1]

### 2.6.2.2 Thermal based:

Due to the heat flow inside the Earth, rocks experience an increase in temperature when getting buried. For an area with no tectonic influences this thus results in a general thermal gradient with depth. The thermal based method uses this thermal gradient and the vitrinite reflectance ( $V_r$ ) data to give insight in the movement of rocks relative to depth.

Vitrinite reflectance data of a rock always shows the maximum temperature reached by the rock, so when compared with the thermal gradient, the maximum reached depth of the rock can be determined. Vitrinite reflectance data will never decrease in value. Therefore, when the burial depth of a rock is less than its maximum burial depth it can be said the rock has experienced uplift (figure 6). This could be in the form of erosion. [3].

By using this method it is assumed that the thermal gradient is the same throughout the geological history.

### 2.6.2.3 Compaction based:

This technique is based on the fact of compaction of sediments during burial, and therefore losing their porosity. This method uses the porosity to make an estimate of the maximum burial. First, a theoretically porosity-depth curve is made based on a large number of porosity measurements over a wide depth range of a given rock unit in a 'normally buried' sequence. These measurements can be calculated from wireline logs. Secondly, a porosity-depth curve is made (based on sonic transit time versus depth) of individual wells. This can then be compared with the theoretical reference curve (figure 7).

Note that this method assumes that the porosity decreases exponentially with depth only if it happens under hydrostatic conditions. Under overpressured conditions the porosity will be larger than expected and wrong depth relations will be made.

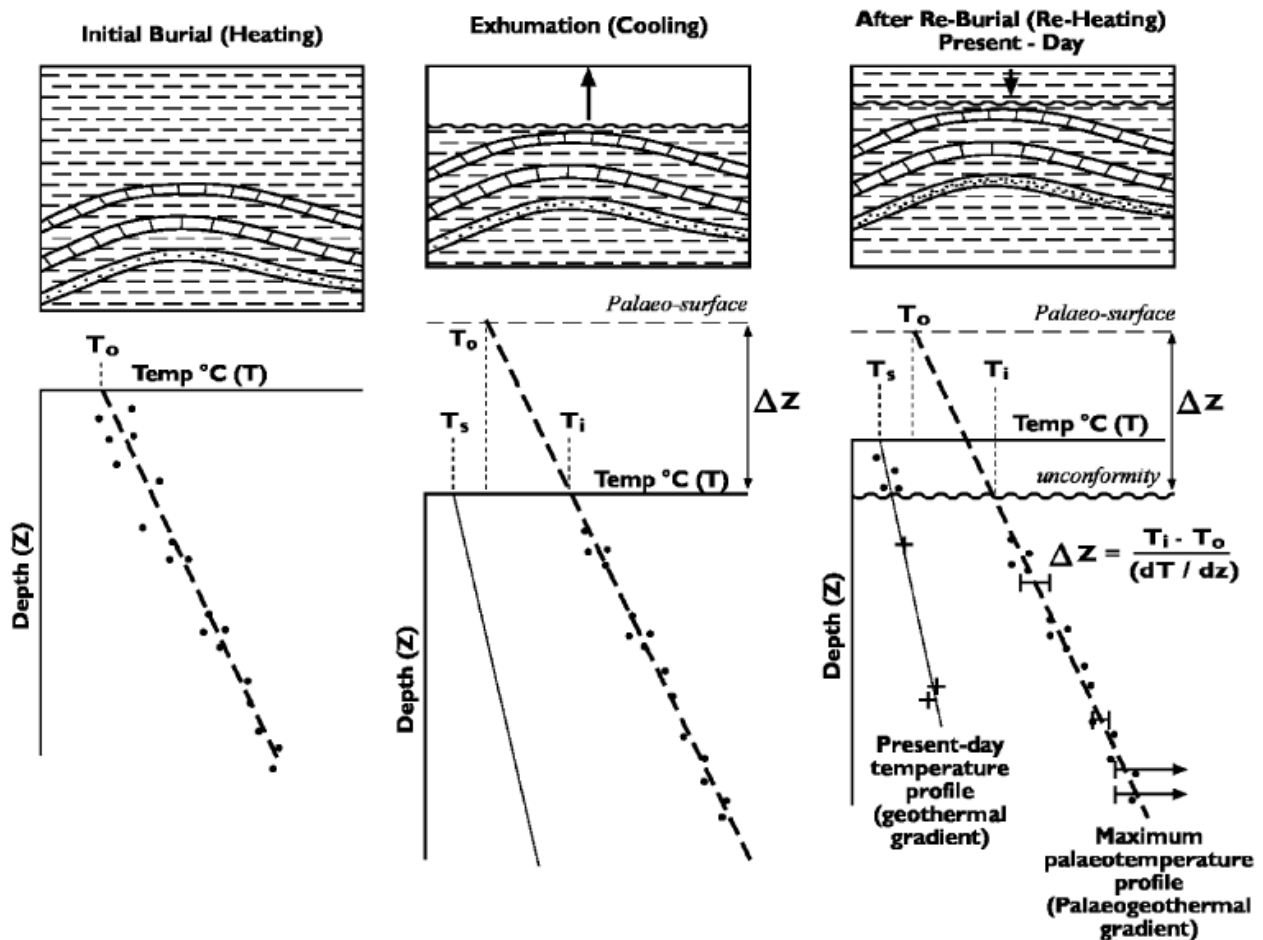


**Figure 6: Thermal based erosion determination.** This figure shows the thermal heating curve as it needs to adapt after erosion.  $T_i$  = palaeo temperature at the unconformity boundary;  $T_o$  = palaeo surface temperature  $T_s$  = present surface temperature (from[3]).

### 2.6.2.4 Stratigraphically based:

With this method an estimate of timing and magnitude of erosion can be determined by using only the stratigraphic sequence of a well and seismic data. Studying the stratigraphy of wells will result in the identification of unconformities and section correlations and restorations. Together with seismic data this can offer an additional constrain with respect to erosion estimates. The quantification of erosion is determined by identifying the maximum preserved section beneath the unconformity, the eroded section (figure 8) [2].

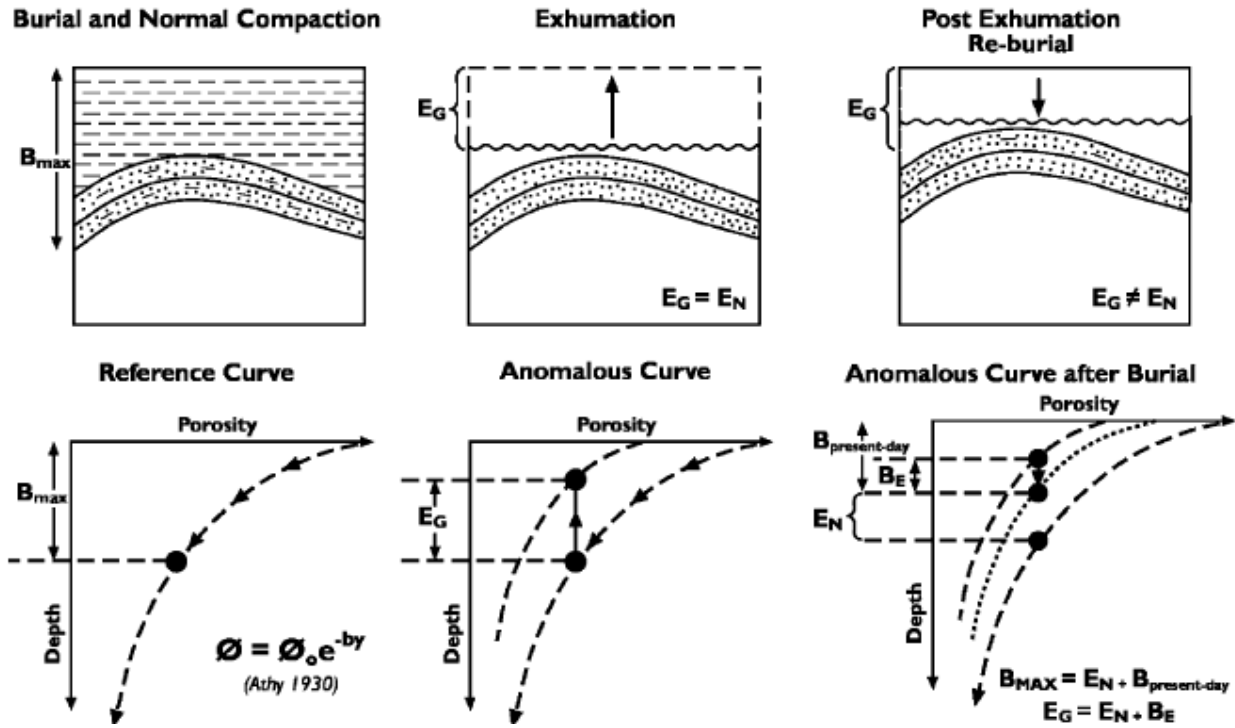


**Figure 7: Compaction based erosion determination.** As rock compress when buried, the porosity will decrease with depth. This figure shows the porosity curve with depth as it needs to adapt through time after an erosion phase.  $E_g$  = estimate of gross erosion;  $E_n$  = estimate of nett erosion;  $B$  = re-burial (from [2]).



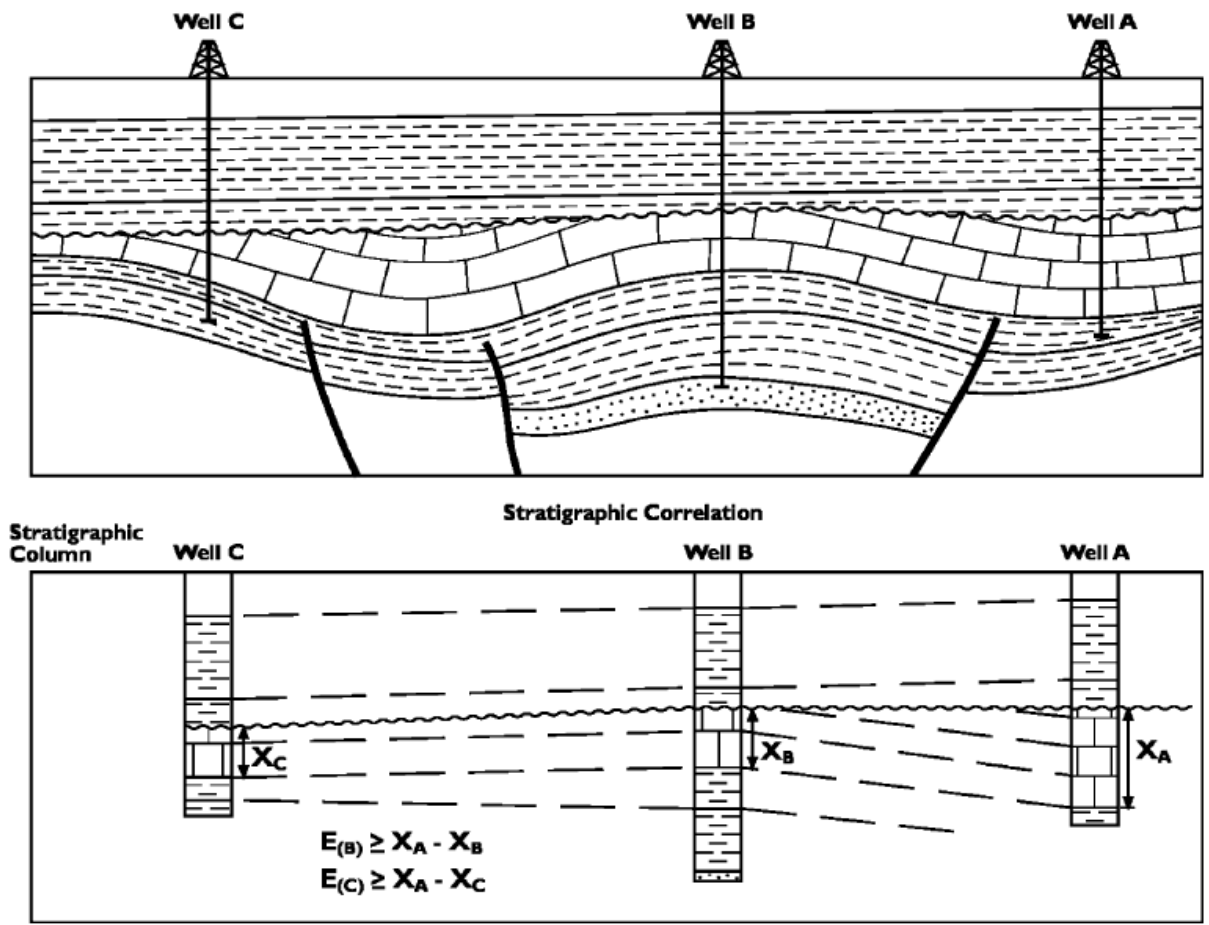


**Figure 8: Stratigraphic based erosion determination.** By stratigraphic correlation the timing and the minimum amount of erosion can be determined. Dating the oldest sediments above the unconformity and the youngest sediments below the unconformity gives the maximum timing of erosion (from [2]).

**2.6.3 Programs used**

To work with all these data and backstripping techniques, several modeling programs were used. Petrel® v. 2009.2 and PetroMod® v.11 of Schlumberger were used to determine the stratigraphic continuation through the basin and to assist in the determination of the depositional thickness per unit. ArcGIS was used to serve as reference and visualization support.

The modeling was based on some basic assumptions. These include the boundary conditions on which the model can run including, palaeo sea level, the palaeo surface temperature and the heat flow. These are discussed further on in the report and listed in Appendix C.

**Petrel® v. 2009.2**

The program Petrel® is a 3D modeling program used to visualize the 3D layer model of the studied area. This model is needed for the interpretation of the structural elements map as mostly faults are bounding the elements from each other. The model can also be used to generate 2D cross sections through the basin. This is very useful for the first estimates of thicknesses that have been removed per well, as are used in the scenario's. A well interpreted model is therefore crucial for this research.

### PetroMod® v. 11

PetroMod® is a basin modeling program, including a backstrip program, which is based on the backstripping principles specified throughout the years [2, 35, 36, 38]. It therefore can make calculations and create burial history diagrams of multi-layer backstripping processes. The program combines seismic information, well data, and the geological knowledge to model the evolution of a sedimentary basin.

An example of an input table in PetroMod® 1D can be seen in table 3. The main input in PetroMod shows not only the top and base of the stratigraphic layer, but also the period in which it is deposited and the lithology defined in percentages. The ages are based on the Geological Time Scale, 2004 [40] and the lithology are derived from the report of Van Adrichem-Boogaert and Kouwe (1993-1997) [21]. This latter variable is an important feature in the modeling as they determine the conductivity of heat through the basin.

As said before, in this report the vitrinite reflectance data is the main property used for the calculation of the erosion values. For this PetroMod® makes use of the algorithm of Burnham and Sweeney (1989) [41] to determine the temperature and maturity histories of the vitrinite reflectance data:

$$VRr = e^{(-1.6 + 3.7F)}$$

Where **VRr** is the mean vitrinite reflectance and **F** is a stoichiometric factor ranging from 0 to 0.85.

PetroMod® does not only generate burial history diagrams, but also generates depth and time related relationships, such as porosity-depth or maturity-time relationships. A best-fit relationship between the theoretical line and the measured data can be made when the geophysical measured values are also putted in. By this method the most likely burial history is determined.

One has to keep in mind, however, that the amount of erosion determined can never be proven as a true fact, but can be well grounded with this method and the use of programs.

**Table 3: Input table of PetroMod® 1D.** This table shows part of the main input for well K14-06

Main Input for K14-06									
Layer	Top [m]	Base [m]	Thick. [m]	Eroded [m]	Depo. from [Ma]	Depo. to [Ma]	Eroded from [Ma]	Eroded to [Ma]	Lithology
RNKPL	1940	2007	67		233.50	225.60			80_Shale_10_Anhy_10_Lime
RNMUU	2007	2036	29		237.00	233.50			50_Marl_50_Lime
RNMUA	2036	2062	26		238.90	237.00			100_Marl
RNMUE	2062	2152	90		240.70	238.90			75_Salt_25_Anhy
RNMUL	2152	2214	62		244.00	240.70			50_Marl_50_Lime
RNROC	2214	2292	78		245.30	244.00			50_Shale_50_Silt
RNRO1	2292	2345	53		245.60	245.30			90_Salt_10_Anhy
RNSOC	2345	2352	8		246.00	245.60			100_Shale
RBMH	2352	2372	19		247.20	246.20			75_Sand_25_Shale
RBMDL	2372	2384	13		247.60	247.20			100_Shale
RBMDL	2384	2390	6		247.80	247.60			75_Sand_25_Shale
RBMVC	2390	2458	68		248.60	247.80			34_Shale_33_Sand_33_Silt
RBMWL	2458	2550	93		249.00	248.60			100_Sandstone
RBSHR	2550	2702	152		250.00	249.00			50_Shale_25_Lime_25_Silt
RBSHM	2702	2852	150		251.00	250.00			75_Shale_25_Silt
ZEUC	2852	2880	28		251.60	251.00			100_Shale
ZEZ4H	2880	2912	32		252.44	252.20			100_Salt

## 2.7 Scenario's

### 2.7.1 Sedimentation & Erosion during the Mesozoic

Sedimentation, and also erosion, in a basin is controlled by the balance of 1) tectonic subsidence and 2) sea level fluctuations causing long term accommodation and 3) sediment influx. This balance can be disrupted when one factor suddenly changes, e.g. a tectonic event or a water level rise due to global warming.

Several major tectonic events occurred in the Dutch North Sea area, which disrupted the sedimentation in several basins, during the Mesozoic. In this study the separate influence of the Kimmerian tectonic phases, the Sub Hercynian phase and the Laramide tectonic phase are studied.

However, before this can be done the timing of the sedimentation and erosion phases have to be defined (see table 4).

#### *Timing the Kimmerian I tectonic & the Kimmerian II tectonic phases*

During the Jurassic several tectonic rifting phases influenced the area, which are responsible for the erosion of Early Cretaceous till Early Triassic sediments. These tectonic events together are known as the Kimmerian tectonic phases. Because the phases follow each other closely no clear division was made when erosion started or ended. Therefore the phases are grouped together and are discussed as two separate main events: the Early Kimmerian tectonic event (~220-170 Ma) and the Late Kimmerian tectonic event (~160-120 Ma). Note that the duration of one of the periods does not stand for the total duration of erosion that could have occurred during that period.

#### *Timing of the Sub Hercynian & the Laramide tectonic phases*

During the Late Cretaceous two other tectonic phases took place, the Sub Hercynian and the Laramide tectonic phases. In this report the dating of these two events, described by van der Molen (2004), are used. In the report of van der Molen the Sub Hercynian is thought to start having influence on the deposition at the end of the Early Campanian. This tectonic event is the cause of a major erosion phase in which sediments up to the Altena Group (Mid-Jurassic) were eroded.

The Laramide tectonic phase influenced the Late Upper Chalk Group, which started Early Danian. This tectonic phase did not have such a great influence as the prior tectonic event, as the erosion period took place for a short time and was not intense. During the Late Danian part of the area already subsided thermally and, mostly on the platforms in the Broad Fourteens basin, the top of the Chalk Group, the Ekofisk Formation, was deposited [42].

**Table 4:** Timing of erosion in the Broad Fourteens Basin

<b>Erosion phase</b>	<b>Duration (Ma)</b>
Kimmerian I	~220-170
Kimmerian II	~160-120
Sub Hercynian	78-67
Laramide	65-61,5

### **2.7.2 The Scenarios**

Erosion was estimated taking into account 3 scenarios, based on the continuation of the stratigraphic layers and their thickness. PetroMod® was used to model the scenarios. The final selection of the best scenario per well was based on the best fit curve with the measured vitrinite reflectance data. With the determination of a scenario per well, the final step is to determine an overall scenario per structural element and for the entire basin, i.e. the evolution of the Broad Fourteens Basin.

As visible on seismic, the Sub Hercynian inversion event had a major influence on the Broad Fourteens. During this time a lot of sediments were eroded from the basin. It is therefore that the scenarios present here are for the most part based on this period. Here, scenario 1 assumes an increase in thickness of the layers toward the centre, i.e. the axis, of the basin. This is a liable assumption as the Broad Fourteens basin is under continuous rifting from the Triassic till Late Cretaceous, with sedimentation in the deeper parts of the basin. Scenario 2 assumes that the stratigraphic layers continued with an equal thickness in the basin at the places where they are now removed. The last scenario, scenario 3, presumes that the inversion period and the erosion during the Late Cretaceous, started during the start of the deposition of the Chalk Group, and therefore will show thinning for the Chalk towards the centre of the basin as the centre moved up first.

A more detailed description of the scenarios is given below.

#### ***Scenario 1: Thickening towards centre***

In this model it is assumed that during every marine setting the whole basin was under water and that during lagoonal or sub-marine phases only the basin was filled with water. This thus describes the timing of sedimentation and the area where deposition occurred, but also when areas were eroded or were occupied by non-deposition.

In this scenario it is assumed that the entire Lower Chalk Group (from Cenomanian till Middle Campanian) is deposited before the Sub Hercynian tectonic phase started to have influence. After the tectonic phase (and erosion) the relative sea level had to rise again or the basin had to subside again, so the Ekofisk Formation (CKEK) could be deposited at different areas in the Broad Fourteens. The Laramide tectonic phase took place after this sedimentation, but did not have much influence on the whole area.

#### ***Scenario 2: Continuous thickness***

This scenario describes that the layers have a thickness that is continuous throughout the basin. At the places where the stratigraphic units are thought to be eroded, it will obtain the same thickness as it is measured at the nearest margin or nearest total sequence of that stratigraphic unit. Here the seismic model plays an important role in determining the initial erosion thickness.

The timing of the sedimentation and the erosion is, however, still different throughout the basin as the structural elements have moved separately from each other.

#### ***Scenario 3: Thinning towards the basin***

Sedimentation in scenario 3 is thought to decrease towards the axis of the basin. This indirectly states that also the amount of erosion will be less related to what is found at the margins.

Scenario 3 assumes that during the beginning of the Sub Hercynian inversion sediments near the NW-SE-axis of the basin were already eroding or experienced less deposition. Meanwhile, sedimentation of Chalk kept on going at the margins and on the platforms. This scenario is also apparent in the Vlieland Basin where in the centre of the basin a thin package of Chalk can be found, which increases towards the margins [27].

Unfortunately, in some cases the erosion can not be determined in detail. Here the erosion values can not be determined, as the maximum burial is reached at its present date and therefore also its maximum temperature. For some wells it can, therefore, only be said what the maximum eroded thickness could be with the present vitrinite reflectance. Per well this is also correlated with the seismic 3D model if these values are acceptable.

### 3. Results:

By using PetroMod® the resulting output of the 1D basin modeling do not represent the erosion values looked for, but modeled maturity values, porosities and temperature values. The principle of the method of PetroMod® is to intersect these modeled values with the measured values of porosity, temperature and vitrinite reflectance by changing the only left variable input, i.e. the estimated erosion. The initial erosion values are based on the 3D structural and stratigraphic model of the subsurface of the North Sea and the different scenarios made.

Below, the erosion values are discussed, giving three wells per main structural element; the Basin, the Lower Platforms and the Higher Platforms with the High. Not all the wells are discussed in this report. Ten wells have been selected and discussed in the text, which represent the structural elements or are remarkable. The burial history and the maturity diagram of these wells can be found in Appendix D. For the results of the other wells, i.e. the estimated erosion values, the reader is referred to Appendix B.

The three scenarios that are used to obtain these values are not further discussed in the results, but are taken into account when the evolution of the structural elements and the entire basin are discussed.

#### 3.1 The Basin:

For the basin element, the wells K14-01, P03-01 and P06-02 were used as representable wells to discuss the sedimentary evolution during the Mesozoic. As suggested by other studies and also by the results of the present research, erosion had much influence on this element. The Sub-Hercynian and the Laramide tectonic event eroded much of the Chalk, Rijnland, Schieland and part of the Altena Group, during the Late Cretaceous, a total time span of 14.5 Ma.

The total removal of sediments during these two events, differ quite a lot from place to place throughout the basin. This can be seen on the erosion maps of both the Chalk and the Rijnland Group. The figures show that the amount of erosion decreases from the southeastern part of the basin towards the northwestern part. This also results in the maximum difference between the southern part and the northern part represented by the two wells K14-01 and P06-02 with respectively 1000 meter and 3100 meter of eroded sediments. This represents an erosion rate between the ~70 m/Ma and the ~210 m/Ma.

It, however, has to be noted that the maximum erosion value of 3100 meter is based on one single vitrinite data point.

Another difference between the northern and the southern part of the basin can be seen in the maturity diagrams, which show an increasing maturity at 2km depth towards the southeastern part of the basin. This leads to a maximum difference of 0.64 %Ro and 1.10 %Ro, found respectively in the northern and southern part of the basin.

Just before the erosion in the basin started (~80-75 Ma), the maximum burial depth for most of the wells in the basin element was reached. Therefore a thickness map (Figure 9) has been made of total thickness at the end of the Late Cretaceous. The map includes the total sediment deposits during the Triassic till the Cretaceous before the major inversion (251-70 Ma) and shows when the wells have reached their maximum burial depth. The map shows that the southern part of the basin had the thickest package of sediment, which decreased towards the northern part. Also now the southern part of the basin reaches a

greater depth than the northern part (Figure 10). This correlates with the measured vitrinite reflectance.

A small remark is made on the stratigraphy of well P03-01. In the composite well log of this well a small layer of ~18 meter of Ekofisk has been found. This suggests that the entire Chalk at this location was removed during the Sub Hercynian, while during the Laramide tectonic phase, the area was underwater again which caused the Ekofisk Formation to be deposited. This is also suggested by de Lugt *et al.* (2003).

**Figure 9: Thickness map,** showing the total sedimentation from the Triassic till the Late Cretaceous, just before the inversion phase of the Sub Hercynian. The dots represent the wells that are selected during this research. The red colored dots are not modeled wells, used to generate the map. The age of the maximum burial depth is given in the colors blue green, representing 78 Ma and 5 Ma.

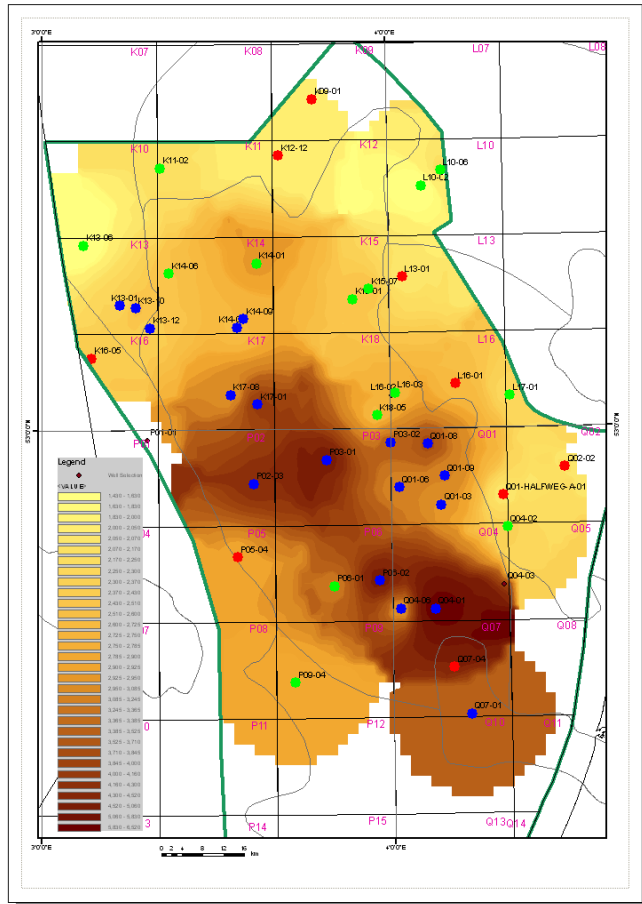
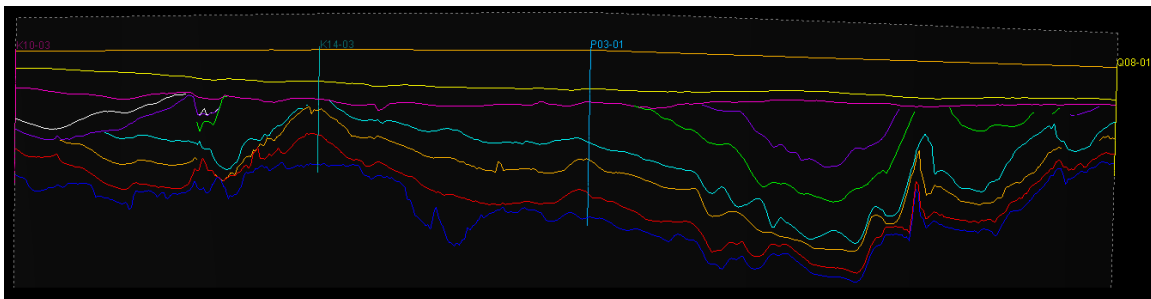


**Figure 10: Cross section D of the basin axis.** The southern part of the basin element lies ~1000 meter deeper than the northern part.



### 3.2 The Low Platforms:

The burial histories of the wells K13-01, L16-03, P09-04 and Q01-08 are used here to represent the structural evolution of the low platform elements. Results show that the wells on these elements had some minor influence of the Late Kimmerian event and were affected by the uplift and erosion during the tectonic event in the Late Cretaceous. In most of the wells a total stratigraphic sequence of the units can be found, which makes it harder to state if all is present or if some sediments are lost due to erosion or non deposition.

Modeling suggests, with a mean of 607 meters of removed sediments, that mainly the erosion of the Chalk Group controlled the evolution of these elements. This suggestion can be made when correlating it with the mean of the total amount of erosion, which is measured to be 725 meter.

The erosion rate on the platforms of respectively between the 20 and 40 m/My, is much lower when compared with the erosion rate in the basin. These values, however, are also based on the Late Kimmerian phase, which give a possible erosion period of 54.5 My in total. When only taking the Late Cretaceous event, into account the erosion rate lies between the 20 and 90 m/My, which is still lower than the erosion rate calculated for in the basin during the same time.

Comparing well L16-02 with well L16-12 shows the result of the different erosion rates. The cross section through L16-02 and L16-12 in figure 11 shows that today's Chalk base of Cenomanian age differs by 2 kilometer in depth. Because the two wells also contain the entire Chalk sequence, with a thickness of respectively ~600 and ~1700 meter, it suggests that the sedimentation of the Chalk was syn-inversion.

The vitrinite reflectance lies lower in comparison with the basin wells, respectively with values between the 0.55 %Ro and 0.65 %Ro. The variation in vitrinite reflectance of the platform elements is, however, not big and could represent a general behavior experienced by all the platform elements.

One outlier, however, is present in the dataset for the low platform wells, Q01-08. Well Q01-08 has got a relative high vitrinite reflectance datapoint at 2 kilometer, 0.73 %Ro. The surrounding wells in the area do not show this high reflectance data and show little evidence that much erosion has taken place. The model has calculated an erosion of 2300 meter of Chalk to correlate with the measured data, but this amount is questionable.

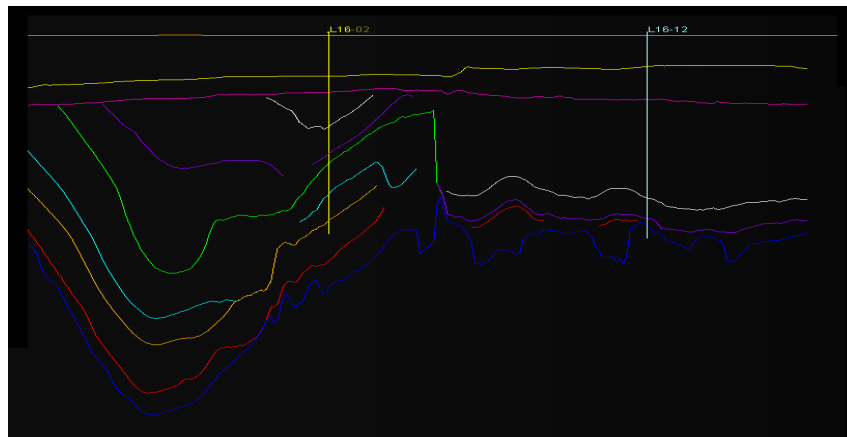


**Figure 11: Cross section E between well L16-02 and L16-12.** On this cross section the 2 kilometer uplift between the basin (to the left) and the high platform (to the right) can clearly be seen.



### 3.3 The Higher Platforms and High:

For the High Platforms and the Highs the burial history diagrams of the wells K13-06, L10-02 and L17-03 are taken to represent the evolution of this main element. The high platforms and the highs are mostly influenced by the Kimmerian I phase and for a minor part by the Sub Hercynian tectonic phase as the wells in these structural elements contain a major hiatus between the Lower Triassic and the Lower Cretaceous. Sediments between these two periods are either never deposited or eroded.

The platforms and the highs started to subside during the mid-Cretaceous, which caused the Vlieland Claystone Formation to overstep the basin margins on to the platforms and the highs [5]. Figure 12 shows two cross sections displaying this overstep.

A mean thickness of 1260 meter of the entire Chalk sequence can now be found on the platforms and highs, representing the continuing subsidence of the Late Cretaceous. The maximum thickness of Chalk can be found at well L16-12 with ~1700 meter. Any removed sediments are, therefore, mostly expected at the boundary between the Lower Triassic and Lower Cretaceous.

Wells of this element can show difficulty when modeling them to estimate the erosion. Some wells show that their maximum burial depth is at present and with it also their vitrinite reflectance of the wells. For these wells the vitrinite reflectance can not be used for estimating the erosion as they are overprinted by the present maximum, which varies between the 0.49 %Ro and the 0.59 %Ro.

Estimates of the erosion have been made by correlating the thicknesses of the units with the surroundings. A maximal estimate of 350 meter for both the removed Triassic sediments and a minor part of the Chalk Group is found in well L17-01. No Delfland has been interpreted to be deposit and eroded. There is no evidence found that suggests the deposition and is therefore interpreted as a non depositional phase.

As found in the other structural elements also in these elements wells have been found, which correspond with a higher vitrinite reflectance than expected. Well L17-03 and L10-06 both show a maturity diagram with measured data that suggests the sediments experienced a much warmer period, even during Cenozoic times. Unlike for wells on the Lower Platforms and the Basin elements, the wells on this element, show evidence of magmatism for this area, suggesting an external heat source [16].

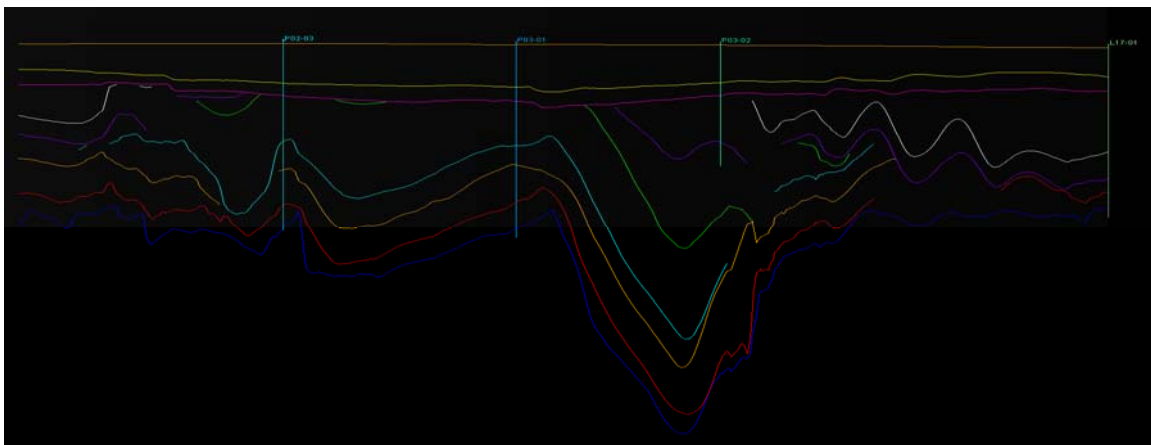


**Figure 12: Cross section A and B.** Both cross sections show the overstepping of the Rijnland Group (purple line) on the platforms from the basin. This creates a major hiatus between the Early/Late Triassic and the Early Cretaceous

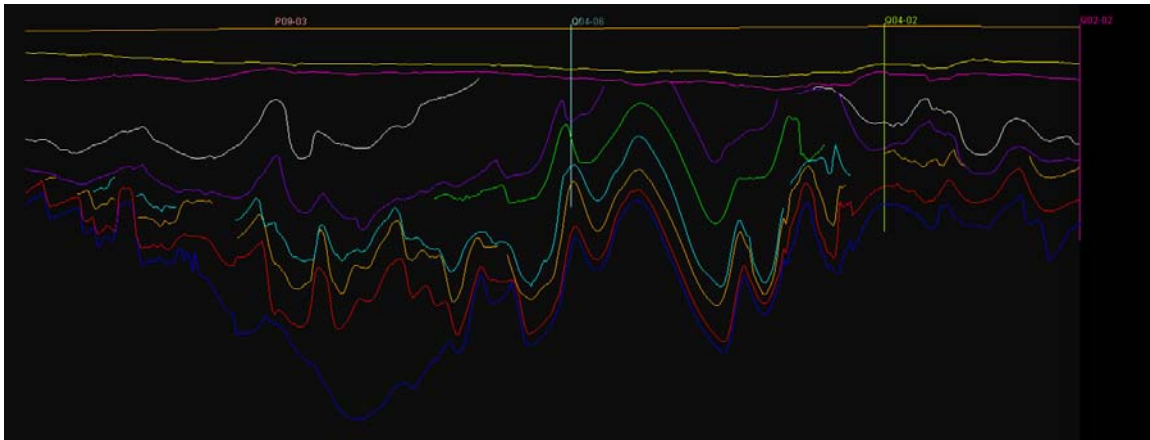


**Figure 12: continued, Cross section B**

### 3.4 The erosion maps (figure 13 and Appendix E)

Of all the erosion values obtained erosion maps are made. The figures give a good impression where the erosion concentrates and which areas are untouched by erosion of that sedimentary unit. The erosion of the Chalk Group, the Rijnland Group, the Schieland Group and the Altena Group are mostly to be found in the structural Basin element and the Low Platform elements of the Broad Fourteens, while the erosion of the Upper and Lower Germanic Trias Group are located at the High Platforms and the Highs.

The figures show the maximum erosion in red decreasing to blue, representing minimum erosion. Note that the scale of the legend differs per figure.

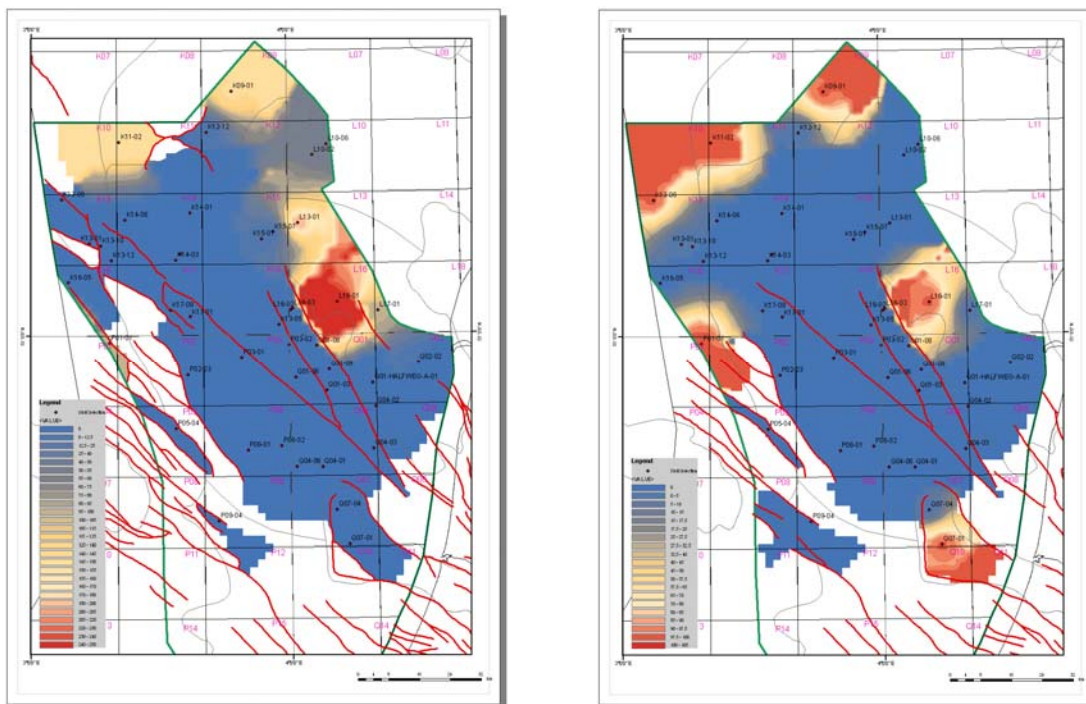


**Figure 13: Erosion maps of the six main stratigraphic units of the Mesozoic based on 30 wells and the fault systems of their age.**

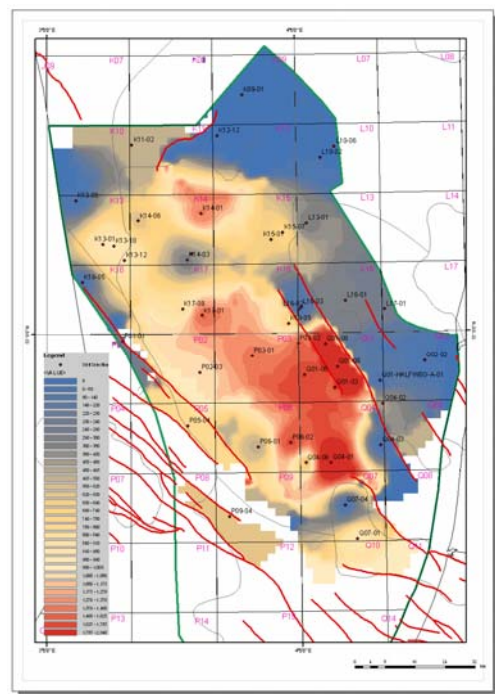
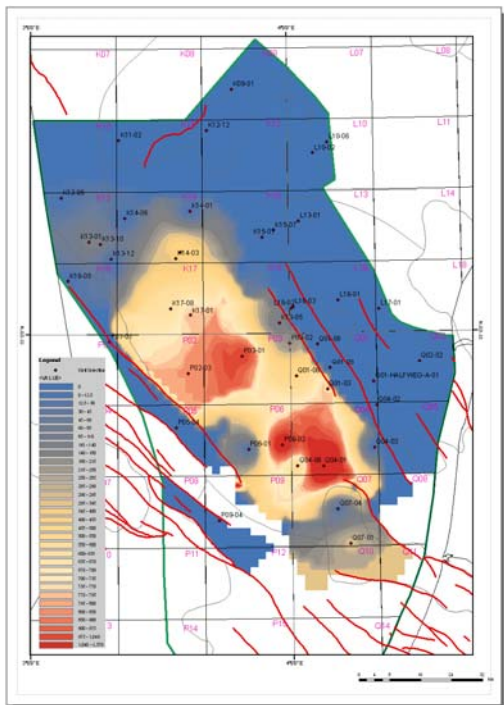
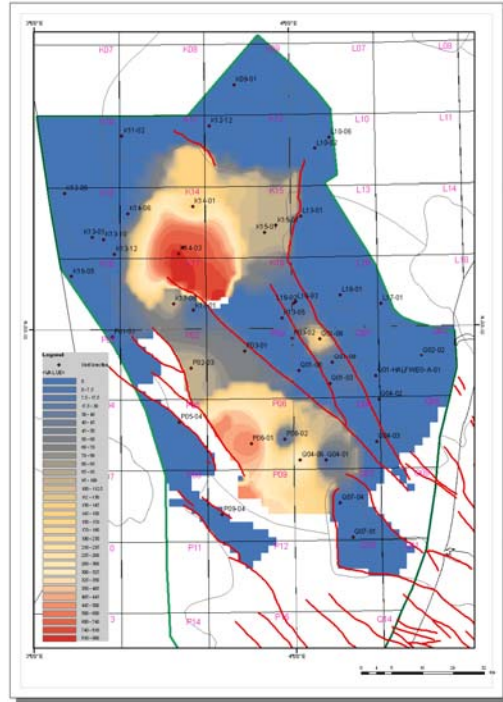
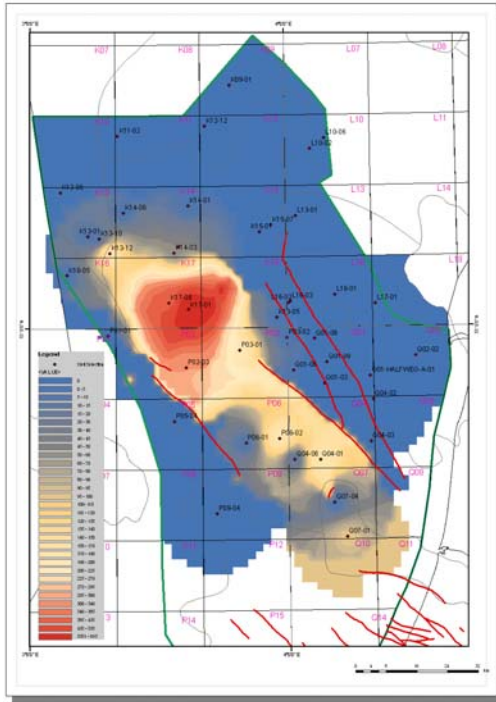


**Figure 13: Erosion maps continued**

## **4. Discussion:**

### **4.1 Structural elements**

The wells of the Broad Fourteens basin that contain the same stratigraphic sequence of the main units were grouped together and shown as the structural elements map (fig 4. and Chap. 10). This division has shown that the entire basin has experienced differential subsidence and uplift periods. However, some wells have been behaving differently in their own structural element.

This differential movement in a structural element can for example be seen by well K14-03 and Q01-08. Well K14-03 lies in the basin area, but suggests a thermal heating history the same as wells from the platform elements. Also well Q01-08 shows a different erosion value than the other wells from the same element do. Instead of showing the same general features of the platform wells, the model suggests Q01-08 has endured a basin-like evolution. It is therefore said that not only the structural elements moved vertically different from each other, but also that the wells moved vertically different within a structural element.

### **4.2 The input data**

Data for the model are crucial input and care has been put into the reliability of these data.

The data set of the vitrinite reflectance is the most important data set from this research. All values were checked on their reliability as the tables in which the geophysical values were provided, included a quality column, stating the reliability of the data.

The chosen structural elements all obtained similar vitrinite values. The few wells that however, have an outlying reflectance value inside a structural element, are either flaws in measurements, are influenced by external heating or are incorrectly put in one of the main structural elements. As the data contains a reliability column, flaws in the measurement are not taken into account. When outliers are found they thus are related to a different evolution of that area compared to their surroundings.

### **4.3 Basic Assumptions**

The basic assumptions mentioned in Chapter 2 have been adapted manually per well when needed. This has mainly been done for the sea level. The sea level was manually adapted when erosion was expected in an area and the reference sea level curve was not set on 0 meter.

The heat flow is also of great influence on the temperature and thus the maturity of the sediment and is therefore of importance for the determination of erosion. In most cases during the research more sediment was added to the interpreted removed material to increase the maximal burial and to compensate with the calculated maturity diagram. However, by increasing the heat flow the same result can be achieved.

It is expected that the heat flow is different per well, but not in such manner that it will change the maturity diagram. For this, the heat flow has to increase or decrease more than likely. Therefore, not much has been changed on the heat flow per well.

Evidence from wells inside and outside the basin have shown that heat, caused by magmatism, has influenced the sediment locally by an increase in temperature and therefore also increased the vitrinite reflectance [8, 43, 44]. It is thought that except for intrusions also the fault systems of the Broad Fourteens play a role in transporting the heat up higher and thus increasing the temperature locally.

During the research 4 well, Q01-03, Q01-08, L17-03 and L10-06, are thought to be influenced by an external heat source. The maturity diagrams show that the calculated

maturity per well does not correlate with the measured vitrinite reflectance. This suggests that somewhere sediment was lost and the entire sedimentary column was deeper in the past, or, that the temperature of the subsurface was higher. If the amount of sediment, needed to be added to correlate with the measured vitrinite reflectance is unlikely, it is chosen in this research, to give more weight to the seismic model and the correlation between wells, to come to a more correct estimate of the erosion. This results in a more balanced erosion value and therefore a better estimate for the evolution of the basin.

#### 4.4 Evolution of the Broad Fourteens Basin

The scenario's used for the modeling are a great help in quickly discovering the depositional evolution of the entire basin. As shown by the results of the modeling during the Triassic, Jurassic up to the Early Cretaceous the basin was influenced by a phase of rifting and the corresponding subsidence, causing a continuous period of sedimentation. The scenario that describes this evolution best is scenario 1, i.e. increasing sedimentation towards the centre of the basin. Scenario 3 most certainly did not take place during this period. No well modeled showed a resulting burial history that represented scenario 3.

For the Lower Cretaceous the modeled wells show both characteristics of scenario 1 as scenario 2. This was also suggested by the results of the cross section between well L16-02 and L16-12 and was also indicated in other basins [27]. It is therefore that the deposition of the sediments was not all pre-inversion.

A combined scenario has taken place in the Broad Fourteens, which is mainly due to the period of the inversion. During the Late Cretaceous sedimentation continued to take place at the margins of the structural basin, while erosion already took place from south to north over the axis of the basin (figure 14) [45].

Sedimentation during the inversion can be more grounded when depositional directions are shown running perpendicular from the axis of the basin and towards the margins of the basin.

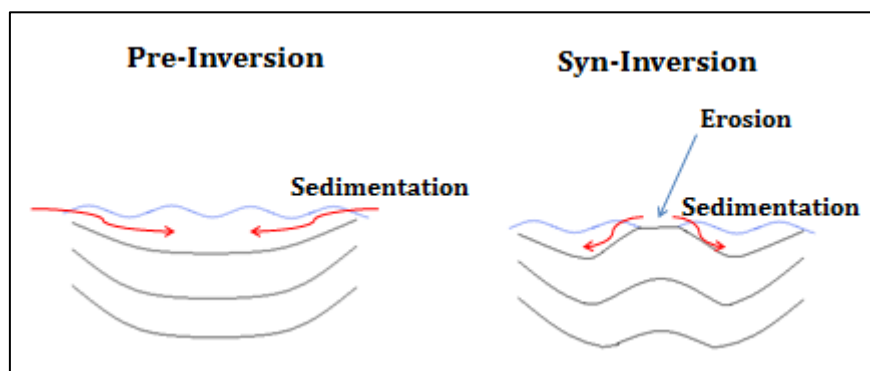


**Figure 14: Uplift, erosion and sedimentation during the Late Cretaceous inversion phase**

## **4.5 The erosion maps**

The erosion maps are made of the highest density of wells possible and show a good correlation with the general evolution of the basin, based on earlier researches [6]. Also the main faults of the Broad Fourteens are integrated in the erosion maps. Mainly between the basin and the platforms the faults play an important role as they can be seen as the boundaries between the structural elements.

When interpolating the erosion values from the wells over the entire basin, the 'influence' of the values is cut-off at these faults. This is done because on the other side of the fault another element lies and thus got other erosion values, i.e. a different evolution. These faults thus cause the erosion maps not to be smooth, but to result in maps where the erosion at some places suddenly stops.

### ***4.5.1 Erosion maps of the Lower and Upper Germanic Trias Group***

A clear difference was made between the basin part and the higher parts of the Broad Fourteens after the Early Triassic. The basin was subsiding while the margins remained around sea level. This caused a period of minor deposition to non-deposition and some erosion in the areas where platforms and highs were generated. The dispersed erosion during the Late Triassic has a strong correlation with the start of the salt doming and are therefore explained by these [46]. This control on the sediment supply causes, that Cretaceous sediments now overlie Lower Triassic or even Zechstein sediments at the higher Platforms and Highs.

For several areas on the high platforms and the highs no erosion has been interpreted using the vitrinite data. Because no maturity data is available from these wells and erosion can not be proven by seismic interpretation no erosion values can be given to these areas. Using other techniques for the determination of erosion could help to obtain values for these areas.

### ***4.5.2 Erosion maps of the Altena and Schieland Group***

The erosion maps of the Altena and Schieland Group show that not much erosion has taken place during the Jurassic. Only in the basin element erosion occurred during this time. Noticeable is that the most erosion took place in the northern part of the basin element. This is probably due to a more subsided southern part of the basin.

The absence of sediment on the platforms and the highs and the thinning towards the margins suggest that there was a period of non-deposition and minor erosion or that the entire Upper Triassic and Jurassic were eroded during the Kimmerian phase. Because no further evidence has been found that possible sedimentation has occurred at the higher platforms and highs, and also the vitrinite reflectance data can not determine this, it is interpreted as a non depositional phase. This is in contrast with other reports [5], which state that due to deep marine Jurassic sediments found in the basin, the platforms and highs also should have lain under water. This then suggest that sedimentation has occurred on the platforms and thus also have been eroded during the Late Kimmerian phase.

At this point both statements can not be proven. A detailed sedimentological study from Jurassic sediments at the margins of the basin should point out if the sediments thin out, or that erosion has occurred during that time. This can then be correlated with the platforms and the highs.

### ***4.5.3 Erosion maps of the Rijnland and Chalk Group***

The erosion maps of the Rijnland and Chalk Group and also the total thickness map of the Broad Fourteens show that the uplift and the erosion of the Late Cretaceous started in the southern part of the basin. The effect of erosion then moved over the axis of the basin in NW

direction. Meanwhile sediments were still deposited at the margins of the basin, while also these margins were eventually inverted and started to erode.

By the amount of erosion and the area it influenced it can be stated that the Sub Hercynian and Laramide tectonic events have had the most influence on the overall structure of the basin.

The maximum amounts of erosion, and thus also the amount of deposited sediment determined for the basin element, are questionable. The thickness of Chalk estimated to be deposited in the basin exceeds the amount of the total package of Chalk on the higher platforms, while these are not influenced by erosion and the basin erosion started Early Campanian. However, the PetroMod model needs this amount of sediment to fit with the measured vitrinite reflectance data.

Several factors are optional that can cause this difference. These include: a higher heat flow in these parts of the basin, the sediments were reworked, or the sediment was indeed that thick but moved also in a lateral sense. Other research has to be done to answer this.

#### **4.5.4 Comparing with others**

The obtained data from this research can be compared with the results from other reports. Doing so there is a close resemblance between the data.

**Erosion values:** The obtained erosion values in this report can be compared with the values generated by Nalpas *et al.* (1995) [6]. In this report the erosion map made is based on maturation modeling calibrated by vitrinite reflectance measurements and sonic velocities of the Lower Triassic shale. When compared with the Early and Late Cretaceous erosion map in the presented report it can be seen that the maps show the same distribution of erosion and also lie in the same range of amount of erosion. They both suggest that local more than 3000 meter of sediments have been removed, which can also be validated by others [15, 26, 47-49].

In the report of Verweij (2003) [5] this maximum amount of erosion is, however, put in doubt. Here the amount of sediments eroded was estimated by multiplying the time of sedimentation times the sedimentation rate based on one well. With this method a total erosion value for P06-02 during the Sub Hercynian and Laramide period is determined on 2528 meter. However, the Altena Group is, according to Verweij, partly eroded during the Late Kimmerian period and not during the Sub Hercynian and Laramide period. When also taking the Altena Group into account a total package of 3092 m (2528 + 564 m) is obtained. This is almost equal to the erosion value determined during this report.

**The timing:** The timing of mainly the erosion phase at the Late Cretaceous, as discussed in Hayward & Graham (1989) [45] can be confirmed by the reports of Huyghe (1995), Nalpas (1995), van der Molen (2003) and this study. Hayward and Graham they show with a detailed study of unconformities that the onset of structural inversion, in the southern part of the basin, began as early as the end of the Turonian. The major thrust faults in the northern part of the basin, controlled by the Zechstein evaporites, were generated during the Late Coniacian to Early Santonian. This is in agreement with the evolution reconstruction presented in this report, based on the calculated erosion values and erosion rates.

**Thickness:** The comparison of the two thickness maps presented in this report and in Nalpas (1995) shows a relatively same thickness map for the initial Mesozoic sediments. Only a small difference can be found stating the centre of the maximum thickness, which lies on the map of this report more towards the south relative to the map of Nalpas (1995).

Overall the obtained data during this research are not surprisingly different with other studies on this area. It can, however, be stated that due to the more and different data the erosion maps presented here are more accurate.



## **5. Conclusions:**

During this research erosion maps of the Mesozoic have been made using, well log information, a 3D seismic model and geophysical data of some core data 30 cores (figure 13).

### ***Sedimentation***

Reconstruction of the basin element of the Broad Fourteens Basin shows that the stratigraphic units were continuously deposited before they were eroded during the Late Cretaceous.

On the highs and the higher platforms sediments of the Upper Triassic and the Jurassic is very thin or absent. This is due to erosion and non-deposition during the Early Kimmerian. During the Early Cretaceous, sedimentation started again on these higher structures with the deposition of the Rijnland Group, as can be seen on the cross/sections (figure 11 & 12). Due to a relative subsidence of the higher parts of the basin during overall uplift of the basin the thickest package of Chalk occur at the highs.

The overall sedimentation during the Mesozoic shows a clear thinning of the units from the basin towards the platforms.

### ***The Method***

The reliability of the geophysical data from core measurements can be tested by comparing it with the 3D seismic model. Using this method, the model shows the structural style of the region, such as fault systems and small structural elements, in which the stratigraphy and the determined erosion can be related. The erosion method, based on mainly vitrinite reflectance is a quick and a, in general, reliable method.

### ***Erosion***

Erosion varies throughout the Broad Fourteens. These variations illustrate the differential subsidence and uplift of the internal structure of the basin during the tectonic phases. Most of the erosion is found in the basin element, which is caused by the inversion period during Late Cretaceous. The maximum total erosion of 3100 meter is found in the basin, in well P06-02. Also other wells in the basin show erosion values more than 2000 m.

A heat flow model of the Broad Fourteens Basin is needed to give more accuracy in the determined erosion values.

### ***The Maps***

This detailed study of the structure of the basin show that erosion values can differ sudden over a small scale. This is mostly seen at the boundaries of the chosen structural elements. Here the added faults on the erosion maps play an important role. Because the present hydrocarbons systems can be found near the boundaries of these structural elements this method can be very useful in future exploration.

The method of estimating the erosion is, due to the 3D aspect, of higher accuracy and can therefore benefit in making better palaeo reconstructions of the area.

## 6. Recommendations:

-In this research most of the erosion estimates are based on vitrinite reflectance data. It is recommended, in future research, to use more different erosion determination methods to increase the erosion estimation, and thus the erosion maps. A usable method is, for example, the sonic velocity method.

It is also advised, when making initial erosion estimations, to bear in mind the sedimentological environment of the region. Doing so, more accurate and reliable erosion values will be determined for, as example, the platforms and the highs, during the Jurassic.

-Because the present method does not take into account lateral displacements it is suggested for further research to use a structural modeling program such as 'Move 3D'. This program can reconstruct and backstrip the basin layer by layer. This is very useful for the inspection of chosen values for removed sediment, such as the maximum erosion values in the basin element.

-A research after the influence of external heat due to magmatism, thinning of the crust and/or heat transport through faults will result in a better heat flow of the basin. This will lead to more accuracy in erosion values determination and thus the reconstruction of the palaeo evolution.

## 7. Acknowledgements:

At the end of this research there are some people who helped me during this research and I would like to thank. First of all I like to thank Johan ten Veen for guiding me through the process and showing me the essence and the contentment of determining the sediment control. Also Poppe de Boer, my supervisor from the UU, is thanked for his quick reviews, ideas and useful comments.

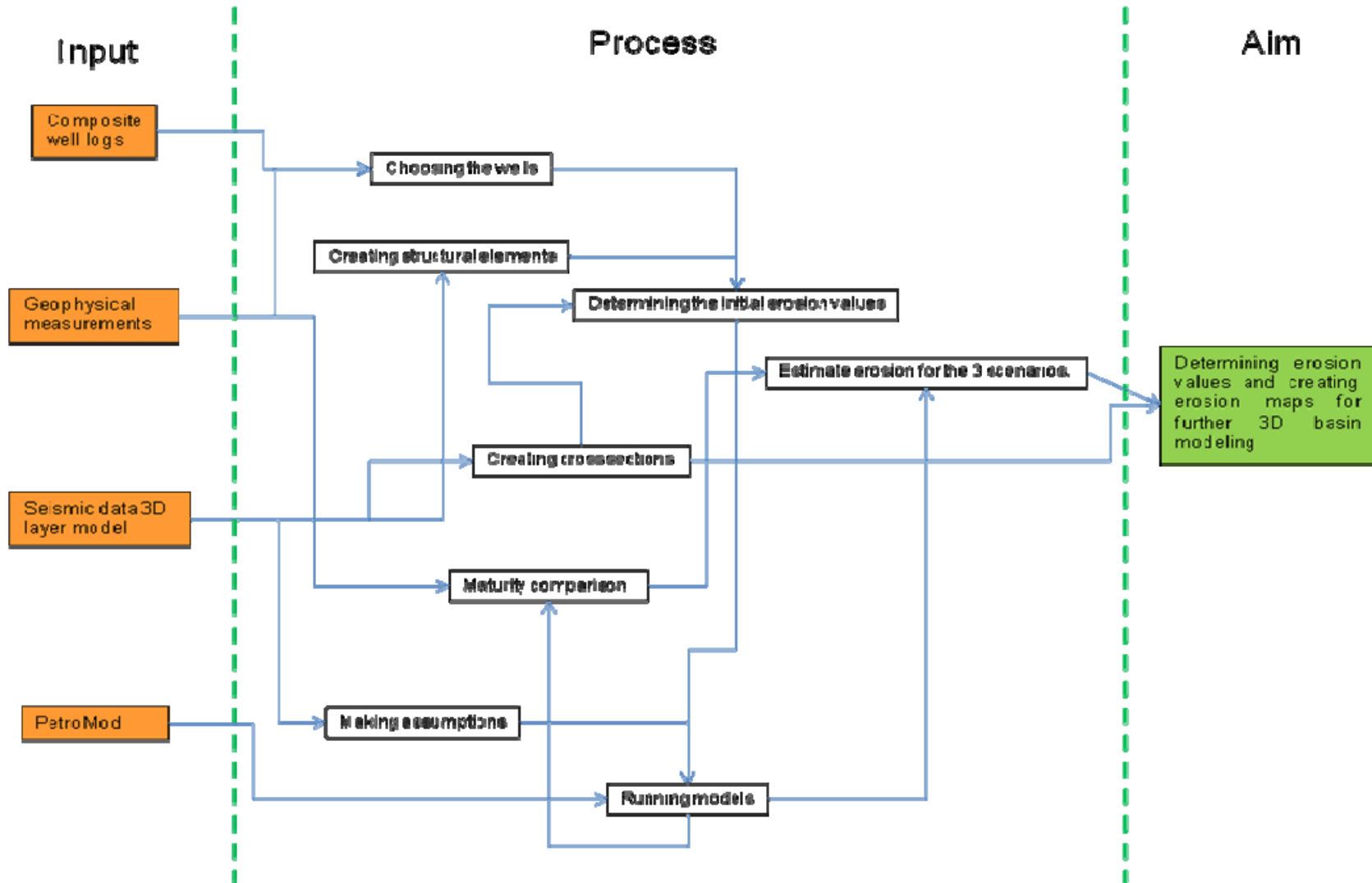
Of the Basin Modeling Group of TNO, I would especially thank Hanneke Verweij and Rader Abdul Fattah for their cooperation during the research period, thinking along and being enthusiastic about the results I made.

Also Nora Witmans and Ed Duin are thanked for the discussion and ideas we shared.

I would like to thank all my roommates: Johan ten Veen, Henk Kombrink, Hans Doornenbal, Nora Witmans, Maryke den Dulk, Tom van der Putte and Jenny Hettelaar for their good company and their beautiful humor. I had a very good time: *'Keurig!'*

And at last, my fellow students at TNO: Thijs Boxem, Pieter Vernooij and Mart Zijp, for the many, many coffee breaks.

## 8. Appendix: A. Workflow



## B. Well selection & Erosion values

Wells		K14-06	K13-12	K14-03	K14-09	K17-08	P02-03	P03-01	P03-02	Q01-09	Q01-03	Q01-06	K18-05	
Structural Element		Basin 1	Basin 1	Basin 2	Basin 2	Basin 2	Basin 2	Basin 2	Basin 3.1	Basin 3.1	Basin 3.1	Basin 3.1	Basin 3.2	
Official name Nomenclator	Code	Cross sections												
		E						C2		B				
Upper North Sea Group	NU	Eroded (m)												
Upper North Sea Group	NU	Present thickness (m)	648	609	727	902	789	1043	1097	1014	898	1004	994	778.2
Upper North Sea Group	NU	Original thickness (m)	648	609	727	902	789	1043	1097	1014	898	1004	994	778.2
Middle North Sea Group	NM	Eroded (m)												
Middle North Sea Group	NM	Present thickness (m)	22	0	42	70	33	0	0	0	0	0	0	22.7
Middle North Sea Group	NM	Original thickness (m)	22	0	42	70	33	0	0	0	0	0	0	22.7
Lower North Sea Group	NL	Eroded (m)												
Lower North Sea Group	NL	Present thickness (m)	355	272	350	451	289,5	0	0	0	0	0	0	265.6
Lower North Sea Group	NL	Original thickness (m)	355	272	350	451	289,5	0	0	0	0	0	0	265.6
Chalk	CK	Eroded (m)	600	1000	600	500	800	1000	1400	1500	2000	1600	1500	700
Chalk	CK	Present thickness (m)	131	70	0	0	12	22	19	0	3	0	0	0
Chalk	CK	Original thickness (m)	731	1070	600	500	812	1022	1419	1500	2003	1600	1500	700
Rijnland Group	KN	Eroded (m)			300	500	600	800		200		800	500	150
Rijnland Group	KN	Present thickness (m)	183	168	0	0	0	0	1050	976	603	342.5	727	1007.5
Rijnland Group	KN	Original thickness (m)	183	168	300	500	600	800	1050	1176	603	1142.5	1227	1157.5
Niedersaksen Group	SK	Eroded (m)												
Niedersaksen Group	SK	Present thickness (m)	0	0	0	0	0	0	0	0	0	0	0	0
Niedersaksen Group	SK	Original thickness (m)	0	0	0	0	0	0	0	0	0	0	0	0
Delfland Group	SL	Eroded (m)		200	50	50	400	300						
Delfland Group	SL	Present thickness (m)	0	0	0	0	0	200	825	187	849.5	457	573	
Delfland Group	SL	Original thickness (m)	0	200	50	50	400	300	200	825	187	049.5	457	573
Altena Group	AT	Eroded (m)			900	700	100	100	50					
Altena Group	AT	Present thickness (m)	418	154	0	146	228	860	884	0	377	219	0	109
Altena Group	AT	Original thickness (m)	418	154	900	846	328	960	934	0	377	219	0	109
Upper Germanic Trias Group	RN	Eroded (m)												
Upper Germanic Trias Group	RN	Present thickness (m)	595	507	412	263	336	570	543	0	0	0	0	0
Upper Germanic Trias Group	RN	Original thickness (m)	595	507	412	263	336	570	543	0	0	0	0	0
Lower Germanic Trias Group	RB	Eroded (m)												
Lower Germanic Trias Group	RB	Present thickness (m)	500	240	469	571	474	620	543	0	0	0	0	0
Lower Germanic Trias Group	RB	Original thickness (m)	500	240	469	571	474	620	543	0	0	0	0	0
Zechstein Group	ZE	Eroded (m)												
Zechstein Group	ZE	Present thickness (m)	179	0	657	298	689	390	526	0	0	0	0	0
Zechstein Group	ZE	Original thickness (m)	179	0	657	298	689	390	526	0	0	0	0	0
Upper Rotliegend Group	RO	Eroded (m)												
Upper Rotliegend Group	RO	Present thickness (m)	123	0	217	268	222,5	160	137	0	0	0	0	0
Upper Rotliegend Group	RO	Original thickness (m)	123	0	217	268	222,5	160	137	0	0	0	0	0
Lower Rotliegend Group	RV	Eroded (m)												
Lower Rotliegend Group	RV	Present thickness (m)	0	0	0	0	0	0	0	0	0	0	0	0
Lower Rotliegend Group	RV	Original thickness (m)	0	0	0	0	0	0	0	0	0	0	0	0
Limburg Group	DC	Eroded (m)												
Limburg Group	DC	Present thickness (m)	73	0	35	47	26,5	0	0	0	0	0	0	0
Limburg Group	DC	Original thickness (m)	73	0	35	47	26,5	0	0	0	0	0	0	0
<b>Totale erosion thickness</b>			<b>600</b>	<b>1200</b>	<b>1850</b>	<b>1750</b>	<b>1900</b>	<b>2200</b>	<b>2700</b>	<b>1700</b>	<b>2000</b>	<b>2400</b>	<b>2000</b>	<b>950</b>

<b>Totale present thickness</b>	<b>3227</b>	<b>2020</b>	<b>2909</b>	<b>3016</b>	<b>3099,5</b>	<b>3665</b>	<b>3749</b>	<b>2815</b>	<b>2068</b>	<b>2415</b>	<b>2178</b>	<b>2756</b>
<b>Totale original thickness</b>	<b>3827</b>	<b>3220</b>	<b>4759</b>	<b>4766</b>	<b>4999,5</b>	<b>5865</b>	<b>6449</b>	<b>4515</b>	<b>4068</b>	<b>4815</b>	<b>4178</b>	<b>3706</b>

		Wells	Q04-06	Q07-01	Q10-02	P06-02	K13-06	L10-02	L10-06	L17-01	L16-03
		Structural Element	Basin 3.2	Basin 4	Basin 4	Basin 5	High Platform (1)	High Platform (2)	High Platform (2)	High Platform (2)	Low Platform (LJ)
Official name Nomenclator	Code	Cross sections	A			B				B	
Upper North Sea Group	NU	<b>Eroded (m)</b>									
Upper North Sea Group	NU	<b>Present thickness (m)</b>	741	711	624	785	870	1250	1447	928,5	775
Upper North Sea Group	NU	<b>Original thickness (m)</b>	741	711	624	785	870	1250	1447	928,5	775
Middle North Sea Group	NM	<b>Eroded (m)</b>									
Middle North Sea Group	NM	<b>Present thickness (m)</b>	9	0	74	29	0	0	0	0	0
Middle North Sea Group	NM	<b>Original thickness (m)</b>	9	0	74	29	0	0	0	0	0
Lower North Sea Group	NL	<b>Eroded (m)</b>									
Lower North Sea Group	NL	<b>Present thickness (m)</b>	137	0	0	139	0	0	0	0	259,5
Lower North Sea Group	NL	<b>Original thickness (m)</b>	137	0	0	139	0	0	0	0	259,5
Chalk	CK	<b>Eroded (m)</b>	500	1400		1700				250	100
Chalk	CK	<b>Present thickness (m)</b>	0		0	0	821	1319	1314	1162,5	458,5
Chalk	CK	<b>Original thickness (m)</b>	500	1400	0	1700	821	1319	1314	1412,5	558,5
Rijnland Group	KN	<b>Eroded (m)</b>	500	300		1200					
Rijnland Group	KN	<b>Present thickness (m)</b>	521	999	935	0	253	61	125,5	448	454
Rijnland Group	KN	<b>Original thickness (m)</b>	1021	1299	935	1200	253	61	125,5	448	454
Niedersaksen Group	SK	<b>Eroded (m)</b>				200					
Niedersaksen Group	SK	<b>Present thickness (m)</b>	0	0	0	0	0	0	0	0	0
Niedersaksen Group	SK	<b>Original thickness (m)</b>	0	0	0	200	0	0	0	0	0
Delfland Group	SL	<b>Eroded (m)</b>		100							
Delfland Group	SL	<b>Present thickness (m)</b>	446	0	0	672	0	0	0	0	107,5
Delfland Group	SL	<b>Original thickness (m)</b>	446	100	0	672	0	0	0	0	107,5
Altena Group	AT	<b>Eroded (m)</b>	350								
Altena Group	AT	<b>Present thickness (m)</b>	0	0	0	236	0	0	0	0	455,5
Altena Group	AT	<b>Original thickness (m)</b>	350	0	0	236	0	0	0	0	455,5
Upper Germanic Trias Group	RN	<b>Eroded (m)</b>		100			100		200		
Upper Germanic Trias Group	RN	<b>Present thickness (m)</b>	109	130	187	404	0	0	163,5	0	540
Upper Germanic Trias Group	RN	<b>Original thickness (m)</b>	109	230	187	404	100	0	363,5	0	540
Lower Germanic Trias Group	RB	<b>Eroded (m)</b>						50	50	100	
Lower Germanic Trias Group	RB	<b>Present thickness (m)</b>	438	360	360	488	259	0	512	264	517
Lower Germanic Trias Group	RB	<b>Original thickness (m)</b>	438	360	360	488	259	50	562	364	517
Zechstein Group	ZE	<b>Eroded (m)</b>						250			
Zechstein Group	ZE	<b>Present thickness (m)</b>	276	175	178	305	89	881,5	190	337	568
Zechstein Group	ZE	<b>Original thickness (m)</b>	276	175	178	305	89	1131,5	190	337	568
Upper Rotliegend Group	RO	<b>Eroded (m)</b>									
Upper Rotliegend Group	RO	<b>Present thickness (m)</b>	209	193	0	90	111	291,5	307	192	153
Upper Rotliegend Group	RO	<b>Original thickness (m)</b>	209	193	0	90	111	291,5	307	192	153
Lower Rotliegend Group	RV	<b>Eroded (m)</b>									
Lower Rotliegend Group	RV	<b>Present thickness (m)</b>	0	0	0	0	0	0	60	0	0
Lower Rotliegend Group	RV	<b>Original thickness (m)</b>	0	0	0	0	0	0	60	0	0
Limburg Group	DC	<b>Eroded (m)</b>									
Limburg Group	DC	<b>Present thickness (m)</b>	121	32	0	0	137	22	0	0	0
Limburg Group	DC	<b>Original thickness (m)</b>	121	32	0	0	137	22	0	0	0
<b>Totale erosion thickness</b>			<b>1350</b>	<b>1900</b>	<b>0</b>	<b>3100</b>	<b>100</b>	<b>300</b>	<b>250</b>	<b>350</b>	<b>100</b>

<b>Totale present thickness</b>	<b>3007</b>	<b>2600</b>	<b>2358</b>	<b>3148</b>	<b>2540</b>	<b>3825</b>	<b>4119</b>	<b>3332</b>	<b>4288</b>
<b>Totale original thickness</b>	<b>4350</b>	<b>4500</b>	<b>2358</b>	<b>6248</b>	<b>2640</b>	<b>4125</b>	<b>4369</b>	<b>3682</b>	<b>4388</b>

		Wells	K15-07	K13-01	K13-10	P09-04	Q01-Halfweg-A-01	Q01-08	Q04-02	K14-01	Q08-01
		Structural Element	Low Platform (LJ)	Low Platform (2)	Low Platform (2)	Low Platform (3)	Low Platform (4)	Low Platform (LJ)	Low Platform (4 ?)	Rest	Rest
Official name Nomenclator	Code	Cross sections									
Upper North Sea Group	NU	Eroded (m)									
Upper North Sea Group	NU	Present thickness (m)	747,5	788,5	605	618	923,5	930	637	958	821
Upper North Sea Group	NU	Original thickness (m)	747,5	788,5	605	618	923,5	930	637	958	821
Middle North Sea Group	NM	Eroded (m)									
Middle North Sea Group	NM	Present thickness (m)	57,5	0	0	0	0	0	0	0	54
Middle North Sea Group	NM	Original thickness (m)	57,5	0	0	0	0	0	0	0	54
Lower North Sea Group	NL	Eroded (m)									
Lower North Sea Group	NL	Present thickness (m)	475	0	288,5	108	0	0	158	0	39
Lower North Sea Group	NL	Original thickness (m)	475	0	288,5	108	0	0	158	0	39
Chalk	CK	Eroded (m)	800	1000	1000	800	50	2300	500	500	1500
Chalk	CK	Present thickness (m)	277,5	81	172,5	755	1021,5	290	663	290	0
Chalk	CK	Original thickness (m)	1077,5	1081	1172,5	1555	1071,5	2590	1163	790	1500
Rijnland Group	KN	Eroded (m)		120	100					350	800
Rijnland Group	KN	Present thickness (m)	413,5	215,5	361	1174	257	423	546	423	0
Rijnland Group	KN	Original thickness (m)	413,5	335,5	461	1174	257	423	546	773	800
Niedersaksen Group	SK	Eroded (m)									
Niedersaksen Group	SK	Present thickness (m)	0	0	0	0	0	0	0	0	0
Niedersaksen Group	SK	Original thickness (m)	0	0	0	0	0	0	0	0	0
Delftland Group	SL	Eroded (m)									200
Delftland Group	SL	Present thickness (m)	166,5	0	0	0	0	394	0	394	0
Delftland Group	SL	Original thickness (m)	166,5	0	0	0	0	394	0	394	200
Altena Group	AT	Eroded (m)	100					150		150	
Altena Group	AT	Present thickness (m)	200,5	0	0	28	0	299	0	269	463
Altena Group	AT	Original thickness (m)	300,5	0	0	28	0	449	0	419	463
Upper Germanic Trias Group	RN	Eroded (m)									
Upper Germanic Trias Group	RN	Present thickness (m)	372	317	412,5	0	140,5	0	165	30	266
Upper Germanic Trias Group	RN	Original thickness (m)	372	317	412,5	0	140,5	0	165	30	266
Lower Germanic Trias Group	RB	Eroded (m)									
Lower Germanic Trias Group	RB	Present thickness (m)	113	520	430,5	0	466,5	0	425	0	330
Lower Germanic Trias Group	RB	Original thickness (m)	113	520	430,5	0	466,5	0	425	0	330
Zechstein Group	ZE	Eroded (m)									
Zechstein Group	ZE	Present thickness (m)	904	577	24	0	344	0	430	0	243
Zechstein Group	ZE	Original thickness (m)	904	577	24	0	344	0	430	0	243
Upper Rotliegend Group	RO	Eroded (m)									
Upper Rotliegend Group	RO	Present thickness (m)	297	180	231	0	325	0	351	0	272
Upper Rotliegend Group	RO	Original thickness (m)	297	180	231	0	325	0	351	0	272
Lower Rotliegend Group	RV	Eroded (m)									
Lower Rotliegend Group	RV	Present thickness (m)	0	0	0	0	0	0	0	0	0
Lower Rotliegend Group	RV	Original thickness (m)	0	0	0	0	0	0	0	0	0
Limburg Group	DC	Eroded (m)									
Limburg Group	DC	Present thickness (m)	41	3	23	0	93,6	0	75	0	33
Limburg Group	DC	Original thickness (m)	41	3	23	0	93,6	0	75	0	33
<b>Totale erosion thickness</b>			<b>900</b>	<b>1120</b>	<b>1100</b>	<b>800</b>	<b>50</b>	<b>2450</b>	<b>500</b>	<b>1000</b>	<b>2500</b>

---

<i>Totale present thickness</i>	4065	2682	2548	2683	3571,6	2336	3450	2364	2521
<i>Totale original thickness</i>	4965	3802	3648	3483	3621,6	4786	3950	3364	5021

### C. Boundary Conditions:

In PetroMod® several boundary conditions are used to further determine the erosion values per well. These boundary conditions are the Palaeo Water Depth, the Palaeo Surface Temperature and the Heat Flow. During the research the values of the two wells K14-02 and P06-04 have been used. The values of each condition for both wells are shown here in a table.

#### *Palaeo Water Depth*

---

##### *Well K14-02*

Year	Mean				
0.00	30.00	170.10	98.20	247.20	17.00
3.10	150.00	170.90	117.40	247.60	22.29
11.70	50.00	171.00	151.30	247.80	18.79
19.90	25.30	177.60	184.20	248.60	11.70
28.00	0.00	183.00	151.80	249.00	15.80
36.00	50.00	199.60	32.30	250.00	18.20
38.60	61.10	203.60	5.00	251.00	17.00
42.10	86.00	207.20	8.70	251.60	18.20
50.00	110.90	211.40	14.40	252.40	13.09
53.00	120.40	213.60	21.40	253.60	15.29
56.50	135.10	220.10	17.00	258.00	15.09
60.50	143.40	221.50	18.80	262.00	8.70
65.00	24.00	225.60	30.60	263.00	6.80
83.00	0.00	233.50	47.90	267.50	1.70
99.00	200.00	237.00	52.00	275.00	0.00
140.20	3.00	238.90	51.10	290.00	0.00
152.00	0.00	240.70	51.10	308.70	0.00
164.70	34.60	244.00	12.60	311.00	0.00
165.40	42.70	245.50	15.01	312.30	6.50
168.20	54.30	246.00	11.70	313.10	9.40
		246.20	13.50	313.60	0.00

##### *Well P06-04*

Year	Mean				
0	0	121	150	242	10
1.64	50	130	40	245	10
5.2	200	140.7	0	250.5	20
10	50	154	0	255	20
23.3	10	158	0	258	10
35	50	167	50	268.8	0
40	80	173	200	290	0
60.5	150	180	180	300	0
65	20	204	0	307	0
70.6	0	212	20	309	0
80	0	220	20	313	5
83.5	50	231	50	328	50
97	200	240	50	350	50
		241	30		



**Surface Water Temperature**

**Well K14-02**

Year	Mean				
0.00	9.78	170.10	19.38	247.20	24.66
3.10	5.00	170.90	18.54	247.60	24.77
11.70	19.83	171.00	17.99	247.80	24.55
19.90	14.60	177.60	16.75	248.60	24.72
28.00	14.66	183.00	47.46	249.00	24.51
36.00	16.95	199.60	19.96	250.00	24.15
38.60	16.81	203.60	20.55	251.00	24.78
42.10	16.27	207.20	20.47	251.60	23.91
50.00	19.36	211.40	20.46	252.40	23.87
53.00	18.77	213.60	19.84	253.60	24.15
56.50	16.96	220.10	21.62	258.00	23.67
60.50	16.29	221.50	21.52	262.00	23.72
65.00	19.41	225.60	22.26	263.00	23.91
85.00	21.90	233.50	22.99	267.50	23.78
99.00	17.46	237.00	23.02	275.00	23.80
140.20	23.91	238.90	22.96	290.00	24.00
152.00	23.45	240.70	23.09	308.70	24.00
164.70	21.47	244.00	25.18	311.00	24.07
165.40	20.97	245.50	24.43	312.30	23.42
168.20	20.48	246.00	25.25	313.10	23.24
		246.20	24.76	313.60	23.50

**Well P06-04**

Year	Mean				
0	10	26	14.5	167	22.17
0.02	0	31	15	173	21.37
0.8	0	35	18	212	20.3
1.5	3	39	18	231	24.15
2.5	5	44.5	18	240	24.76
3	10	51	22.4	241	25.68
3.3	14	53	21.6	242	25.58
6.8	14	54.3	23	245	25.4
7.7	18	54.7	25	250.5	24.76
8.3	21	55.6	27	255	24.13
14	21	55.7	25	258	24
14.2	20	58.5	18	268.8	23.68
15.2	20	60	19.3	270	23.54
15.6	21	64	20	300	25
16.5	21	70.6	19.84	307	24
19.2	15	83.5	21.64	328	23
21.5	15	97	22.6	350	25
22	17	121	22.88		
24.5	13.5	140.7	24		
		156	23.49		

**Heat Flow**

---

**Well K14-02**

Year	Mean
0.00	53.50
3.10	57.63
11.70	54.42
19.90	56.14
28.00	54.85
36.00	55.52
38.60	56.32
42.10	56.78
50.00	56.52
53.00	56.36
56.50	56.11
60.50	56.57
65.00	57.62
85.00	58.26
99.00	59.94
140.20	65.45
152.00	52.99
164.70	54.29
165.40	54.66
168.20	55.18

170.10	55.85
170.90	56.19
171.00	56.33
177.60	56.64
183.00	56.52
199.60	58.04
203.60	58.59
207.20	58.81
211.40	59.03
213.60	59.09
220.10	60.29
221.50	60.39
225.60	60.70
233.50	61.26
237.00	61.18
238.90	61.88
240.70	61.90
244.00	61.54
245.50	60.90
246.00	60.36
246.20	59.53

247.20	59.93
247.60	59.89
247.80	59.87
248.60	59.70
249.00	60.31
250.00	60.29
251.00	61.22
251.60	62.18
252.40	62.26
253.60	62.26
258.00	63.61
262.00	64.87
263.00	65.06
267.50	66.91
275.00	71.65
290.00	58.30
308.70	56.85
311.00	56.86
312.30	57.81
313.10	56.58
313.60	61.57

**Well P06-04**

Year	Mean
0	52.49
3.1	53.01
5.8	54.77
20.1	53.67
33.1	54.79
37.9	51.71
50.2	52.38
53	53.3
55.1	53.51
55.4	53.55
61.7	56.21
71	51.55
99	53.25
124.5	52.62
131.1	54.72
137.4	54.63
156.4	57.97
165	53.53
183	53.64
199.6	55.18
203.6	55.39

207.2	55.54
211.4	56.22
213.6	56.32
220.1	56.6
221.5	56.63
225.6	57.21
233.5	57.71
237	57.61
238.9	56.88
240.7	56.77
244	57.25
245.3	57.27
245.6	57.75
246.2	57.76
247.2	57.77
247.6	57.76
247.8	57.74
248.7	57.64
249	57.64
250	58.27
251	58.22
251.6	58.14







252.6	57.97
252.8	58.67
254.3	58.62
254.6	58.58
255	58.54
256	58.31
257.4	58.96
257.6	58.95
257.8	58.94
258	58.93
264	60.7
280	64.03
290	53.74
308.7	49.59
311	52.18
312.3	54.64
313.1	54.2
313.6	60.53
314	56.5

## Appendix D: Burial Histories and Maturity Diagrams

In the following figures the following legend is used

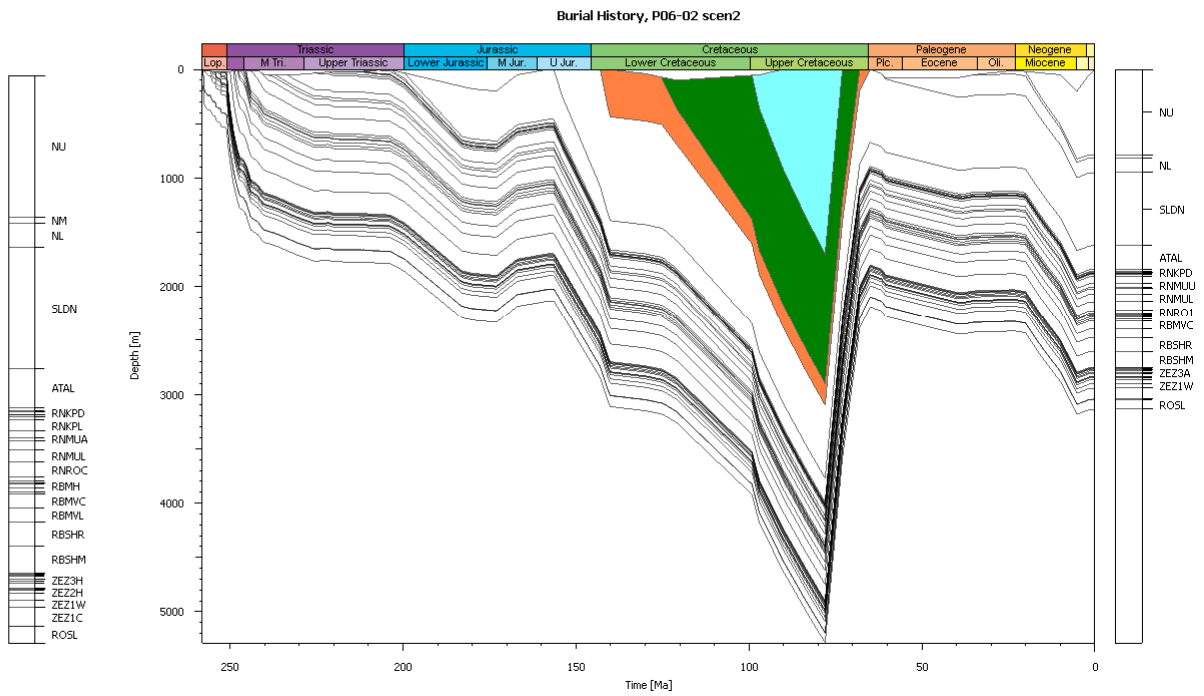
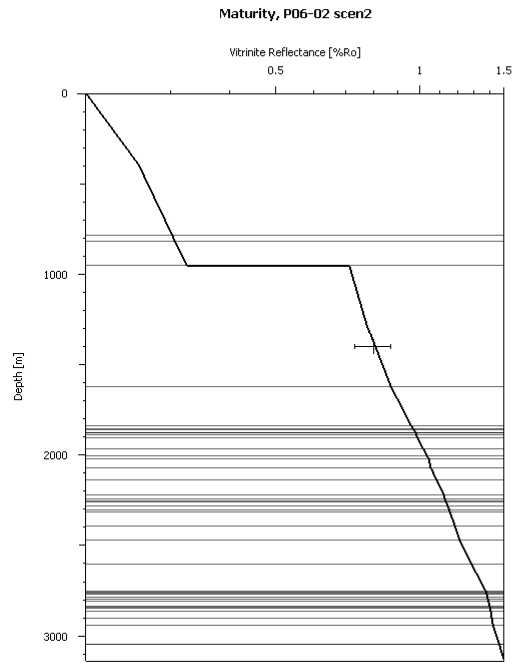
Measured vitrinite reflectance data points	
+	Poor
●	Medium
*	Good
—+—	Error bar

In the legend for the measured vitrinite reflectance data points the Error bar represents the standard deviation measured in the lab.

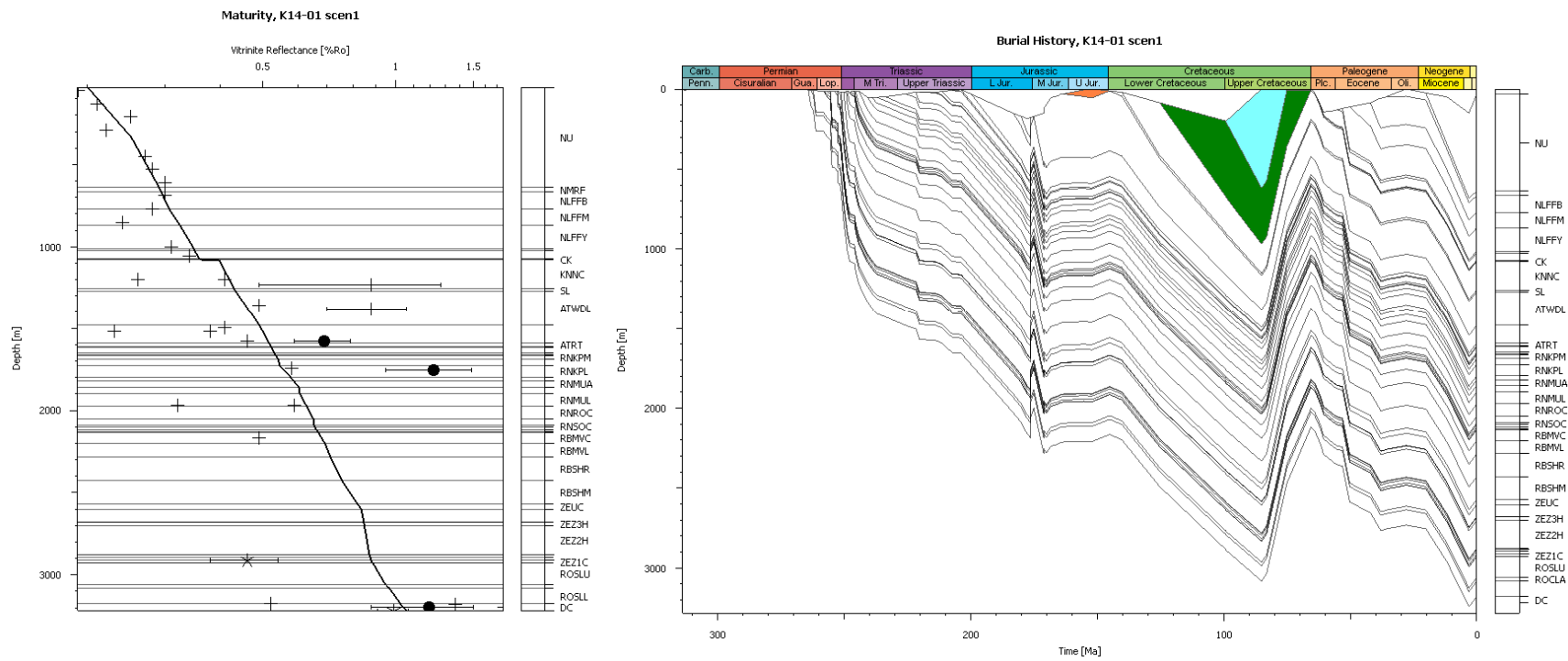
Eroded	
	CK
	KN
	SL
	AT
	RN
	RB



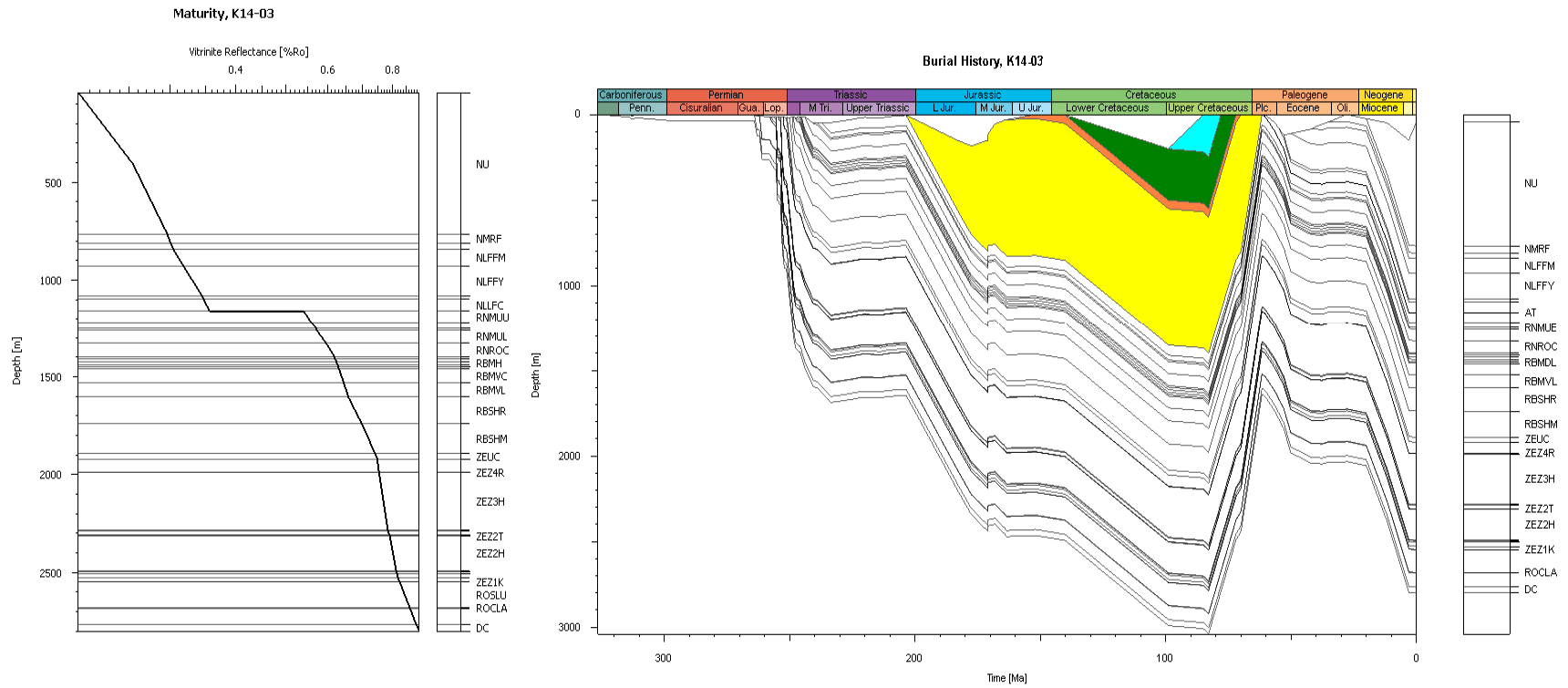
# Burial history and Maturity diagram of P06-02



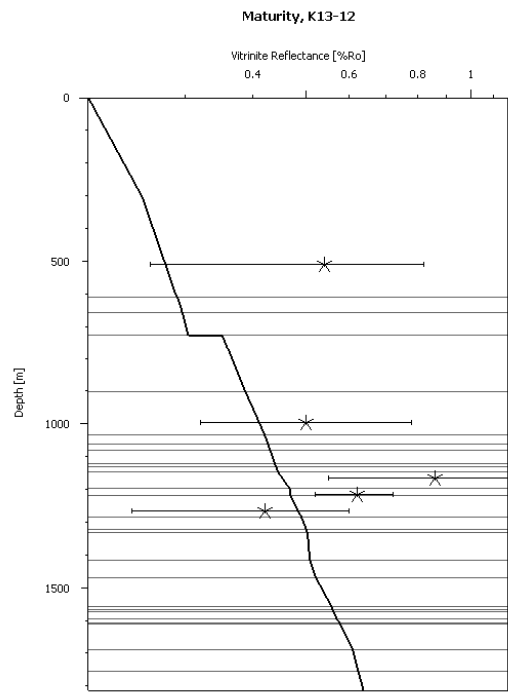
# Burial history and Maturity diagram of K14-01



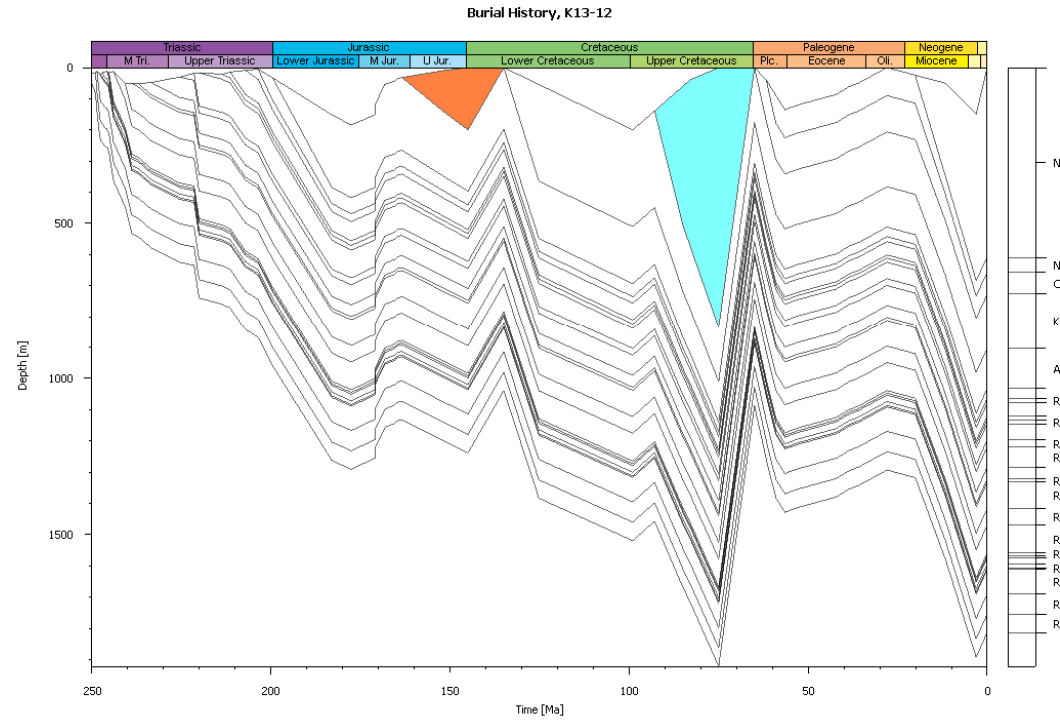
# Burial history and Maturity diagram of K14-03



# Burial history and Maturity diagram of K13-01



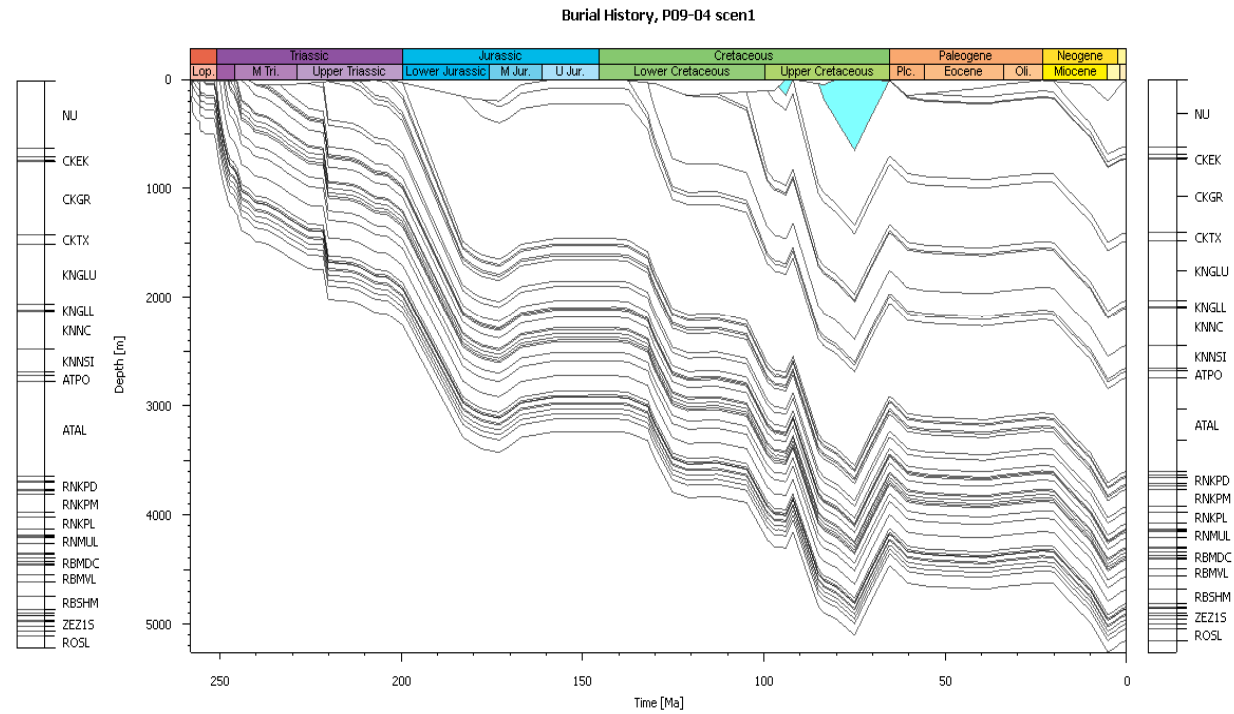
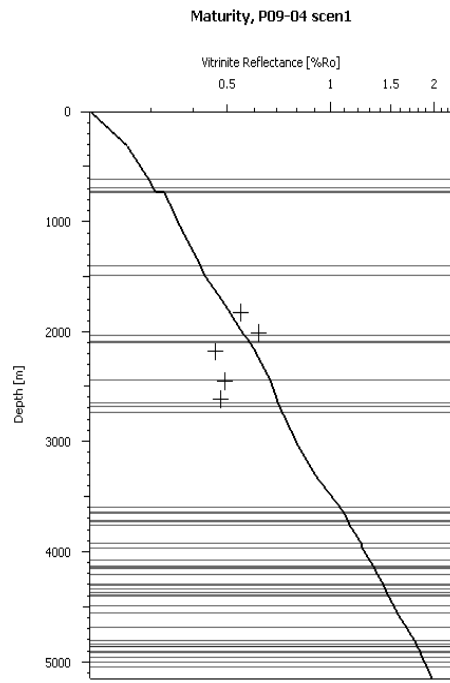
- NU
- NULLFC
- CKGR
- KNNC
- ATAL
- ATRT
- RNKPD
- RNKPE
- RNKPS
- RNKPL
- RNMUA
- RNMUE
- RNMUL
- RNROC
- RNSOC
- RBMDL
- RBMYC
- RBMWL
- RBSH



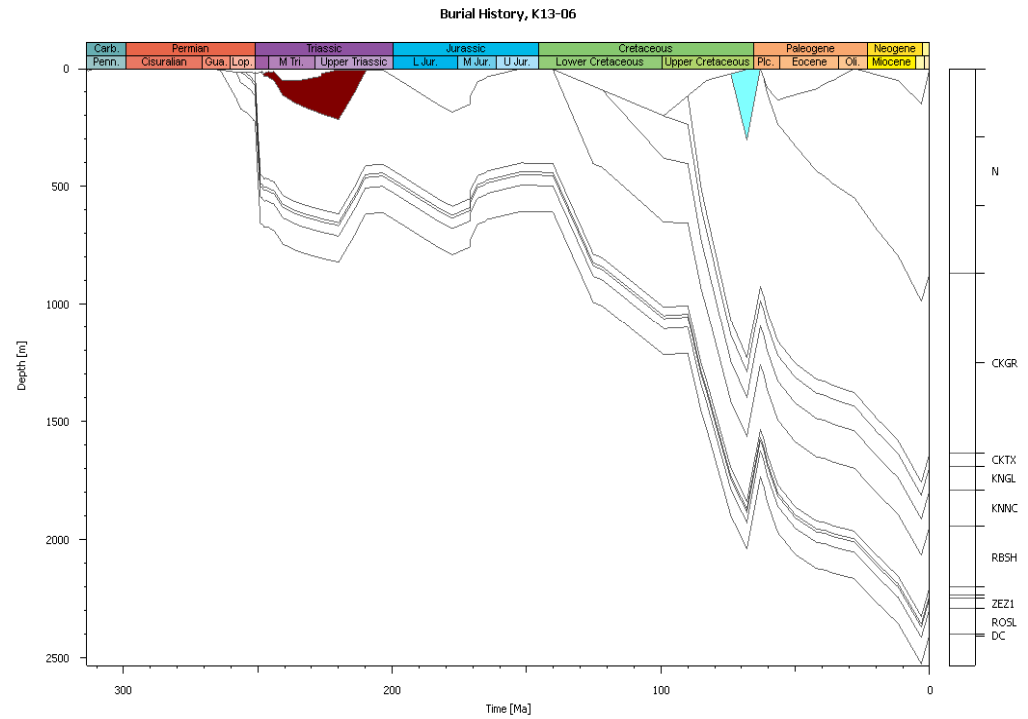
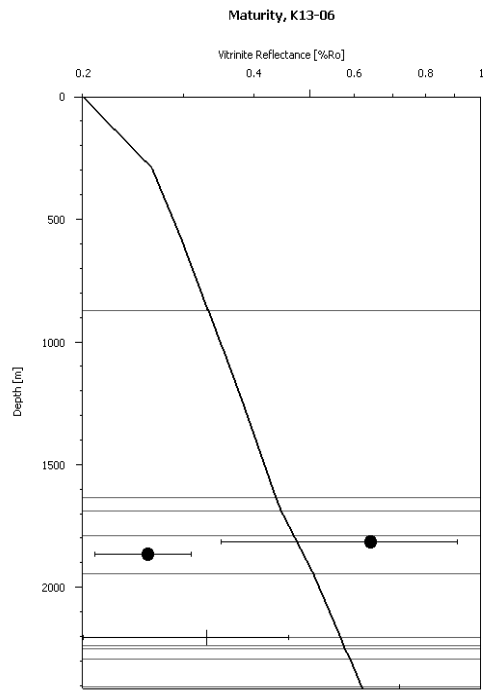




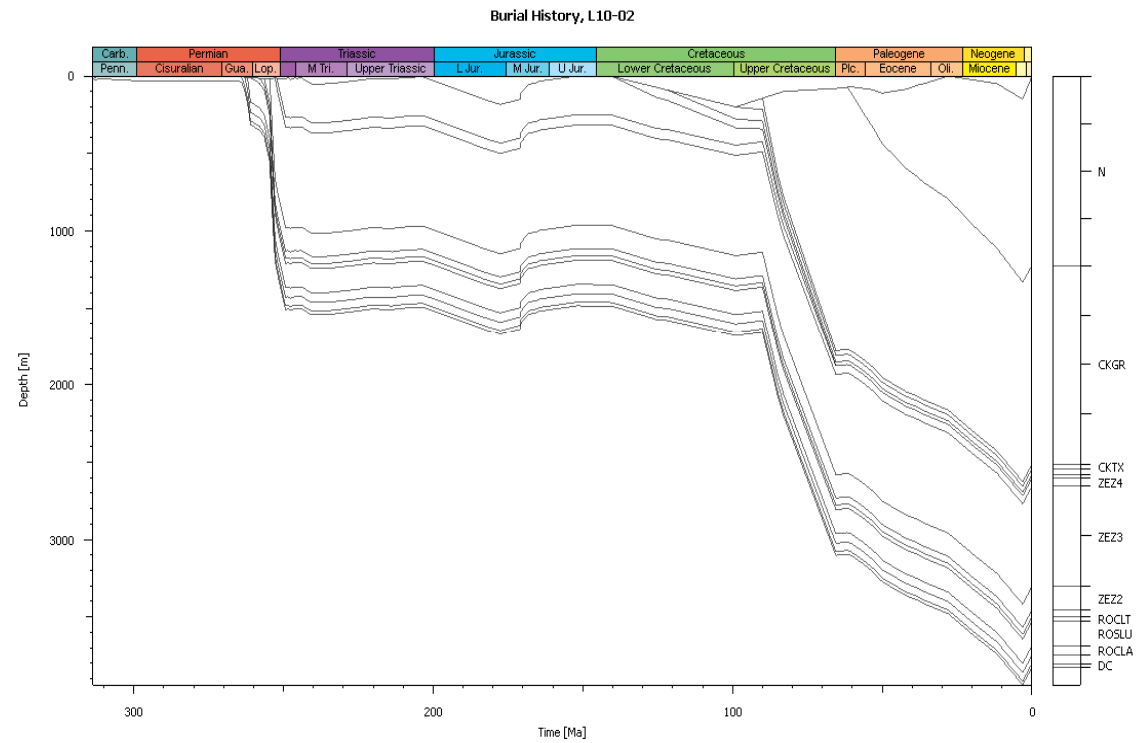
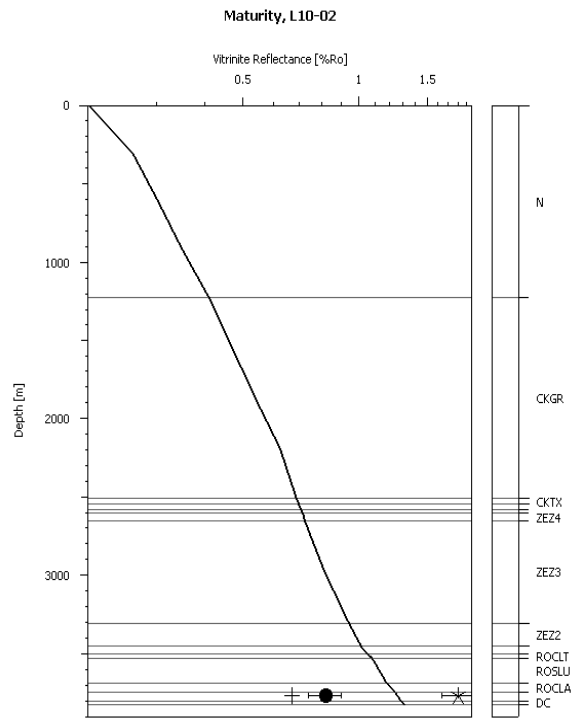
## Burial history and Maturity diagram of P09-04



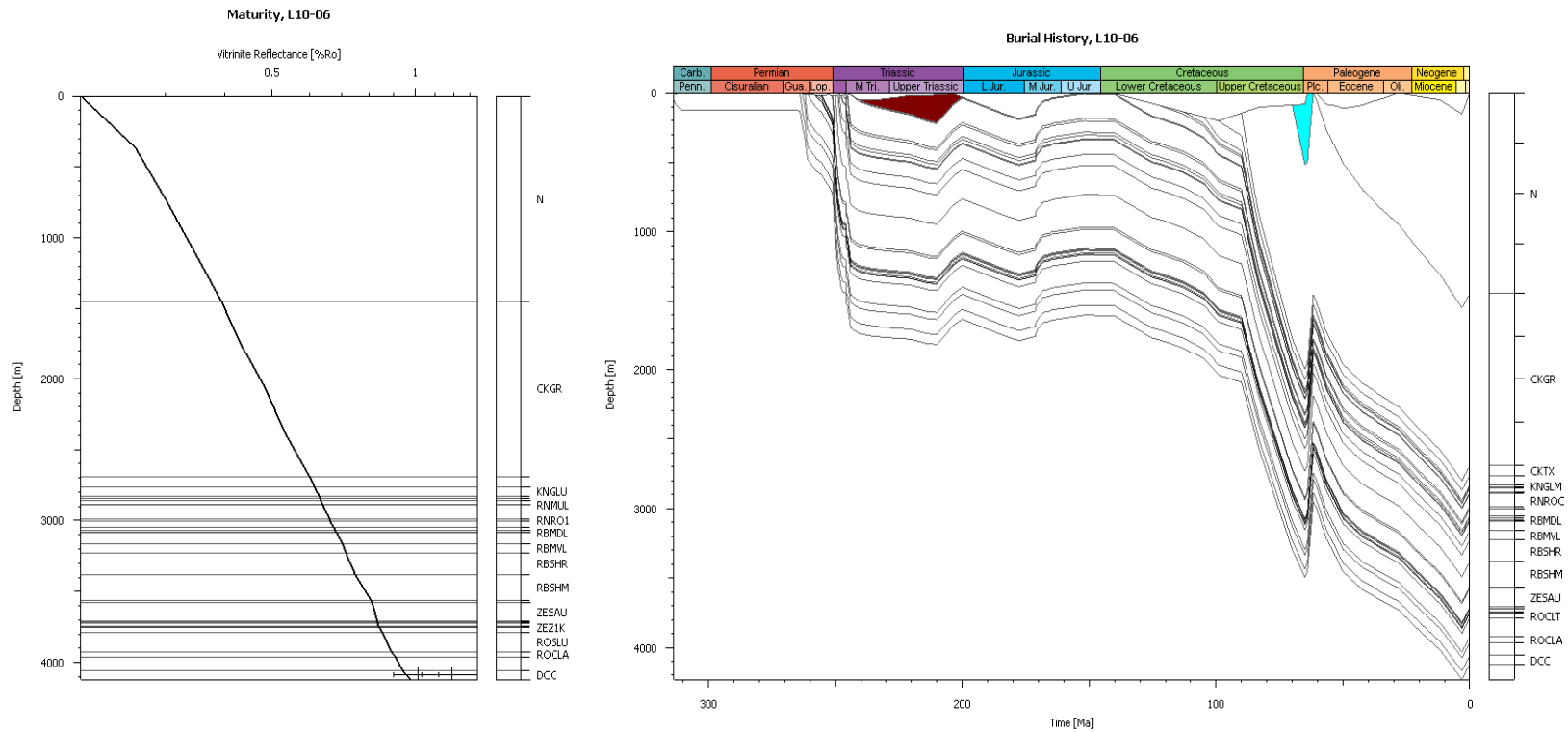
## Burial history and Maturity diagram of K13-06



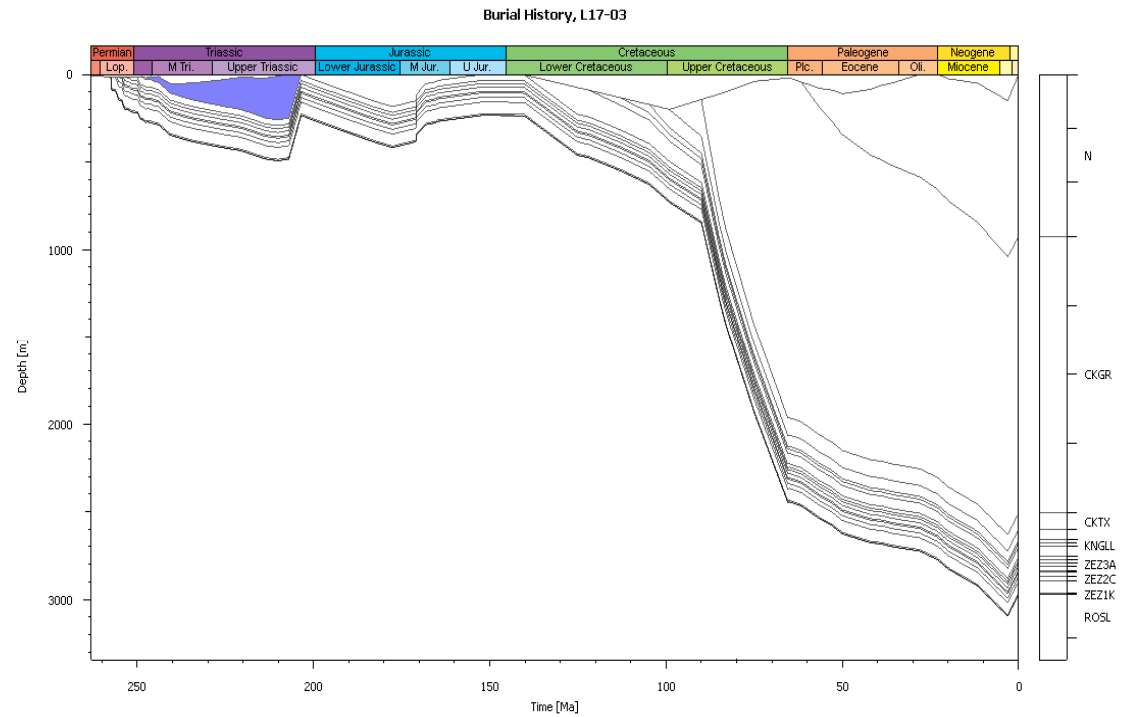
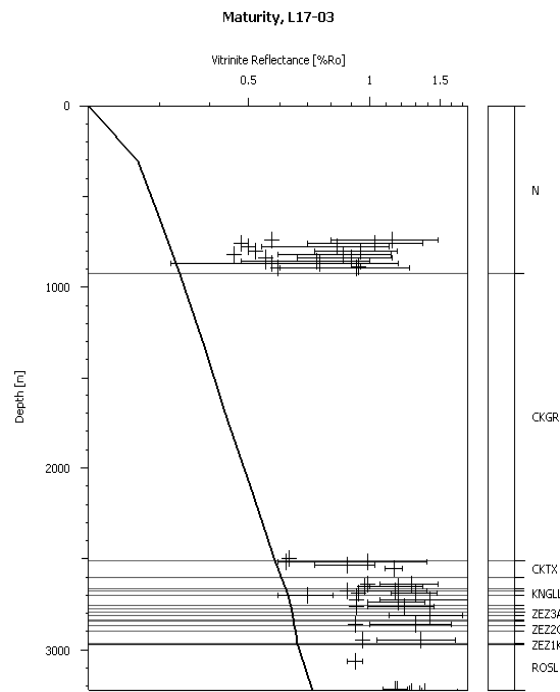
## Burial history and Maturity diagram of L10-02



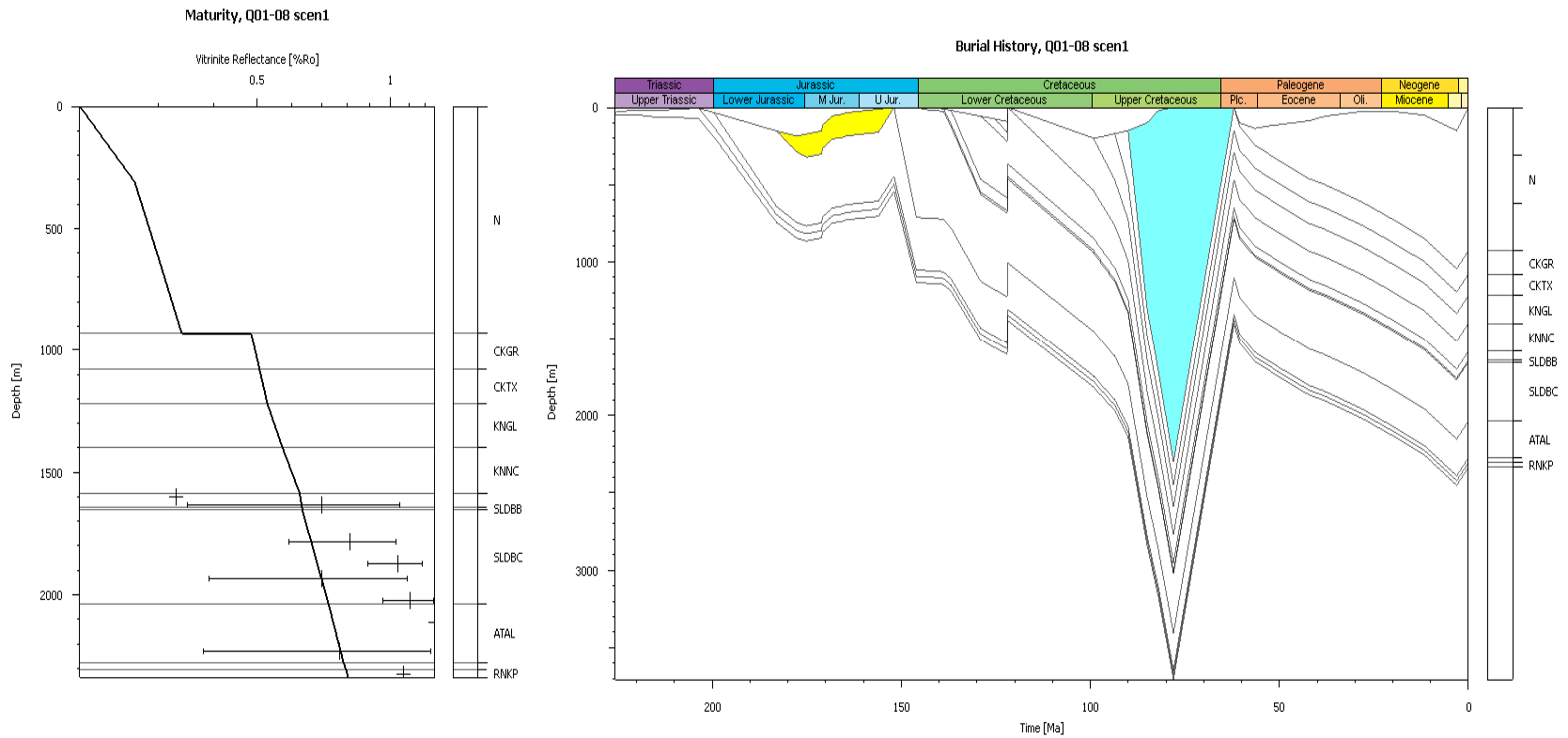
## Burial history and Maturity diagram of L10-06



## Burial history and Maturity diagram of L17-03

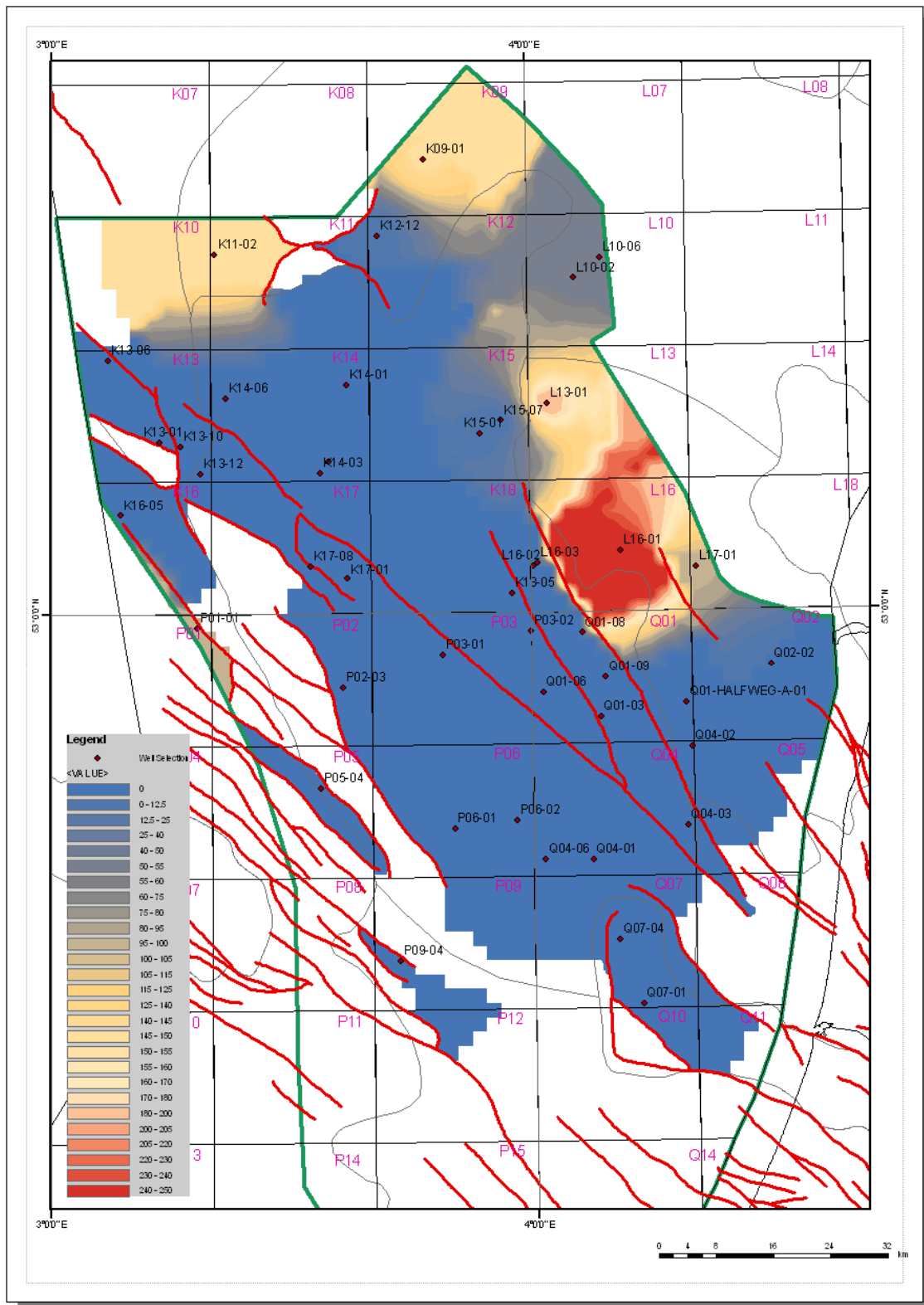


## Burial history and Maturity diagram of Q01-08



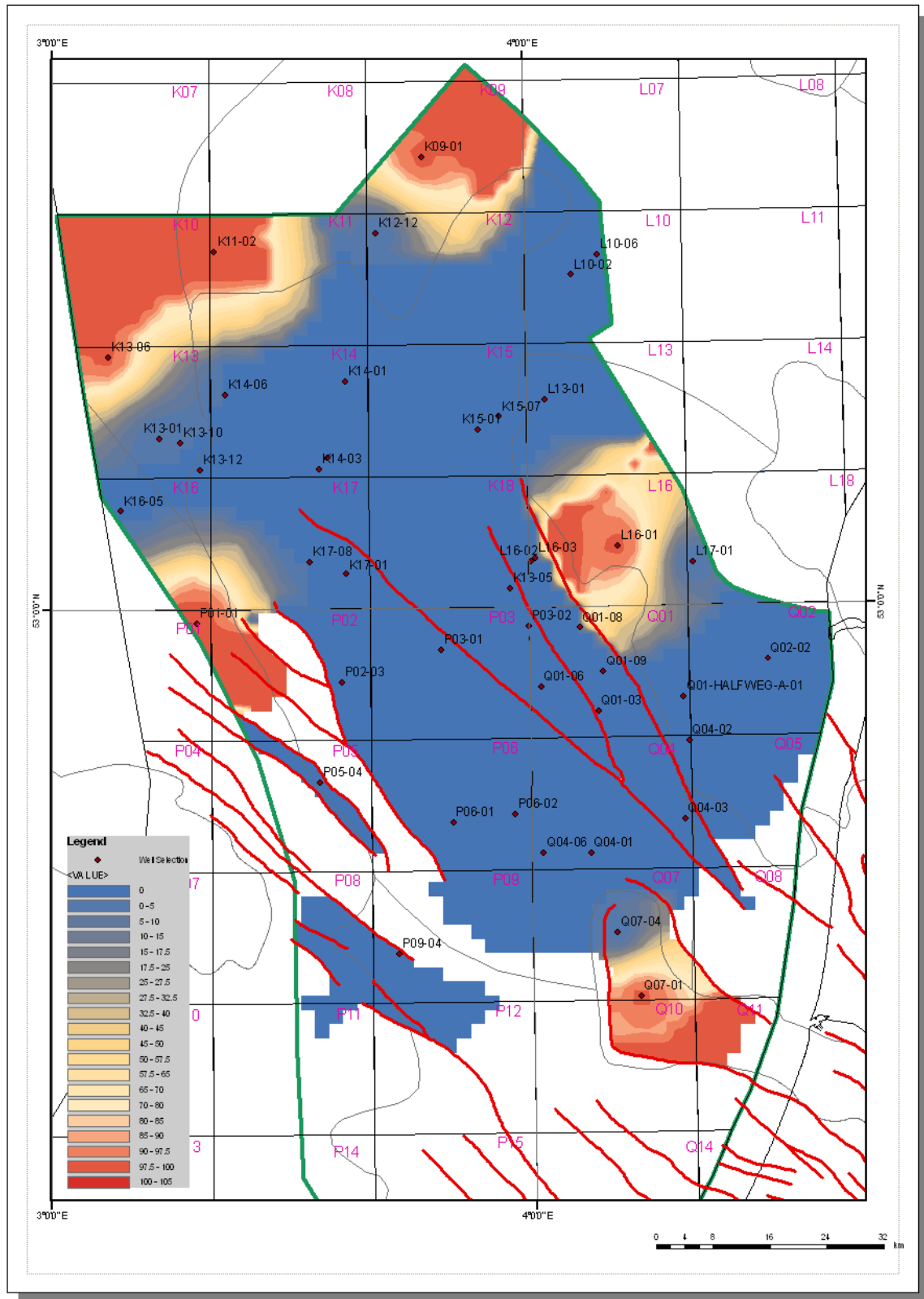
# Appendix E: The Erosion maps

## Erosion map of the Lower Germanic Trias Group

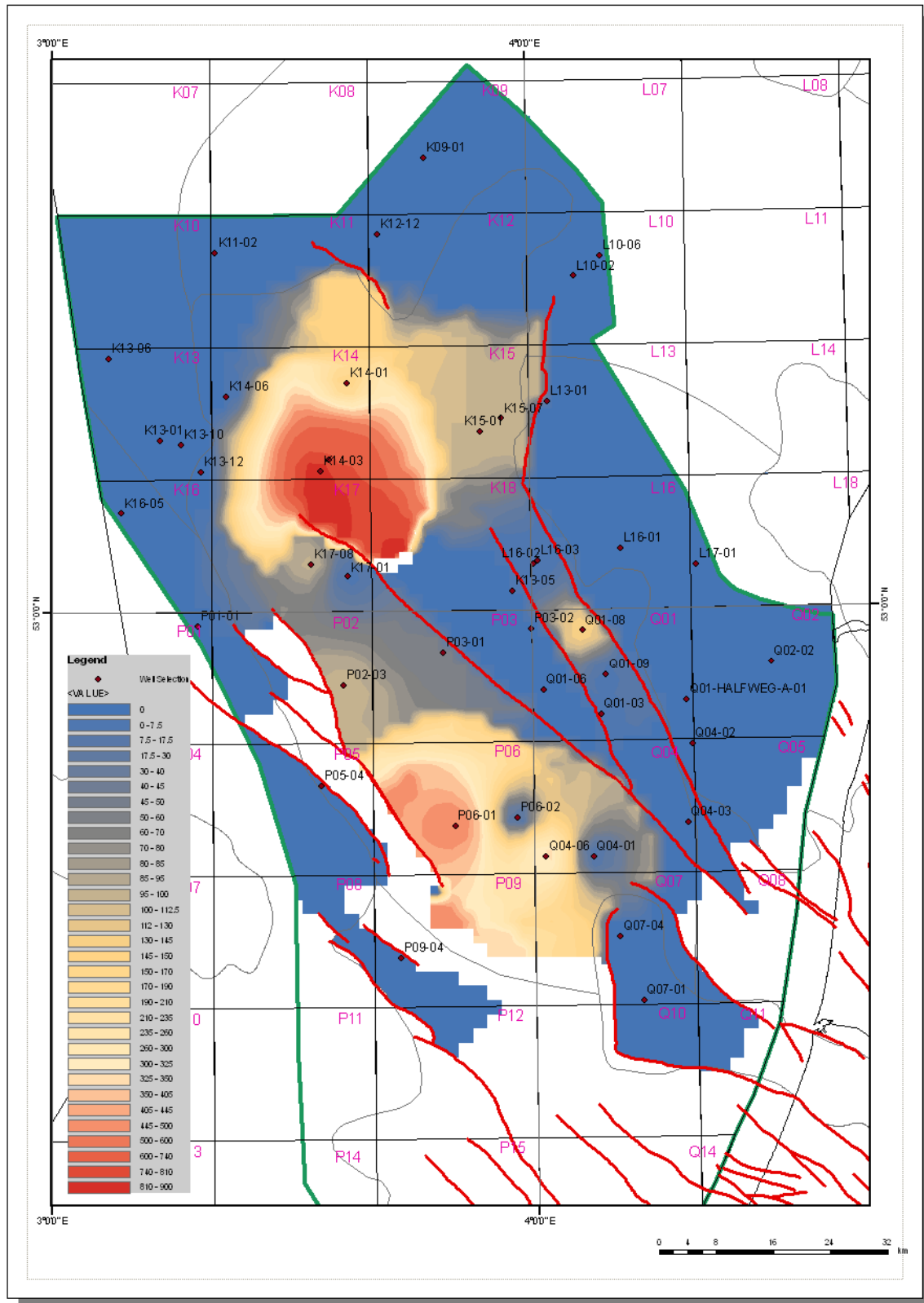




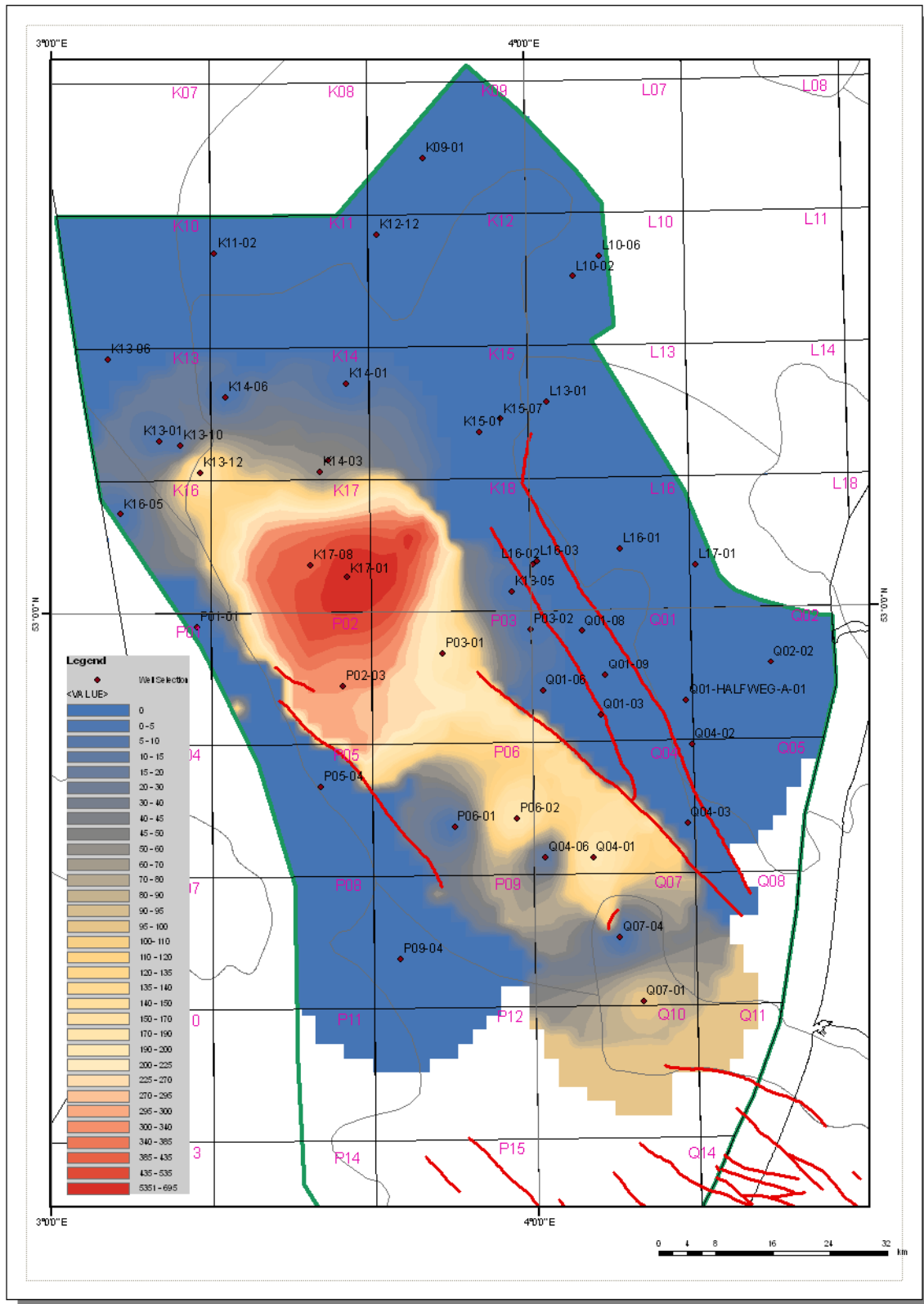
# Erosion map of the Upper Germanic Trias Group



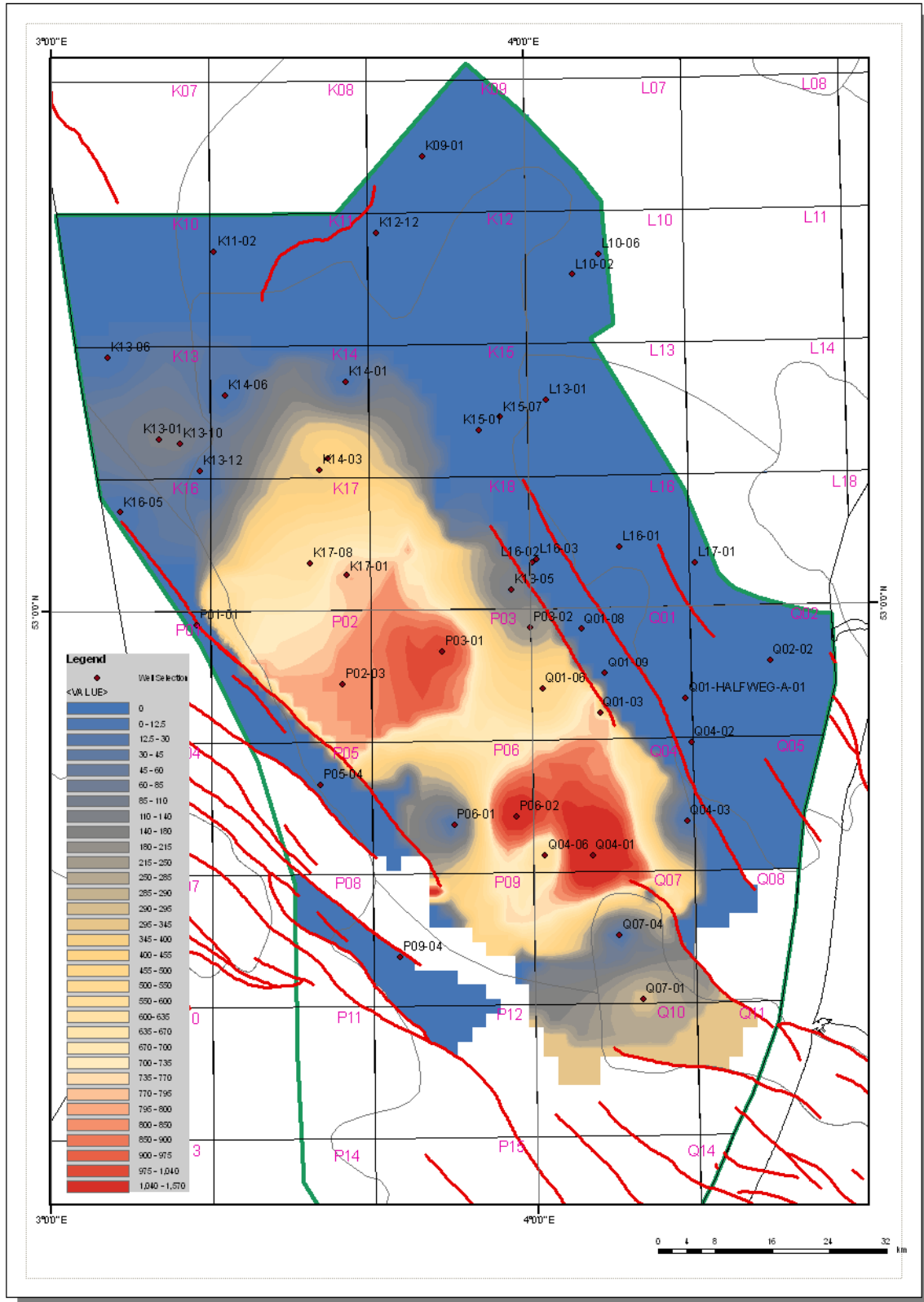
# Erosion map of the Altena Group



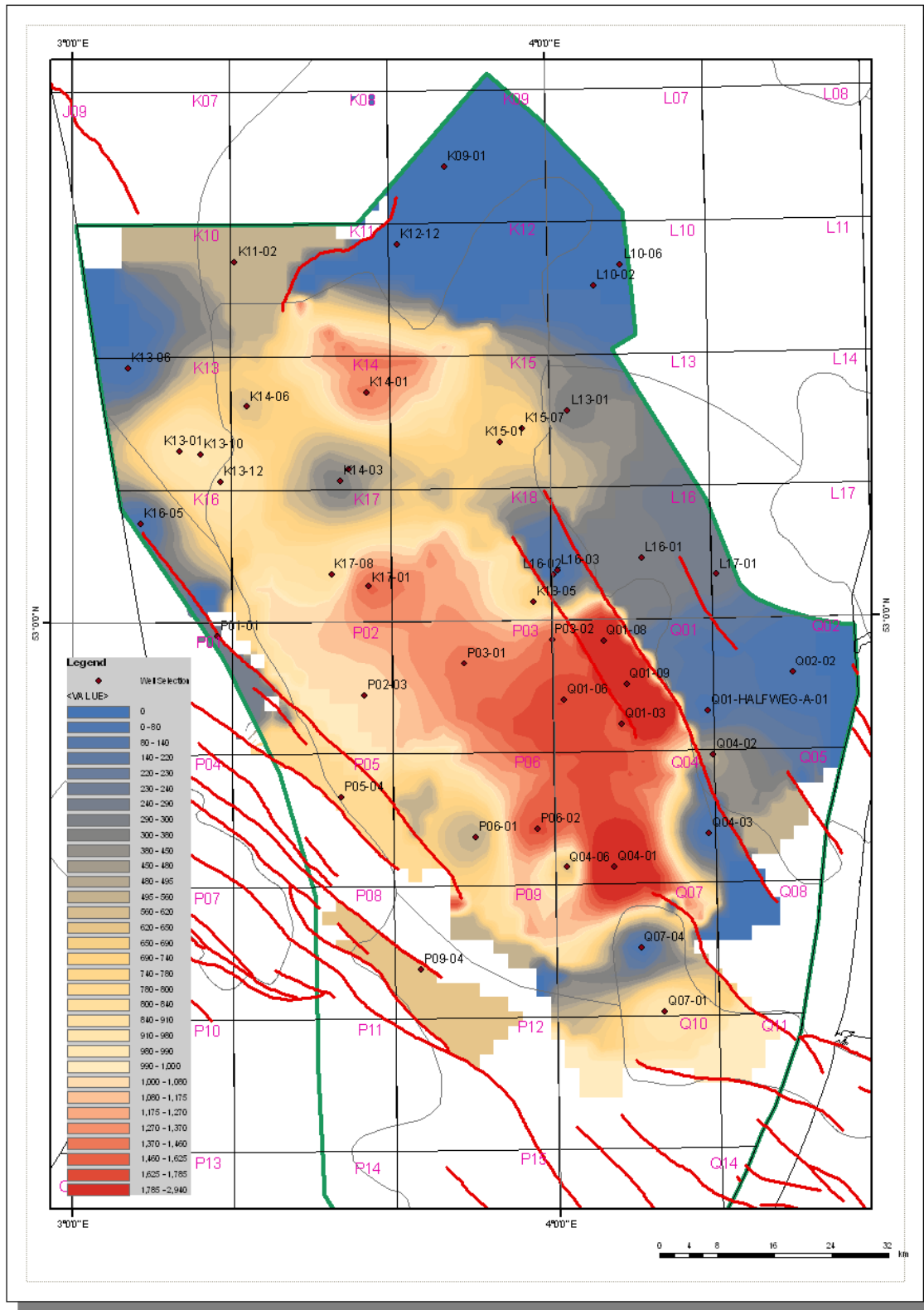
# Erosion map of the Schieland Group



# Erosion map of the Rijnland Group



# Erosion map of the Chalk Group (with the fault system of the Early Cretaceous)



## 9. References:

1. McKenzie, *Some remarks on the development of sedimentary basins*. Earth and Planetary Science Letters, 1978. **10**: p. 25-32.
2. Corcoran, D.V. and A.G. Doré, *A review of techniques for the estimation of magnitude and timing of exhumation in offshore basins*. Earth-Science Reviews, 2005. **72**(3-4): p. 129-168.
3. Green, P.F., I.R. Duddy, and K.A. Hegarty, *Quantifying exhumation from apatite fission-track analysis and vitrinite reflectance data: precision, accuracy and latest results from the Atlantic margin of NW Europe*. Geological Society, London, Special Publications, 2002. **196**(1): p. 331-354.
4. Glennie, K.W., *Petroleum Geology of the North Sea: Basin Concepts and recent Advances*. 4 ed. 1998: Wiley-Blackwell. 656.
5. Verweij, J.M., *Fluid flow systems analysis on geological timescales in onshore and offshore Netherlands; With special reference to the Broad Fourteens basin*. Earth and Life Sciences, 2003. **PhD**: p. 278.
6. Nalpas, T., et al., *Inversion of the Broad Fourteens Basin (offshore Netherlands), a small-scale model investigation*. Sedimentary Geology, 1995. **95**(3-4): p. 237-250.
7. Bouw, L. and G.H.P. Oude Essink, *Fluid flow in the northern Broad Fourteens Basin during Late Cretaceous inversion*. Netherlands Journal of Geosciences, Geologie en Mijnbouw, 2003. **82**(1): p. 55-69.
8. Dixon, J.E., J.G. Fitton, and R.T.C. Frost, *The tectonic significance of post-Carboniferous igneous activity in the North Sea Basin.*, in *Petroleum Geology of the Continental Shelf of North West Europe*, L.V. Illing and G.D. Hobson, Editors. 1981, Heyden: London. p. 121-137.
9. Latin, D.M., J.E. Dixon, and J.G. Fitton, *Rift-related magmatism in the North Sea basin*, in *Tectonic Evolution of the North Sea rifts*, D.J. Blundell and A.D. Gibbs, Editors. 1990, Claredon Press: Oxford. p. 101-144.
10. Neumann, E.R., et al., *The Oslo Rift: A review*. Tectonophysics, 1992. **208**(1-3): p. 1-18.
11. Ziegler, P.A., *North Sea rift system*, in *Geodynamics of Rifting, Volume I. Case History Studies on Rifts: Europe and Asia*, P.A. Ziegler, Editor. 1992, Tectonophysics. p. 55-75.
12. Ziegler, P.A., *Evolution of the Artic-North Atlantic and the Western Tethys - A visual presentation of a series of paleogeographic-paleotectonic maps*. AAPG Memoir. Vol. 43. 1988: American Association of Petroleum Geologists. 198, 30 plates.
13. Ziegler, P.A., *Geological Atlas of Western and Central Europe*. 2 ed. 1990: Geological Society Publishing House (Bath; distributors). 239, 56 encl.
14. de Lugt, I.R., J.D. van Wees, and T.E. Wong, *The tectonic evolution of the southern Dutch North Sea during the Palaeogene: basin inversion in distinct pulses*. Tectonophysics, 2003. **373**(1-4): p. 141-159.
15. van Wijhe, D.H., *Structural evolution of inverted basins in the Dutch offshore*. Tectonophysics, 1987. **137**(1-4): p. 171-219.

16. Wong, T.E., D.A.J. Batjes, and J. de Jager, eds. *Geology of the Netherlands*. 2007, Royal Netherlands Academy of Arts and Sciences. 356.
17. Verweij, J.M., et al., *History of petroleum systems in the southern part of the Broad Fourteens Basin*. Netherlands Journal of Geosciences, Geologie en Mijnbouw, 2003. **82**(1): p. 71-90.
18. Wong, T.E., N. Parker, and P. Horst, *Tertiary sedimentary development of the Broad Fourteens area, the Netherlands*. Netherlands Journal of Geosciences - Geologie en Mijnbouw, 2001. **80**(1): p. 85-94.
19. Duin, E.J.T., et al., *Subsurface structure of the Netherlands - results of recent onshore and offshore mapping*. Netherlands Journal of Geosciences, Geologie en Mijnbouw, 2006. **85**(4): p. 245-276.
20. de Jager, J., *Inverted basins in the Netherlands, similarities and differences*. Netherlands Journal of Geosciences - Geologie en Mijnbouw, 2003. **82**(4): p. 355-366.
21. van Adrichem Boogaert, H.A. and W.F.P. Kouwe, *Stratigraphic nomenclature of the Netherlands, revision and update by RGD and NOGEPA*. Mededelingen Rijks Geologische Dienst. Vol. 50. 1993-1997, Haarlem: TNO-NITG, Geological Survey of the Netherlands.
22. Verweij, J.M. and H.J. Simmelink, *Geodynamic and hydrodynamic evolution of the Broad Fourteens Basin (The Netherlands) in relation to its petroleum system*. Marine and Petroleum Geology, 2002. **19**: p. 339-359.
23. van Wijhe, D.H., M. Lutz, and J.P.H. Kaasschieter, *The Rotliegend in The Netherlands and its gas accumulations*. Geol. en Mijnbouw, 1980. **59**: p. 3-24.
24. TNO-NITG, *Geological Atlas of the Subsurface of the Netherlands - onshore*. 2004, Utrecht.
25. Geluk, M.C., *Stratigraphy and tectonics of Permo-Triassic basins in the Netherlands and surrounding areas*. Earth Sciences, 2005. **PhD**: p. 171.
26. Hooper, R.J., L.S. Goh, and F. Dewey, *The inversion history of the northeastern margin of the Broad Fourteens Basin*. Geological Society, London, Special Publications, 1995. **88**: p. 307-317.
27. Hengreen, G.F.W. and T.E. Wong, *Cretaceous*, in *Geology of the Netherlands*, T.E. Wong, D.A.J. Batjes, and J. de Jager, Editors. 2007, Royal Netherlands Academy of Arts and Sciences. p. 127-150.
28. Malcolm H., R., *The Geological Interpretation of Well Logs*. 2 ed. 1996, Caithness: Whittles Publishing.
29. Allen, P.A. and J.R. Allen, *Basin Analysis: principles and applications*. 2 ed. 2005: Blackwell Publishing Ltd. 549.
30. Wórum, G., *Modelling of fault reactivation potential and quantification of inversion tectonics in the southern Netherlands*. Earth- and Life Sciences, 2004: p. 152.
31. Hantschel, T. and A.I. Kauerauf, *Petroleum Generation*, in *Fundamentals of Basin and Petroleum Systems Modeling*. 2009, Springer-Verlag Berlin Heidelberg: Berlin.
32. van Dalfsen, W., et al., *A comprehensive seismic velocity model for the Netherlands based on lithostratigraphic layers*. Netherlands Journal of Geosciences - Geologie en Mijnbouw, 2006. **85**(4): p. 277-292.

33. Duin, E.J.T., F.M.J. van Lieshout, Editor. 2010: Utrecht.
34. Abdul Fattah, R., F.M.J. van Lieshout, Editor. 2010: Utrecht.
35. Watts, A.B. and W.B.F. Ryan, *Flexure of the lithosphere and continental margin basins*. Tectonophysics, 1976. **36**(1-3): p. 25-44.
36. Skagen, J.I., *Methodology applied to uplift and erosion*. Norsk geologisk tidsskrift, 1992. **72**(3): p. 307-311.
37. Watts, A.B., *Backstripping sediments progressively through geological time*. 2005.
38. Doré, A.G., et al., *Exhumation of the North Atlantic margin: introduction and background*. Geological Society, London, Special Publications, 2002. **196**: p. 1-12.
39. Jones, S.M., N. White, and B. Lovell, *Cenozoic and Cretaceous transient uplift in the Porcupine Basin and its relationship to a mantle plume*, in *The Petroleum Exploration of Ireland's Offshore Basins*, P.M. Shannon, P.D.W. Haughton, and D.V. Corcoran, Editors. 2001, Geological Society, London, Special Publications: London. p. 345-360.
40. Gradstein, F.M., et al., *A new Geologic Time Scale, with special reference to Precambrian and Neogene*. 2004, Cambridge: Cambridge University Press.
41. Burnham, A.K. and J.J. Sweeney, *A chemical kinetic model of vitrinite maturation and reflectance*. Geochimica et Cosmochimica Acta, 1989. **53**: p. 2649-2657.
42. van der Molen, A.S., *Sedimentary development, seismic stratigraphy and burial compaction of the Chalk Group in the Netherlands North Sea area*. Earth Sciences, 2004. **PhD**: p. 180.
43. Sissingh, W., *Palaeozoic and Mesozoic igneous activity in the Netherlands: a tectonomagmatic review*. Netherlands Journal of Geosciences / Geologie en Mijnbouw, 2004. **83**: p. 113-134.
44. Kuijper, R.P., *Petrology of a dolerite in Netherlands offshore well G/17-2*. Scripta Geologica, 1991. **97**: p. 33-97.
45. Hayward, A.B. and R. Graham, *Some geometrical characteristics of inversion*, in *Inversion tectonics*, M.A. Cooper and G.D. Williams, Editors. 1989, Geological Society, Special Publication London. p. 17-40.
46. Witmans, N., F.M.J. van Lieshout, Editor. 2010: Utrecht.
47. Trichon, H. and M. Lescoeur, *Maturation dans le "Broad Fourteens Basin"* Rapport interne Elf Petroland, 1992: p. 15.
48. Huyghe, P. and J.-L. Mugnier, *A comparison of inverted basins of the Southern North Sea and inverted structures of the external Alps*. Geological Society, London, Special Publications, 1995. **88**: p. 339-353.
49. Dronkers, A.J. and F.J. Mrozek, *Inverted basins of The Netherlands*. First Break, 1991. **9**: p. 409-425.



# 10. Figures:

Figure 1:

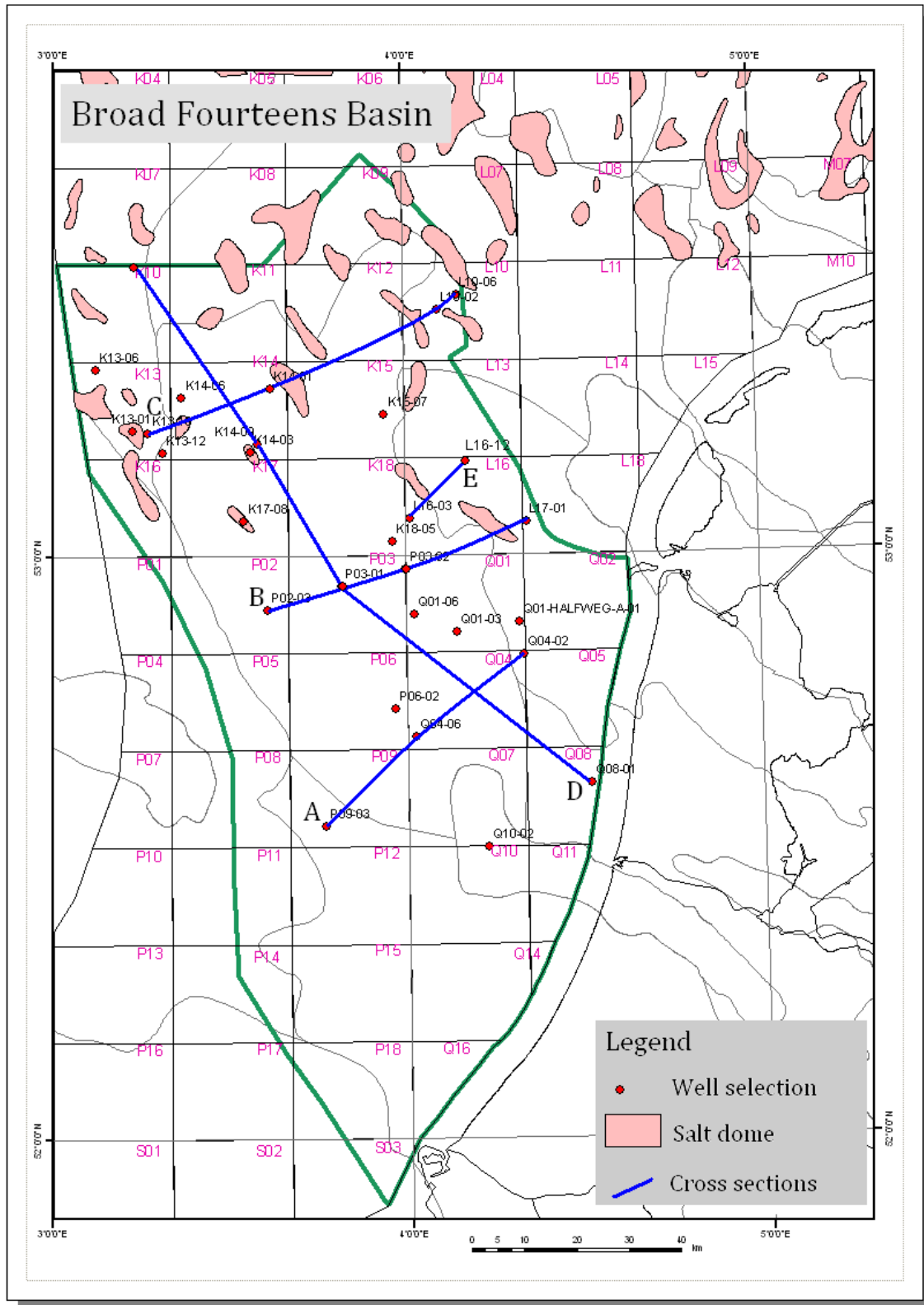


Figure 1: Overview of basin, with axis

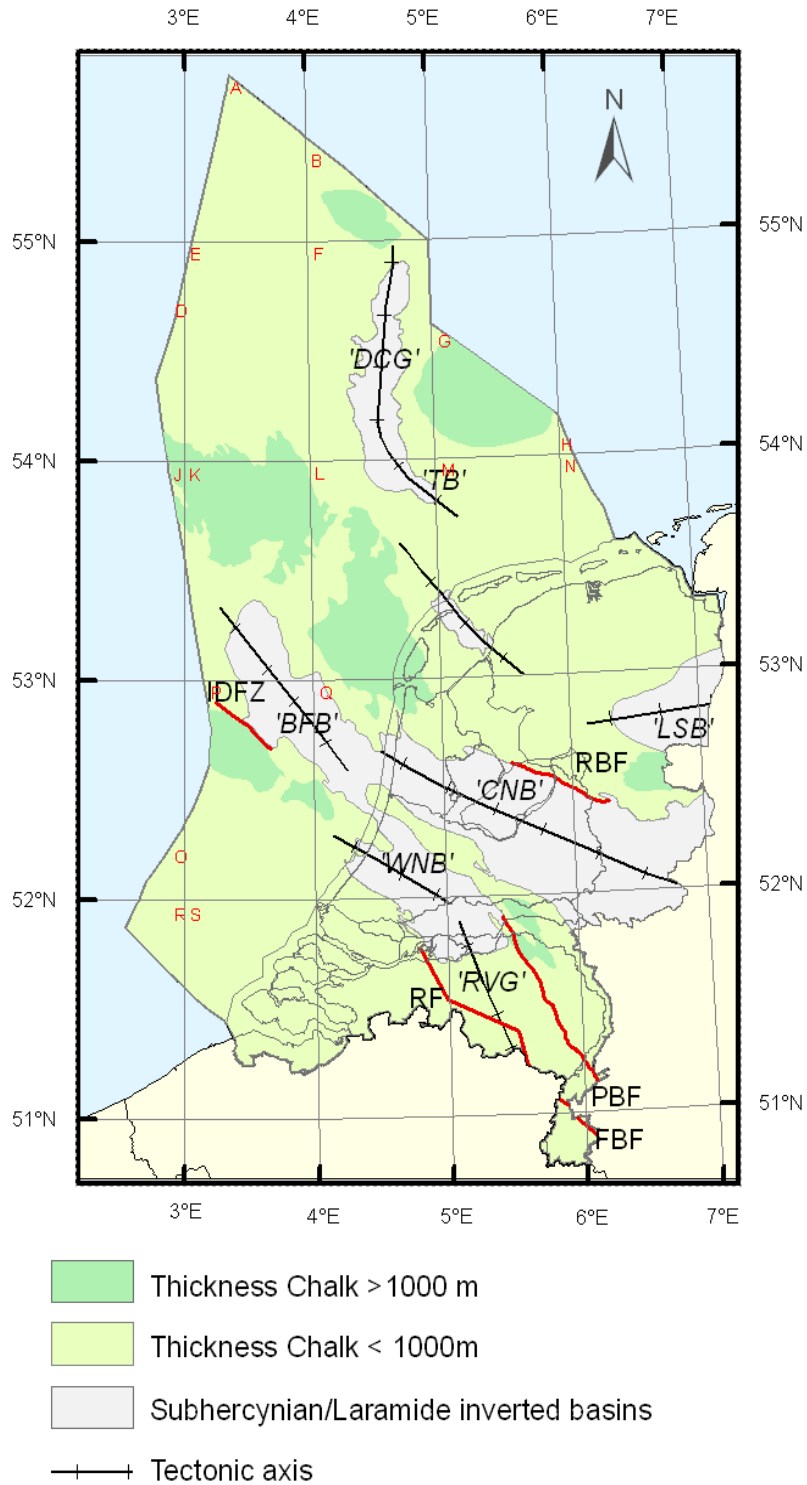


Figure 4: Structural elements map, numbered. The numbered values correspond with the basin, platform or the highs elements. These can also be found in the *'Well selection & Erosion values'* table in Appendix B.

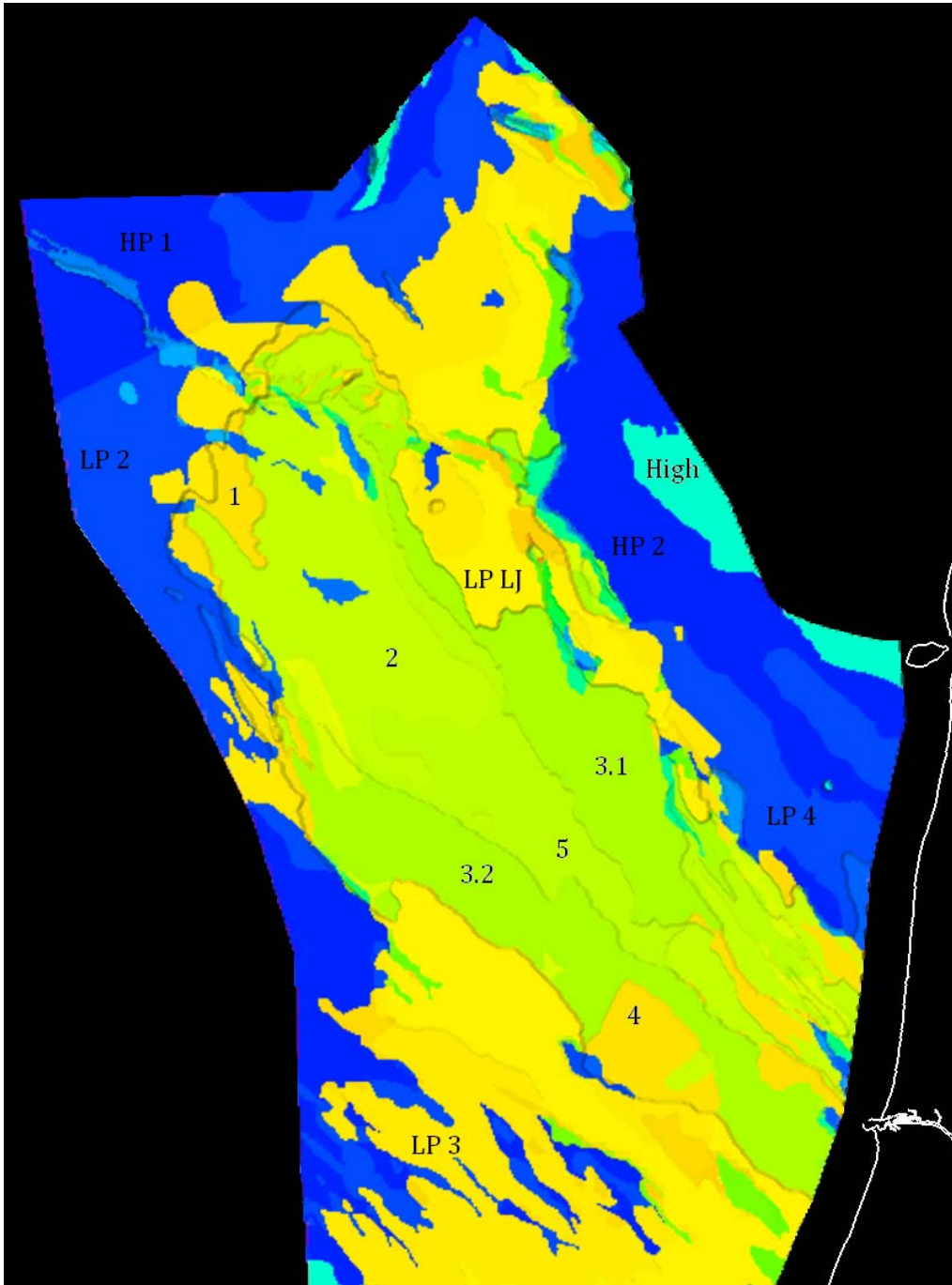
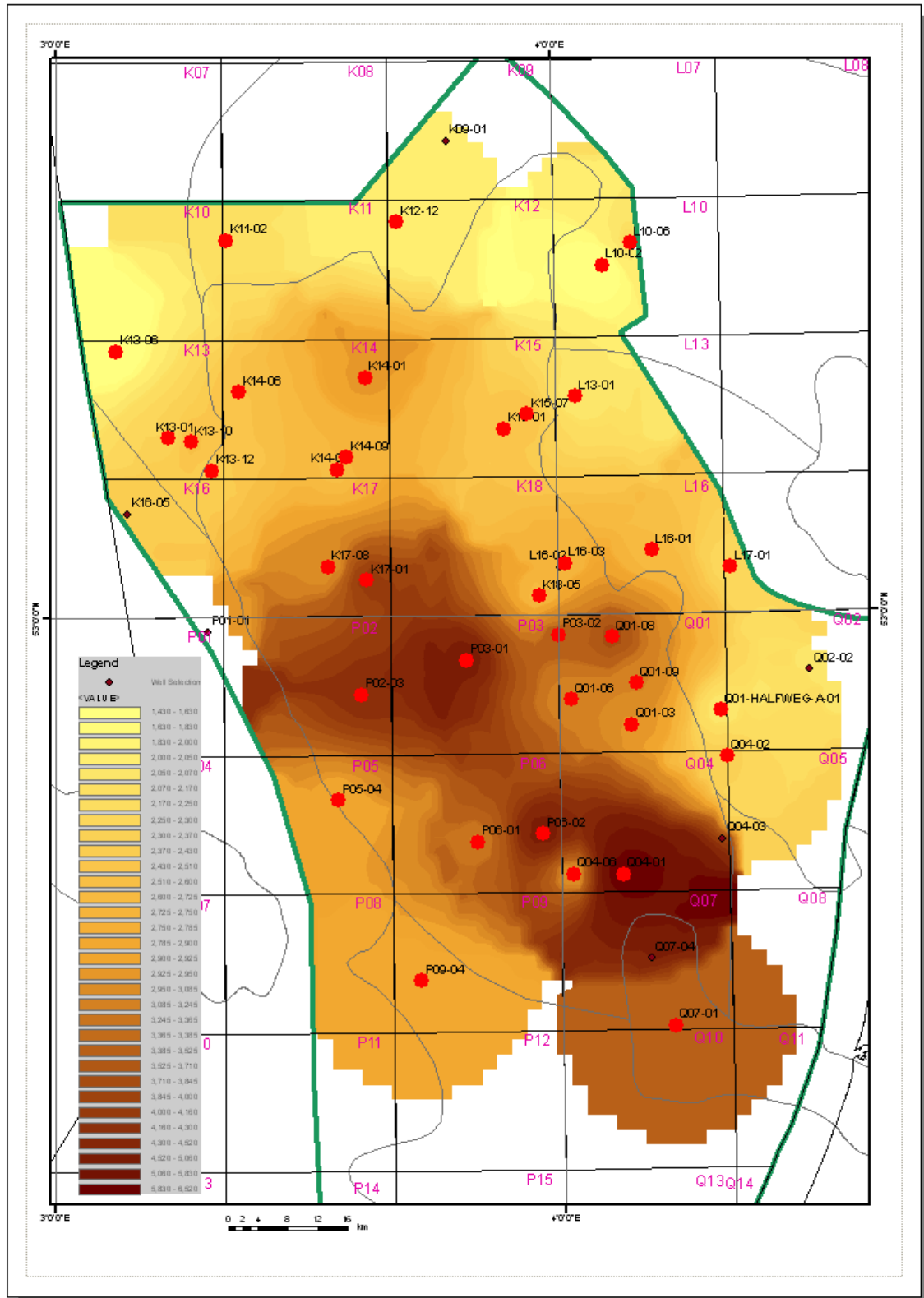


Table 3: Example of an input table of PetroMod® 1D

Layer	Top [m]	Base [m]	Thick. [m]	Eroded [m]	Depo. from [Ma]	Depo. to [Ma]	Eroded from [Ma]	Eroded to [Ma]	Lithology
NUJ	0	648	648		20.10	0.00			49_Sand_49_Shale_2_Coal
NMRF	648	670	22		35.40	28.60			75_Shale_25_Sand
NLFFB	670	757	87		42.00	37.90			100_Shale
NLFFM	757	865	108		50.20	42.00			50_Shale_50_Marl
NLFFY	865	964	99		53.00	50.20			100_Shale
NLFFT	964	982	18		55.10	53.00			50_Shale_50_Tuff
NLLFC	982	1025	43		61.70	55.10			100_Shale
CKEK	1025	1088	63		65.50	61.70			100_Chalk
CKGR	1088	1156	68		72.00	65.50			100_Chalk
CKTX + CKGR	1156	1156	0	600	99.10	80.00	80.00	72.00	75_Chalk_25_Marl
KN	1156	1339	183		140.10	99.10			75_Marl_25_Shale
AT	1339	1757	418		203.60	150.00			75_Shale_25_Silt
RNKPU	1757	1765	8		207.20	203.60			75_Shale_25_Marl
RNKPD	1765	1820	56		211.40	207.20			75_Shale_25_Dolo
RNKPR	1820	1840	20		213.60	211.40			50_Shale_50_Marl
RNKPE	1840	1845	5		220.10	213.60			40_Anhy_40_Shale_20_Silt
RNKPM	1845	1902	58		221.50	220.10			100_Shale
RNKPS	1902	1940	38		225.60	221.50			90_Salt_10_Anhy
RNKPL	1940	2007	67		233.50	225.60			80_Shale_10_Anhy_10_Lime
RNMJU	2007	2036	29		237.00	233.50			50_Marl_50_Lime
RNMUA	2036	2062	26		238.90	237.00			100_Marl
RNMUE	2062	2152	90		240.70	238.90			75_Salt_25_Anhy
RNMUL	2152	2214	62		244.00	240.70			50_Marl_50_Lime
RNR0C	2214	2292	78		245.30	244.00			50_Shale_50_Silt
RNR01	2292	2345	53		245.60	245.30			90_Salt_10_Anhy
RNS0C	2345	2352	8		246.00	245.60			100_Shale
RBMH	2352	2372	19		247.20	246.20			75_Sand_25_Shale
RBMD0C	2372	2384	13		247.60	247.20			100_Shale
RBMDL	2384	2390	6		247.80	247.60			75_Sand_25_Shale
RBMVC	2390	2458	68		248.60	247.80			34_Shale_33_Sand_33_Silt
RBMVL	2458	2550	93		249.00	248.60			100_Sandstone
RB5HR	2550	2702	152		250.00	249.00			50_Shale_25_Lime_25_Silt
RB5HM	2702	2852	150		251.00	250.00			75_Shale_25_Silt
ZEUC	2852	2880	28		251.60	251.00			100_Shale
ZE24H	2880	2912	32		252.44	252.20			100_Salt
ZE24A	2912	2912	0		252.56	252.44			100_Anhydrite
ZE24R	2912	2913	0		252.80	252.56			75_Shale_25_Anhy
ZE22H	2913	2983	70		255.32	254.60			100_Salt
ZE22A	2983	2984	2		255.68	255.32			100_Anhydrite
ZE22C	2984	2995	10		256.40	255.68			75_Lime_25_Dolo
ZE21W	2995	3024	30		257.40	256.40			100_Anhydrite
ZE21C	3024	3031	6		257.80	257.40			100_Limestone
ZE21K	3031	3032	0		258.00	257.80			100_Shale
ROSL	3032	3104	72		260.00	258.00			100_Sandstone
FLT_N	3104	3104	0		260.00	260.00			
ROSL	3104	3228	124		264.00	260.00			100_Sandstone
DCC	3228	3300	72		315.40	311.00			48_Shale_25_Sand_25_Silt_2_Coal
						315.40			

Figure 12: Thickness map of sedimentation during Triassic till Cretaceous



**Afstuderen...**

**Het lijkt een grote  
chaos...**

**Maar het einde is,**

**inzicht**

*Flo'tje*

---